ALZHEIMER'S DISEASE DRUG DISCOVERY AND RISK FACTORS IDENTIFICATION

By

Mengyu Liu

A DISSERTATION

Submitted to
Michigan State University
in partial fulfillment of the requirments
for the degree of

Biochemistry and Molecular Biology – Doctor of Philosophy

2019

ABSTRACT

ALZHEIMER'S DISEASE DRUG DISCOVERY AND RISK FACTORS IDENTIFICATION

By

Mengyu Liu

Pathological deposition of hyperphosphorylated tau protein (p-tau) into neurofibrillary tangles in selective neurons is the most revealing molecular feature for a group of neurodegenerative disorders collectively known as tauopathies, including Alzheimer's disease (AD) which is the most common form of dementia. Tau pathology has a strong correlation with the progression and severity of cognitive functions, suggesting a pathogenic role of this protein, and critically, that measures that control tau deposition may afford promising therapy for tauopathies. The first hurdle for tangle-centric drug discovery would be the procurement of hyperphosphorylated tau (p-tau) exhibiting characters that are relevant to the disease. I have employed the PIMAX system (Protein Interaction Modules-Assisted function X) developed in our laboratory to produce recombinant p-tau. PIMAX p-tau is phosphorylated at multiple sites with strong links to the disease, and forms fibrils spontaneously. At sub-micromolar concentrations, p-tau triggers apoptosis, causes cytoplasmic superoxide levels to increase drastically, and causes death of two different cultured cells. Consistent with the neurodegeneration model that cytotoxic tau in the brain acts in a prion-like fashion, p-tau is able to potentiate the aggregation and cytotoxicity of the unphosphorylated tau that is otherwise benign to cultured cells. These unique features strongly suggest that p-tau is a novel and pathophysiologically relevant subject for AD drug discovery. I therefore developed a high-throughput screening platform for the identification of small-molecule compounds

that may modulate the cognitive symptoms of AD through controlling the fibrillization and cytotoxicity of p-tau. In a pilot screen, I discovered two brain permeant prescription drugs, R-(–)-apomorphine and raloxifene to be cytoprotective p-tau aggregation inhibitors. In contrast, selective prescription benzodiazepines were found to exacerbate the cell killing activity of p-tau by enhancing its aggregation. Together, my results suggest that the p-tau aggregation-based screens may uncover candidates for AD therapy as well as potential avoidable risk factors for this devastating disease, therefore breaking through the current stagnant status of AD drug discovery.

ACKNOWLEDGEMENTS

My PhD career is indebted to many people, and I would like to thank them for their help and contribution. First I want to thank my thesis advisor, Dr. Min-Hao Kuo. He teaches me how to be a scientist and think as an independent PhD student. Without his instruction, I cannot overcome all the difficulties during my experiment and data presenting. I really appreciate his encourage and patience when I was struggling to find the right direaction of my research. Next, I want to thank my committee members, Dr. David L. DeWitt, Dr. Erik Martinez-Hackert, Dr. Heedeok Hong and Dr. Lee R. Kroos. They provide really helpful advices on my thesis work. It's a big challenge for me to make good presentation to them, but I learned a lot and made progress after each committee meeting and talk with them. I am also grateful to my labmates and collaborators. Thank for the support from Christopher Buehl, Witawas Handee, Xiexiong Deng and Stacy Hovde from Kuo lab. And I would like to thank Dexin Sui and Thomas Dexheimer for their help on my thesis project. Last but not least, I want to thank my family for the encouragement that supports my confidence of finishing my PhD degree.

TABLE OF CONTENTS

LIST OF TABLES

LIST OF FIGURES

CHAPTER I

LITERATURE REVIEW

Part I: Alzheimer's disease is a disease of tau

Alzheimer's disease

Alzheimer's disease (AD) is a degenerative brain disease that causes problems with memory, thinking and behavior [1]. AD accounts for more than half of all dementia cases. Currently, 5.7 million Americans of all ages are living with AD in 2018 [2]. This number includes 5.5 million people age 65 and older and approximately 200,000 individuals under an age of 65. The cause of AD is not fully understood, but is believed to be a combined result of genetic predispositions, environmental factors and lifestyle. Increasing age is the greatest risk factor for AD. The prevalence of AD is 10% among people age 65 years and older, and the number reaches 32% among those 85 years and older [2]. Gender is another important AD risk factor: two-thirds of AD patients in the USA are women [3]. AD is the sixth-leading cause of death and the fifth-leading cause of death among those 65 years and older in the United States [2, 4]. There is no cure or prevention.

Biomarkers of AD: Amyloid beta

The two defining biomarkers of AD are the progressive accumulation of amyloid beta (Aβ) plaques outside neurons and the neurofibrillary tangles (NFTs) consisting of hyperphosphorylated tau (p-tau) protein inside neurons [5, 6]. Aβ peptides are proteolytic products of the amyloid precursor protein (APP) which is a single-pass transmembrane protein concentrated in the synapses of neurons [7]. APP is cleaved by the non-amyloidogenic or amyloidogenic pathway (Fig 1.1) [8, 9]. In the non-

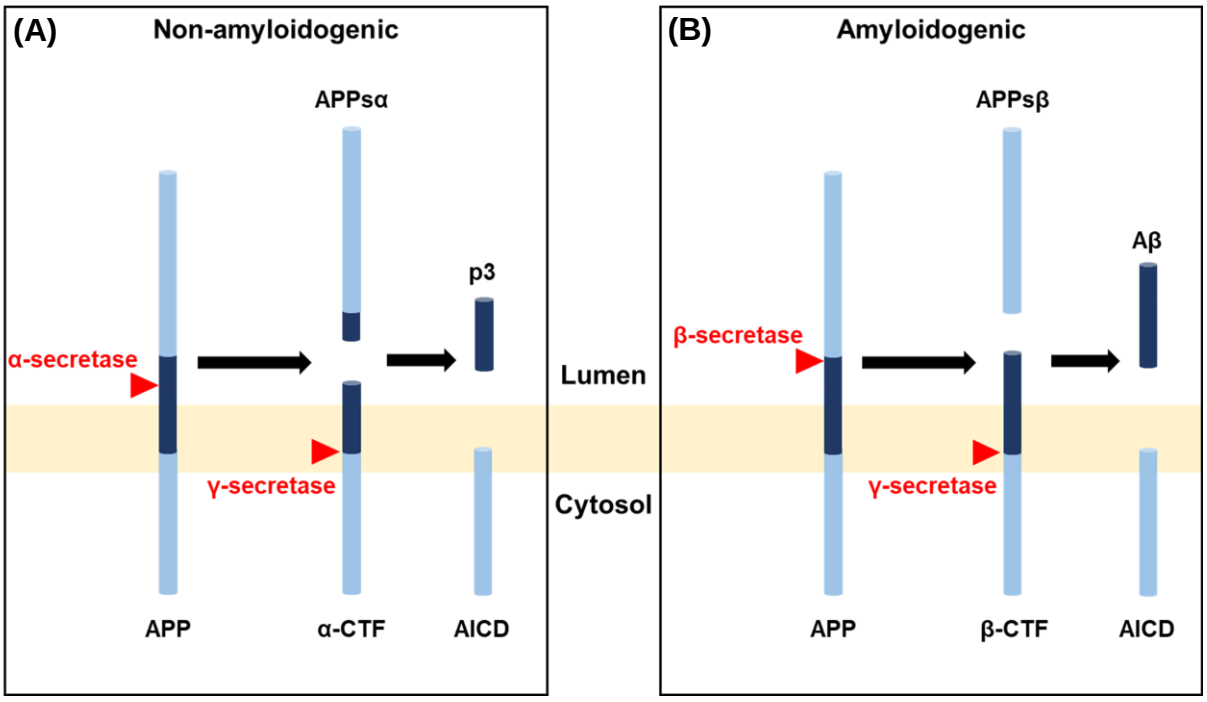

Figure 1.1 Proteolytic pathways of the amyloid precursor protein (APP).

Schematic description of the two APP processing pathways: the non-amyloidogenic pathway (A) and the amyloidogenic pathway (B). APP is first cleaved by either α-secretase or β-secretase to liberate the N-terminal ectodomain (APPsα or APPsβ respectively) and the carboxy-terminal fragment (α-CTF or β-CTF). The α-CTF or β-CTF is then cleaved by the γ-secretase to generate p3 or Aβ and the APP intracellular domain (AICD).

amyloidogenic pathway, APP is first cleaved by the α-secretase to produce an N-terminal ectodomain (APPsα) and a carboxy-terminal fragment (α-CTF). The α-CTF is subsequently cleaved by the γ-secretase to produce a 3 kD peptide (p3) which has no clear biological role [10] and an APP intracellular domain (AICD). In the amyloidogenic pathway, APP is cleaved sequentially by β- and γ- secretases to generate the Aβ peptides which contain 38-43 residues [11]. The Aβ peptides can assembly through a nucleation-dependent polymerization process [12].

The very conspicuous senile plaques of Aβ as well as the ease of detection of Aβ peptides in body fluids [13], Aβ has been regarded as a key pathogenic factor for AD. An amyloid hypothesis posits that Aβ fibril is the primary cause for neurotoxicity and neuron loss [14]. According to this hypothesis, soluble Aβ oligomers impair synaptic functions [14, 15] and induce calcium influx that in turn leads to cell death in neurons and astrocytes [16, 17]. Enormous efforts from different sectors have been committed to Aβ -based AD drug discovery. Twenty-six potential therapeutic agents for AD were tested in Phase III clinical trials in 2018, among which fourteen targeted Aβ [18]. However, every Aβ-centric clinical trial failed to reach the primary outcomes clinically. Even compounds that effectively reduced or even cleared Aβ deposits had no positive effects on cognitive functions [19]. The repetitive failures in Aβ drugs can be explained by the fact that Aβ deposition lacks the correlation with the development of cognitive impairment in AD patients [20], one trait anticipated to be seen with a true pathogenic factor. The prevalence of amyloid pathology is 20-to 30-year earlier than the onset of dementia [21]. Older people may be healthy and show normal cognitive aging even with high levels of Aβ deposition [22, 23]. Together, these findings suggest that Aβ oligomer

is not a direct cause of neurodegeneration, and arouse increased interests in tau-based AD drug discoveries.

Biomarkers of AD: Tau protein

Pathological deposition of hyperphosphorylated tau (p-tau) is shared among a group of neurodegenerative disorders collectively known as tauopathies, including Alzheimer's disease (AD), Pick's disease, frontotemporal dementia with parkinsonism linked to chromosome 17 (FTDP-17), chronic traumatic encephalppathy (CTE), etc. [6]. All tauopathies but AD lack significant Aβ plaques, suggesting a pathogenic role of tau.

Tau is a microtubule-associated protein that locates predominantly in the axons of neurons in the central nervous system [24]. Six tau isoforms are produced by alternative splicing of a single MAPT (microtubule-associated protein tau) transcript [25, Fig 1.2]. The MAPT gene locates on chromosome 17q21 and contains 16 exons [25]. Exons 4A and 6 are maintained in the tau species in the peripheral nervous systems, muscles, pancreas, and other organs, but are spliced out in the CNS [25, 26]. The alternative splicing of exons 2, 3 and 10 gives rise to the six tau isoforms containing different number of insertions at the N-terminus and repeat domains at the C-terminus [26]. K18 is a recombinant peptide that contains only the four microtubule binding repeats. All 6 tau isoforms are expressed in the normal adult human brain with approximately equal amounts of the 3R and 4R isoforms, while the proportion of 1N, 0N, and 2N is 54%, 37% and 9% [27]. Whereas the number of the N domain is generally thought to be less significant, the relative amount of 3R and 4R isoforms may be

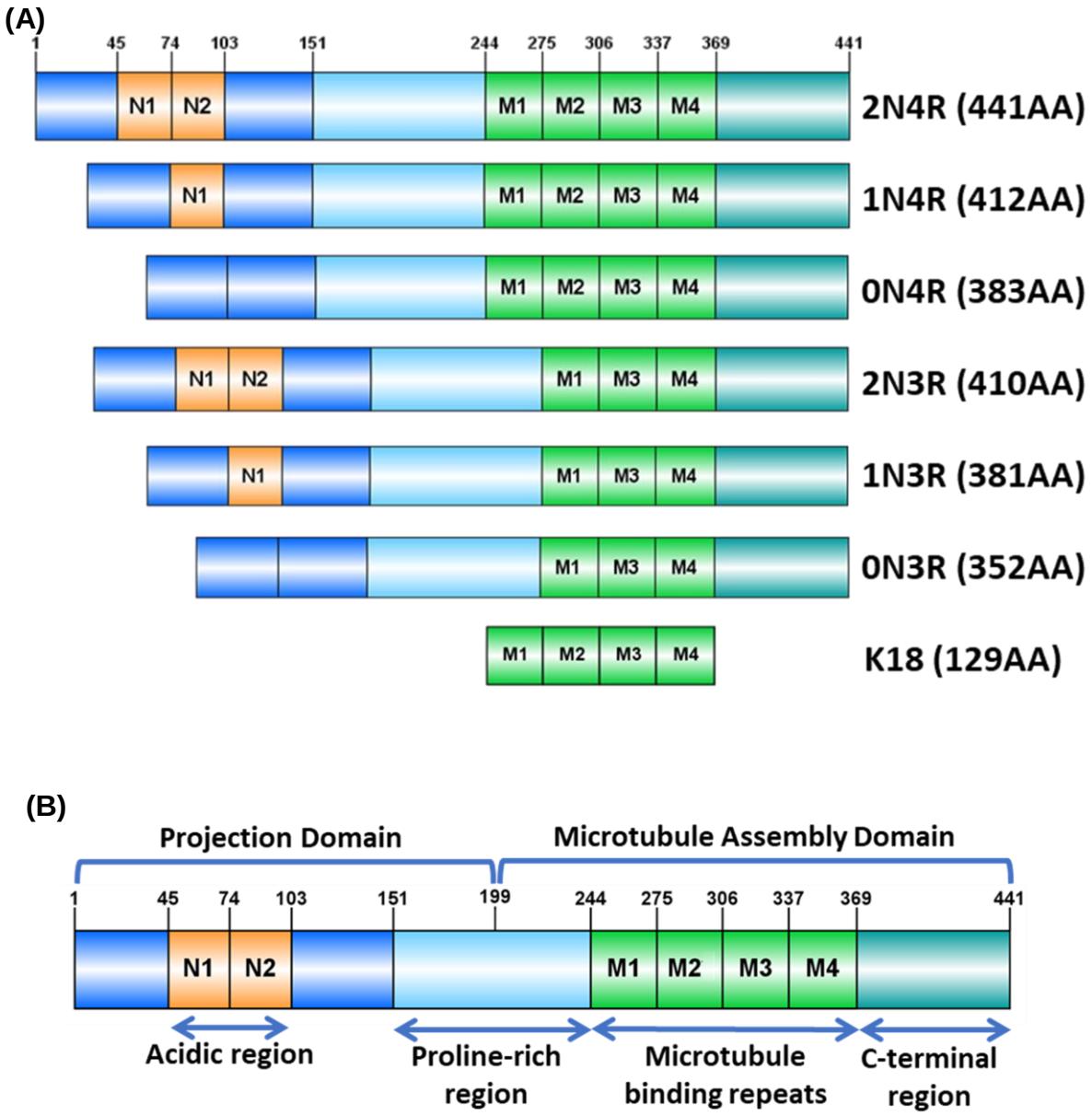

Figure 1.2 Schematic tau isoforms and structure. (A) The six tau isoforms contain different numbers of N-terminal insertions and the repeat-domains. K18 is the construct of the four repeat domains. (B) Tau protein is separated into the projection domain and microtubule assembly domain. The N-terminal of tau is acidic region, followed by a proline-rich region, microtubule binding repeats and C-terminal region.

development- and disease-specific [28]. For example, the normal and AD brains have equal amounts of 3R and 4R [29], but tangles from Pick's disease (PiD), corticobasal degeneration (CBD) and progressive supranuclear palsy (PSP) are composed of either 3R (PiD) or 4R isoforms (CBD and PSP) [30-33].

Tau protein can be roughly separated into the projection domain and the microtubule assembly domain (Fig 1.2B). The projection domain extends from the microtubule surface and interacts with cytoskeletal elements and plasma membrane [34, 35]. The N-terminal insertions are acidic, and are followed by a basic proline-rich region which functions in signal transduction pathways [36, 37]. The microtubule-binding repeats region is positively charged and consists of three (3R) or four (4R) highly conserved 18-amino-acid repeat with less conserved 13- or 14-amino-acid sequences flanking the repeats [27, 38]. The C-terminal region is acidic and is thought to be involved in the regulation of tau polymerization [39] and stability [40].

Tau phosphorylation

In the normal brain, tau protein binds to microtubules and has 2 – 4 phosphates per molecule [41]. In AD, tau protein is about 3 to 4 fold more phosphorylated [41, 42]. Hyperphosphorylation of tau protein reduces its microtubule affinity in vitro [43 – 45], except Thr50, whose phosphorylation promotes microtubule binding [46]. There are 85 potential phosphorylation residues including 45 serine (Ser), 25 threonine (Thr) and 5 tyrosine (Tyr) in the longest CNS tau isoform 2N4R. Twenty-eight phosphorylation sites

have been found specifically in the AD brains, and 10 sites may be phosphorylated in both AD and normal brains [42, 47].

Tau phosphorylation is the consequence of a balance between tau kinase and phosphatase activities. Many kinases have been reported to phosphorylate tau protein in vivo or vitro, and they are grouped into 3 classes: proline-directed serine/threonine-protein kinase (PDPK) including glycogen synthase kinase 3 beta (GSK-3β) and cyclin dependent kinase 5 (Cdk5), the two most potential tau kinase candidates; non-proline-directed serine/threonine-protein kinases such as AMPK; and tyrosine kinases [48]. Among the 42 sites reported to be phosphorylated by GSK-3β, 29 are found in AD tau [49]. GSK-3β co-localizes with NFTs in AD brain [50, 51]. The abundance of the active form of GSK-3β (phosphorylated at Tyr216) is increased in the AD frontal cortex [53] and the activity of active GSK-3β correlates with neurodegeneration in the AD brain [51 - 53]. Overexpression of GSK-3β results in increased tau phosphorylation and neurodegeneration in animal models [54]. Lithium, a GSK-3β inhibitor, can reduce tau phosphorylation at several sites that are phosphorylated in AD, lower tau aggregation level [55], and enhance cognitive performance in both mouse models and clinical studies [56, 57]. Cdk5 binds its co-activator p35 or p25 to phosphorylate tau at 11 sites, all of which are found in AD tau [49]. Activation of Cdk5 by overexpressing the disease-associated cyclin p25 in animal models leads to tau hyperphosphorylation, increased numbers of NFTs and neuronal loss in the brain [58, 59]. Silencing Cdk5 activity reduces tau phosphorylation and the number of NFT number in a mouse model [60]. Cdk5, GSK-3β and tau are found co-localized in rat brain cortex and the phosphorylation of tau at specific sites by Cdk5 facilities the sequential activity of GSK-

3β [61, 62]. At least four kinds of protein phosphatases (PPs) function in the brain to dephosphorylate tau protein: PP1, PP5, PP2B and the major working species PP2A [48]. Reduced PP2A mRNA expression [63] and activity [64] in AD brain have been reported.

Other post-translational modifications of tau

In AD brain, tau is the target of a slew of post-translational modifications (PTM). Except phosphorylation, the biological and pathological significance of these PTMs remains elusive. Acetylation has been proposed to play a role in regulating tau-mediated neurodegeneration. Acetylation at residues Lys174 [65], and Lys280/ Lys281 [66] impairs the interaction between tau and microtubules, promoting tau aggregation and inducing tau pathology in animal models. In addition, acetylation at Lys280 is detected in aggregated tau fibrils from AD and 4R-tau predominant corticobasal degeneration (CBD) brains but not in tau fibrils from 3R-tau predominant Pick's disease brains [67].

O-GlcNAcylation is the attachment of N-acetyl-glucosamine (O-GlcNAc) to the hydroxyl side chain of serine or threonine residues [68]. Because of the mutually exclusive use of the same substrates, O-GlcNAcylation and phosphorylation are thought to be antagonistic of each other. O-GlcNAc transferase (OGT) is the enzyme responsible for adding O-GlcNAc to serine and threonine, while O-GlcNAcase (OGA) removes O-GlcNAc from the protein [69]. Each mole of bovine tau contains 4.2±0.9 mole of O-GlcNAc [70]. Several methods have been used to obtain O-GlcNAcylated tau, including co-expressing tau and OGT in bacteria [71], incubating tau with OGT in vitro

[72] or purifying tau from rat brain [73]. Four O-GlcNAcylation sites have been identified in these tau sources: Thr123 [71], Ser208, Ser238 [72] and Thr400 [71- 73]. Thr123, Ser 208 and Thr 400 are reported phosphorylated sites in AD patients [42], whereas none of these sites is critical in tangle development [74, 75]. O-GlcNAcylation level in tau protein is lower in the cerebellar cortex of AD brains compared to the control brains, while no difference has been detected in the cerebellar cortex, the region that is not affected in AD [76]. The level of O-GlcNAcylation in hyperphosphorylated tau purified from AD brain is only 20% of that in unphosphorylated tau purified from the same brain sample [76]. Expression of OGT [77] and the treatment by the inhibitor of OGA [78] in cultured cells both reduced the phosphorylation level in tau protein. In addition, O-GlcNAcylation inhibits the aggregation of the fourth microtubule-binding repeat of tau [79]. These together suggest that O-GlcNAcylation regulates the level of tau phosphorylation and aggregation in AD.

Nitration [80 - 82], ubiquitylation [83, 84], SUMOylation [85, 86], methylation [87, 88] and prolyl-isomerization [89, 90] are additional post-translational modifications found in tau protein. They influence a small number of residues in tau and more work needs to be done to clarify their function in AD.

Tau aggregation

Neurofibrillary tangles are composed primarily of fibrils of hyperphosphorylated tau (p-tau) [1]. The spatiotemporal distribution of tangles in the brain is different from that of plaques, but correlates well with the progression of cognitive impairments of AD

patients [33, 74]. Braak's staging using a silver stain or later the AT8 antibody recognizing pSer199, pSer202, and pThr205 [91, 92] showed that tau tangles start in the transentorhinal region that functions as the transition between the hippocampus and the neocortex (Stage I), then spreads through the entorhinal region (Stage II), hippocampus (Stage III), superior temporal neocortex (Stage IV), and the entire neocortex (Stages V and VI). This progression pattern coincides with the development of cognitive dysfunction of AD – from short-term and working memory loss to much more severe cognitive symptoms and behavioral changes resulting from neocortex pathology [74, 93-95].

A model for tangle formation is shown in Fig 1.3 [96]. Tau monomer is an intrinsically disordered protein [97] that adopts a random coiled conformation lacking apparent secondary structures [98]. Incubation of 10 μM of recombinant tau monomers with an inducer generates granular tau oligomers (GTOs), which contain 40 ± 3 tau molecules [99]. GTOs can be detected in early and mid- Braak stages in the frontal cortex of human brains [100]. Another fibrillization pathway includes stable dimers and small soluble oligomers as intermediates. Stabilization of partially folded tau monomers via phosphorylation [101] or inducers [102], manifested by increased levels of β-sheet structure, triggers the formation of dimers. A local hexapeptide sequence (^{306}VQIVYK^{311}) in the core region (Fig 1.2, M1-M4) is required for dimerization [103]. Both granular tau oligomers and small soluble oligomers can form paired helical filaments (PHFs), which is the major component of NFTs found in neuronal soma [104].

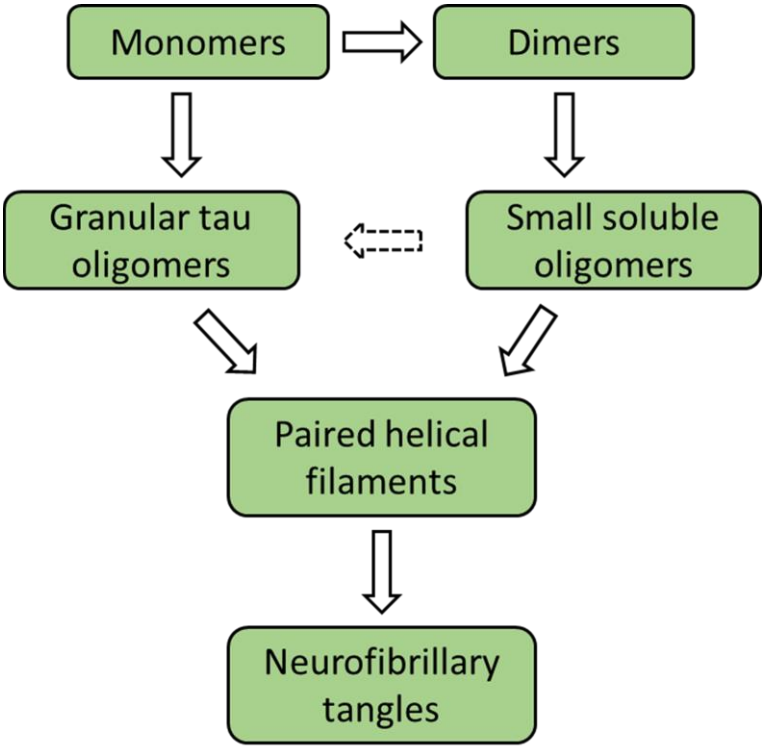

Figure 1.3 Neurofibrillary tangles formation pathway. Tau monomers can polymerize into paired helical filaments via granular tau oligomers or through dimers and small soluble oligomers. The paired helical filaments then assemble into neurofibrillary tangels.

The tau aggregation process is thought to be modulated by post-translational modifications in the brain, and the effect of phosphorylation is the best-understood. Tau hyperphosphorylation reduces affinity for microtubule, thus increases the amount of detached p-tau that can be candidates for building tau fibrils. In addition, multiple lines of evidence support that hyperphosphorylation is critical during the formation of tau tangles. Phosphorylated tau which contains 3 phosphates per molecule via in vitro incubation with GSK-3β, can form tangle-like filaments in the presence of an inducer [105]. Changing the kinase source to a rat brain crude extract increases the number of incorporated phosphate per molecule to 10, and the resulted highly phosphorylated tau can aggregate without an inducer [106]. Phosphorylated tau purified from AD brains undergoes self-assembly in vitro in the absence of an inducer, and this process can be blocked by dephosphorylation [106]. Accumulation of tau aggregates are detected in mouse models overexpressing GSK-3β [54] or CDK5/p25 [59], or wild-type mice after phosphatase 2A inhibitor okadaic acid injection [107]. Kinase inhibitors treatment in mouse models leads to reduced levels of tau phosphorylation and tau aggregates [55, 108]. Taken together, these reports support the notion that dysregulated phosphorylation causes tau to be prone to aggregate, and consequently to form NFTs in AD and other tauopathies.

Tau-mediated neurodegeneration

Substantial evidence supports that tau tangle is the underlying cause for neuron loss and dementia-related neurodegeneration. The spatiotemporal distribution of tau tangles, not Aβ plaques, correlates with the progression of cognitive impairments of AD

patients [33, 74]. Tau pathology is shared by about 15 neurodegenerative tauopathies that, except AD, are without apparent Aβ-related pathology [6]. In addition, mutations in the MAPT gene causing missense or deletion in tau, or even changes in the splicing of exon 10 lead to a tauopathy, FTDP-17 [109, 110]. These findings manifest the likely direct role of tau dysregulation in neurodegeneration.

The mechanism of tau-induced neurodegeneration is likely a gain-of-function cytotoxic defect. From 1994 to 2007, tau knock-out mice have been developed in four different labs and none of them showed an overt phenotype [111], indicating functional redundancy between tau and another protein(s). For its well-documented in vitro microtubule-binding activity, tau is postulated to be involved in microtubule polymerization [112, 113] and axonal transport [114]. Although tau primarily locates in axons, it's also present at both presynaptic and postsynaptic terminals [115]. Tau is therefore suggested to be involved in modulating neuronal excitability, signaling of synaptic neurotransmitter-receptors and synaptic mitochondrial function [116, 117].

The AD pathology is probably more than a simple "unbearable-weight-of-tangles" hypothesis [118, 119]. Accumulating evidence instead shows that smaller, fibrillization intermediates are the more damning species than the large fibrils. As a hallmark of AD, the density of NFTs correlates with the severity of dementia assessed by the degree of cognitive impairment [120, 121]. However, the number of neurons lost in AD brain exceeds the number of NFTs by more than sevenfold [122]. Intraneuronal NFTs fail to disrupt synaptic or neuronal function in vivo [123, 124]. Suppressing transgenic tau expression restores the neuron numbers and memory function, even though NFTs level continues to increase [125]. Neurodegeneration can be induced by tau overexpression

in a Drosophila model without forming large tau filaments [126]. These reports imply that NFTs do not necessarily cause neuronal loss and synaptic deficit.

Instead, the pre-tangle oligomers of abnormally phosphorylated tau are the likely toxic species causing neurondegeneration. Tau oligomers impair SH-SY5Y neuroblastoma cells viability more effectively than monomer or fibrils [127]. Transgenic mice expressing the wildtype human tau shows no tau fibrils formation or overt neurondegeneration phenotype [128]. To study tau pathology, transgenic mice expressing human tau containing a FTDP-17 mutation, P301L has been developed [129]. The P301L mice develop NFT-like inclusions, neuronal loss and neurodegeneration symptoms [129, 130]. However, synapse loss and memory deficit correlate with the level of tau oligomers rather than NFTs in this mouse model [131, 132]. Moreover, injection of tau oligomers prepared by the “the seeded conversion and amplification” method (an approach to propagating prion-like toxic proteins) or that purified from AD brain can induce cognitive impairment and synaptic dysfunction in mouse models [133, 134]. Together, the hypothesis of cytotoxic aggregation intermediates gains momentum [135] and affords a mechanistic basis for therapeutics development.

Prion-like characters of tau

The observation of induced neurodegeneration after injection of tau oligomers in animal models indicates that tau propagates in a prion-like mechanism, which is supported by works done with cultured cells or animals [136]. Endogenously produced tau can transfer from donor cells (expressing tau) to recipient cells (no tau expression)

via direct contacts or the extracellular media in cultured neurons, and the internalized tau can propagate to neighboring cells [137]. Tau aggregates are transferred more efficiently from medium to cytoplasma than monomers [136, 137]. Injection of brain extract from a P301S-tau-expressing line [138] or brain homogenates from human tauopathies [139] into the brain of mice expressing wild-type tau result in the formation of filaments consisting of wild-type tau and the spreading of filaments from injection site to connected brain regions.

The mechanism of transcellular tau propagation in the human brain is not clear. Several pathways have been proposed, including intercellular spreading through tunneling nanotubes (TNTs), via extracellular space or synapses [140]. TNTs are filamentous actin-containing channels bridging cells [141]. In cultured primary neurons, extracellular tau can activate TNTs formation, after that the internalized tau fibrils are transported from cell to cell within TNTs [142, 143]. Besides TNTs, tau may propagate through extracellular space. Although the majority of tau is located in the cytoplasm of neurons, it's also found in cerebrospinal fluid [144] and interstitial fluid [145]. Moreover, accumulating evidence supports that the cellular release of tau is independent of neuron toxicity or cell death [146, 147]. Tau secretion from healthy cells into extracellular space is a physiological process, and is regulated by neuronal activity [148, 149]. The exact mechanism of tau internalization is unknown, but it's supposed to happen via fluid-phase endocytosis [150, 151] and adsorptive endocytosis [152]. Tau has also been reported to spread through a trans-synaptic mechanism [153]. Tau pathology in mouse models can propagate from the entorhinal cortex into synaptically connected brain regions [154, 155]. Synaptic fractions purified from early AD stages present a stronger

tau seeding activity than cytoplasmic fractions, as assessed by their ability to recruit and misfold monomeric tau [156]. Synaptic contacts can increase the tau pathology propagation [157] or be required in exosome-mediated tau transmission [158]. In conclusion, tau propagates in cultured cells or the brain of mouse models via a prion-like mechanism, which may underlie the spreading pathway in AD brain.

Part II: Drug discovery for AD

FDA-approved drugs for AD

Only five prescription drugs are approved by the U.S. Food and Drug Administration (FDA) to treat AD symptoms: donepezil was approved to treat all AD stages, galantamine and rivastigmine for mild to moderate stages, memantine and a combination of donepezil with memantine for moderate to severe stages [159]. They are used to lessen AD symptoms including memory loss and confusion, but insufficient to cure or prevent the progression of the disease. Donepezil, galantamine and rivastigmine are cholinesterase inhibitors, a class of drugs used to stop or inhibit the acetylcholinesterase enzyme from breaking down acetylcholine [160]. Acetylcholine is a neurotransmitter involved in mental processes including memory and cognition, and its dysfunction is related to memory disturbances [161]. Cholinesterase inhibitors are developed to maintain acetylcholine level in brain neurons and have shown positive effects on improving cognitive function [162]. Memantine is a blocker of N-methyl-D-aspartate (NMDA) receptor. NMDA receptors are activated by glutamate to allow positively charged ions to flow into nerve cells [163]. Thus, memantine can protect cells from being overstimulated by excess glutamate. Memantine treatment has been shown to benefit mental functioning and behavioural symptoms in severely demented patients [164].

Amyloid beta-centric therapies

The amyloid cascade hypothesis has been (perhaps wrongfully) dominating the AD pharmaceutical development in the past 25 years. It contends that the deposition of Aβ peptide is the primary cause of AD [165]. Thus, reducing Aβ production, preventing Aβ aggregation, increasing clearance of Aβ or amyloid plaques should have potential therapeutic benefits for the disease. APP is cleaved sequentially by β- and γ-secretases to produce Aβ in the amyloidogenic pathway [8, Fig 1.1]. β- and γ-secretase inhibitors and α-secretase activators have been developed to modulate the level of Aβ. Antiaggregate compounds, metal complexing agents [166] and molecular chaperones [167] have been reported to inhibit the Aβ aggregation in vitro and in animal models. Amyloid fibrils are quite stable and resistant to disaggregating conditions including heat and SDS [168, 169]. Enhancement of Aβ removal has been successful in a mouse model by active immunization in 1999 [170]. Since then, several active and passive vaccines have been developed and tested in clinical trials [171].

Even though Aβ peptides and aggregates have been the subjects of intensive research, none of the Aβ-targeted phase III clinical trials shows benefit in AD patients [18]. Only one recombinant monoclonal antibody, aducanumab which binds to both insoluble amyloid plaques and soluble Aβ, was reported to reduce the level of Aβ aggregates and to slow down the cognitive decline in preclinical or mild AD patients in phase I trial [172]. Two phase III trials were launched to confirm the result [173]. However, far ahead of the originally planned completion date of April 2022, Biogen and Eisai announced on March 12th 2019, that their phase III trials of aducanumab would be terminated immediately [174]. One of the most cited explanations for the failures of Aβ-

centric trials is that the drug is given too late when people start to show symptoms of AD. Prevalence of amyloid pathology assessed by positron emission tomography scanning or biomarkers in cerebrospinal fluid suggests that amyloid plaque may appear 20 to 30 years before the appearance of cognition symptoms [19]. The failures of all plaque-centric clinical trials imply that Aβ is not the proper target for AD therapeutic development, and the Aβ hypothesis should be laid to rest.

Tangle-centric therapies

Tau post-modification modulators

Hyperphosphorylation causes tau to aggregate into oligomers, which are thought to be a transmissible toxic species. The strong correlation between tau hyperphosphorylation and the brain pathology indicates that reducing tau phosphorylation via kinase inhibitors or phosphatases activators is a potential therapeutic strategy for AD. A well-known GSK-3β inhibitor, lithium has shown protection effect on spatial memory deficits via reducing tau hyperphosphorylation and level of insoluble tau in a rat model [56]. However, lithium's clinical effect on patients with AD or mild cognitive impairment was inconclusive [57, 175, 176]. An orally available drug, ANAVEX®2-73, which blocks tau phosphorylation at Ser202, Thr205 significantly in a mouse model [177], is now under phase IIb trial to assess its influence on cognitive and functional efficacy on early AD patients [178]. Since GSK-3β has a wide range of substrates in multiple signaling pathways, one challenge for applying kinase inhibitor on AD is to control the decline of enzyme activity to less than 25% of

total activity, in order to avoid toxic effects [179]. Another tau kinase inhibitor saracatinib (AZD0530) is under a phase IIa trial to assess its safety in mild AD patients, and the benefits on cognitive and behavioral function [180]. Saracatinib is a highly selective inhibitor for Src family kinases [181] including Fyn which can phosphorylate tau in the N-terminal domain [182]. Saracatinib treatment can reverse memory loss and rescue synapse intensity in tau transgenic mice [183]. Similar to kinase inhibitors, developing phosphatase activators also face the problem of specificity and side-effects since they have a broad range of substrates [184]. Sodium selenate, a protein phosphatase 2A (PP2A) activator, is able to reduce tau phosphorylation level in cultured cells and animal models via stabilizing PP2A-tau complex [185]. Sodium selenite treatment inhibits tau filaments formation and improves memory and motor performance in tau transgenic mice [186], and also shows benefit in epileptogenesis [187] and traumatic brain injury rat models [188]. In addition to phosphorylation, candidates that modulate acetylation and glycosylation are also under investigation for potential AD therapies [65, 189].

Microtubule stabilizers

Hyperphosphorylated tau losses its microtubule-binding and stabilizing ability in vitro, which was postulated to impair axonal transport and synapse function [114, 115-117]. Therefore, microtubule stabilizers are developed to rescue the presumptive loss-of-function defects resulting from tau hyperphosphorylation. One microtubule stabilizer, davunetide promotes cognitive function in a mouse model [190] and rescues neuronal dysfunction in a Drosophila model [191]. However, davunetide fails to improve cognition performance in patients with mild cognitive impairments [192] or treat progressive

supranuclear palsy in a randomized, double-blind, placebo-controlled trial [193]. Side effects and neurotoxicity caused by microtubule stabilizer including epothilone D [194] and paclitaxel [195] are concerns as well. A possible explanation is that overstabilization of dendritic microtubules causes dendritic simplification [196] and those microtubule stabilizers may influence microtubule dynamicity in other cells types like microglia [197]. Therefore, therapeutic strategy using microtubule stabilizer should be more does- and compartment-specific to avoid side effects.

Tau aggregation inhibitors (TAIs)

Inhibition of tau aggregation is increasingly drawing attention for AD therapy development due to the strong correlation between tau pathology and cognition impairment, as well as the string of failures in other drug discovery endeavors. Both covalent tau aggregation inhibitor (TAI) and non-covalent TAI have been identified through cell-based and/or in vitro aggregation assays [198]. These TAIs include aminothienopyridazines [199, 200], phenothiazines [201], polyphenols [202], porphyrins [202], anthraquinones [203], N-phenylamines [204], phenylthiazole-hydrazides [205], cyanine [206] and rhodanines [207]. None of these TAIs progress to clinical trials for reasons detailed below.

Methylene blue (methylthioninium chloride, MTC) and its stable reduced form leuco-methylthioninium bis(hydromethanesulphonate) (LMTM) are the most studied TAIs and have entered a phase III clinical trial [18]. Methylene blue has been used as medication to treat malaria and methemoglobinemia since 1891 [208]. In 1996,

methylene blue was first shown to prevent the tau-tau interaction in a dose-dependent manner [201]. Methylene blue treatment in tau transgenic mice reduced the immunoreactivity of AT8 (pSer202/pThr205) and AT180 (pThr231/pSer235) [209, 210], and rescued cognitive impairment in tau transgenic mice [211]. Methylene blue exhibited benefit in mild or moderate AD on a phase II study [212], but was criticized for its side effects [213] and failure to show a dose response [214]. Later, the phase III trial of LMTM was deemed ineffective [215]. Methylene blue turned out to be a non-specific redox modulator that inhibits tau aggregation via oxidation of the two cysteines, Cys 291 and Cys 322 [200]. Similarly, other TAIs such as aminotheienopyridazines [200], cinnamaldehyde and epicatechin [234] fall in the same category of non-selective redox modulator [235], casting doubts on the use of unmodified tau aggregation as the primary screening target. Therefore, future tangle-based drug screen has to be conducted in a system that is free of the interference of tau redox modulators.

Anti-tau immunotherapy

Anti-tau immunotherapy is a promising approach to clearing tau aggregates by targeting hyperphosphorylated or specific conformations of tau with tau vaccines [216]. Both active [217, 218] and passive immunization [219] exhibit reduced level of tau aggregates and improved cognitive function in mouse models. The development of tau-target immunotherapy is at early stage, with only two active immunization vaccines, AADvac-1 containing tau294-305 and ACI-35 containing tau393-408 [pSer396, pSer404] under investigation in clinical trials [18, 216]. AADvac-1 has shown a good safety profile and immunogenicity in a 24-week phase I trial [220] and a subsequent 72-week study in

mild-moderate AD patients [221]. The observation of the 19 patients who finished the cognition assessment indicates a benefit of this vaccine [221], however the result needs to be confirmed by study with a larger number of participants. The safety and immune response of ACI-35 have been studied in animal model [222], and it's now tested under phase I clinical trial [18].

Therapeutic strategy targeting inflammation

Recent results also suggest that inflammation in the brain is related to AD pathogenesis. Neuroinflammation characterized by reactive astrocytes in the vicinity of amyloid plaques [223] and reactive microglia [224] are detected in post-mortem AD brains. The level of Alpha 1-antichymotrypsin (ACT), an acute phase serum glycoprotein is up-regulated by activated astrocytes, which further induces tau phosphorylation [225] and amyloid plaque deposition [226, 227]. Activated microglia induced by lipopolysaccharide also can stimulate the amyloid plaque deposition in a mouse model [228]. Multiple reports suggest that long-term usage of non-steroidal anti-inflammatory drugs (NSAIDs) benefits cognition or AD severity [229, 230]. Several NSAIDs have been assessed in phase III clinical trials but again failed to improve the cognitive performance in AD patients [231], probably due to the adverse effects of NSAIDs at late AD stages [232], and that neuroinflammation may be a comorbidity, rather than a direct cause of neurodegeneration.

Part III: Research interests and significance

Alzheimer's disease is the most common form of dementia, which accounts for 60 to 80 percent of the total cases [2]. There is no cure or prevention for AD, making it the only one of the top-ten causes of death to be without an effective treatment [2, 4]. Only five prescription drugs are approved by the FDA to lessen AD symptoms and to improve the quality of life, but their efficacy declines eventually as the brain damage progresses [159]. Aβ has been the main focus of AD drug development, due to its specificity for AD and the influence of the amyloid cascade hypothesis for the past 25 years [165]. Tangles consisting of hyperphosphorylated tau have become an increasingly important target for AD drug discovery, due to their strong correlation with the progression of cognition impairment in the AD brain, and to a large body of in vitro and animal studies [74]. Current tangle-centric drug discovery attempts use unphosphorylated tau (full-length or the K18 core fragment), and is typically done with an aggregation inducer such as heparin [199, 202]. The pathophysiological relevance of heparin remains to be substantiated. Many hits from these prior screens turned out to be non-selective redox modulators with limited therapeutic values [200]. As such, practically no tau aggregation inhibitors have progressed to clinical trials. To overcome this hurdle, our lab developed the PIMAX system (Protein Interaction Modules-Assisted function X) that produces recombinant hyperphosphorylated tau (p-tau) [233]. My thesis work aims to develop and use a high-throughput screening platform featuring p-tau aggregation to identify compounds that control formation of tangles. These p-tau aggregation inhibitors (PTAIs) and enhancers (PTAEs) are candidates for AD therapeutics and risk factors, respectively. Results presented in the following chapters

as well as their follow-up research have a great potential for breaking the stagnant status of AD drug development.

REFERENCES

REFERENCES

1. Goedert M, Spillantini MG. 2006. A century of Alzheimer's disease. Science. 314(5800):777-81.

2. Alzheimer's Association, 2018. Alzheimer's disease facts and figures. Alzheimers Dement. 14(3):367-429.

3. Christian J. Pike, 2017. Sex and the development of Alzheimer’s disease. J Neurosci Res. 95(1-2): 671–680.

4. James BD, Leurgans SE, Hebert LE, Scherr PA, Yaffe K, Bennett DA. 2014. Contribution of Alzheimer disease to mortality in the United States. Neurology. 82(12):1045-50.

5. Blennow K, Zetterberg H. 2018. Biomarkers for Alzheimer disease - current status and prospects for the future. J Intern Med. 284(6):643-663.

6. Arendt T, Stieler JT, Holzer M. 2016. Tau and tauopathies. Brain Res Bull. 126(Pt 3):238-292.

7. O'Brien RJ, Wong PC. 2011. Amyloid Precursor Protein Processing and Alzheimer’s Disease. Annu Rev Neurosci. 34:185-204.

8. Haass C, Kaether C, Thinakaran G, Sisodia S. 2012. Trafficking and proteolytic processing of APP. Cold Spring Harb Perspect Med. 2(5):a006270.

9. Thinakaran G1, Koo EH. 2008. Amyloid precursor protein trafficking, processing, and function. J Biol Chem. 283(44):29615-9.

10. Chow VW, Mattson MP, Wong PC, Gleichmann M. 2010. An overview of APP processing enzymes and products. Neuromolecular Med. 12(1):1-12.

11. Sadigh-Eteghad S, Sabermarouf B, Majdi A, Talebi M, Farhoudi M, Mahmoudi J. 2015. Amyloid-beta: a crucial factor in Alzheimer’s disease. Med Princ Pract. 24(1):1-10.

12. Roychaudhuri R, Yang M, Hoshi MM, Teplow DB. 2009. Amyloid beta-protein assembly and Alzheimer disease. J Biol Chem. 284(8):4749-53.

13. M. Paul Murphy and Harry LeVine, III. 2010. Alzheimer’s Disease and the β-Amyloid Peptide. J Alzheimers Dis. 19(1): 311.

14. Yankner BA, Lu T. 2009. Amyloid beta-protein toxicity and the pathogenesis of

Alzheimer disease. J Biol Chem. 284(8):4755-9.

15. Shankar GM, Li S, Mehta TH, Garcia-Munoz A, Shepardson NE, Smith I, Brett FM, Farrell MA, Rowan MJ, Lemere CA, Regan CM, Walsh DM, Sabatini BL, Selkoe DJ. 2008. Amyloid-beta protein dimers isolated directly from Alzheimer's brains impair synaptic plasticity and memory. Nat Med. 14(8):837-42.

16. Ekinci FJ, Linsley MD, Shea TB. 2000. Beta-amyloid-induced calcium influx induces apoptosis in culture by oxidative stress rather than tau phosphorylation. Brain Res Mol Brain Res. 76(2):389-95.

17. Abramov AY, Canevari L, Duchen MR. 2004. Calcium signals induced by amyloid beta peptide and their consequences in neurons and astrocytes in culture. Biochim Biophys Acta. 1742(1-3):81-7.

18. Cummings J, Lee G, Ritter A, Zhong K. 2018. Alzheimer's disease drug development pipeline: 2018. Alzheimers Dement (N Y). 4:195-214.

19. Castello MA, Soriano S. 2014. On the origin of Alzheimer's disease. Trials and tribulations of the amyloid hypothesis. Ageing Res Rev. 13:10-2.

20. Giacobini E, Gold G. 2013. Alzheimer disease therapy--moving from amyloid-β to tau. Nat Rev Neurol. 9(12):677-86.

21. Willemijn J. Jansen, Rik Ossenkoppele, Dirk L. Knol, Betty M. Tijms, Philip Scheltens, Frans R. J. Verhey, Pieter Jelle Visser, and the Amyloid Biomarker Study Group. 2015. Prevalence of cerebral amyloid pathology in persons without dementia: a meta-analysis. JAMA. (19):1924-38.

22. Jenalle E. Baker, Yen Ying Lim, Robert H. Pietrzak, Jason Hassenstab, Peter J. Snyder, Colin L. Masters and Paul Maruff. 2016. Cognitive impairment and decline in cognitively normal older adults with high amyloid-β: A meta-analysis. Alzheimers Dement (Amst). 6: 108–121.

23. Aizenstein HJ, Nebes RD, Saxton JA, Price JC, Mathis CA, Tsopelas ND, Ziolko SK, James JA, Snitz BE, Houck PR, Bi W, Cohen AD, Lopresti BJ, DeKosky ST, Halligan EM, Klunk WE. 2008. Frequent amyloid deposition without significant cognitive impairment among the elderly. Arch Neurol. 65(11):1509-17.

24. Buée L, Bussière T, Buée-Scherrer V, Delacourte A, Hof PR. 2000. Tau protein isoforms, phosphorylation and role in neurodegenerative disorders. Brain Res Brain Res Rev. 33(1):95-130.

25. Neve RL, Harris P, Kosik KS, Kurnit DM, Donlon TA. 1986. Identification of cDNA clones for the human microtubule-associated protein tau and chromosomal localization of the genes for tau and microtubule-associated protein 2. Brain Res. 387(3):271-80.

26. D'Souza I, Schellenberg GD. 2005. Regulation of tau isoform expression and dementia. Biochim Biophys Acta. 1739(2-3):104-15.

27. Goedert M, Jakes R. 1990.
Expression of separate isoforms of human tau protein: correlation with
the tau pattern in brainand effects on tubulin polymerization. EMBO J. 9(13):4225-30.

28. Jovanov-Milošević N, Petrović D, Sedmak G, Vukšić M, Hof PR, Simić G. 2012. Human fetal tau protein isoform: possibilities for Alzheimer's disease treatment. Int J Biochem Cell Biol. 44(8):1290-4.

29. Goedert M, Spillantini MG, Jakes R, Rutherford D, Crowther RA. 1989. Multiple isoforms of human microtubule-associated protein tau: sequences and localization in neurofibrillary tangles of Alzheimer's disease. Neuron. 3(4):519-26.

30. Buée L, Delacourte A. 1999. Comparative biochemistry of tau in progressive supranuclear palsy, corticobasal degeneration, FTDP-17 and Pick's disease. Brain Pathol. 9(4):681-93.

31. Ksiezak-Reding H, Morgan K, Mattiace LA, Davies P, Liu WK, Yen SH, Weidenheim K, Dickson DW. 1994. Ultrastructure and biochemical composition of paired helical filaments in corticobasal degeneration. Am J Pathol. 145(6):1496-508.

32. Flament S, Delacourte A, Verny M, Hauw JJ, Javoy-Agid F. 1991. Abnormal Tau proteins in progressive supranuclear palsy. Similarities and differences with the neurofibrillary degeneration of the Alzheimer type. Acta Neuropathol. 81(6):591-6.

33. Delacourte A, David JP, Sergeant N, Buée L, Wattez A, Vermersch P, Ghozali F, Fallet-Bianco C, Pasquier F, Lebert F, Petit H, Di Menza C. 1999. The biochemical pathway of neurofibrillary degeneration in aging and Alzheimer's disease. Neurology. 52(6):1158-65.

34. Hirokawa N, Shiomura Y, Okabe S. 1988. Tau proteins: the molecular structure and mode of binding on microtubules.

35. Maas T, Eidenmüller J, Brandt R. 2000. Interaction of tau with the neural membrane cortex is regulated by phosphorylation at sites that are modified in paired helical filaments. J Biol Chem. 275(21):15733-40.

36. Hwang SC, Jhon DY, Bae YS, Kim JH, Rhee SG. 1996. Activation of phospholipase C-gamma by the concerted action of tau proteins and arachidonic acid. J Biol Chem. 271(31):18342-9.

37. Lee G, Newman ST, Gard DL, Band H, Panchamoorthy G. 1998. Tau interacts with src-family non-receptor tyrosine kinases. J Cell Sci. 111 (Pt 21):3167-77.

38. Butner KA, Kirschner MW. 1991. Tau protein binds to microtubules through a flexible array of distributed weak sites. J Cell Biol. 115(3):717-30.

39. Berry RW, Abraha A, Lagalwar S, LaPointe N, Gamblin TC, Cryns VL, Binder LI. 2003. Inhibition of tau polymerization by its carboxy-terminal caspase cleavage fragment. Biochemistry. 42(27):8325-31.

40. Geng J, Xia L, Li W, Dou F. 2015. The C-terminus of tau protein plays an important role in its stability and toxicity. J Mol Neurosci. 55(1):251-259.

41. Khatoon S, Grundke-Iqbal I, Iqbal K. 1994. Levels of normal and abnormally phosphorylated tau in different cellular and regional compartments of Alzheimer disease and control brains. FEBS Lett. 351(1):80-4.

42. Köpke E, Tung YC, Shaikh S, Alonso AC, Iqbal K, Grundke-Iqbal I. 1993. Microtubule-associated protein tau. Abnormal phosphorylation of a non-paired helical filament pool in Alzheimer disease. J Biol Chem. 268(32):24374-84.

43. Drechsel DN, Hyman AA, Cobb MH, Kirschner MW. 1992. Modulation of the dynamic instability of tubulin assembly by the microtubule-associated protein tau. Mol Biol Cell. 3(10):1141-54.

44. Biernat J, Gustke N, Drewes G, Mandelkow EM, Mandelkow E. 1993. Phosphorylation of Ser262 strongly reduces binding of tau to microtubules: distinction between PHF-like immunoreactivity and microtubule binding. Neuron. 11(1):153-63.

45. Bramblett GT, Goedert M, Jakes R, Merrick SE, Trojanowski JQ, Lee VM. 1993. Abnormal tau phosphorylation at Ser396 in Alzheimer's disease recapitulates development and contributes to reduced microtubule binding. Neuron. 10(6):1089-99.

46. Feijoo C, Campbell DG, Jakes R, Goedert M, Cuenda A. 2005. Evidence that phosphorylation of the microtubule-associated protein Tau by SAPK4/p38delta at Thr50 promotes microtubule assembly. J Cell Sci. 118(Pt 2):397-408.

47. Tapia-Rojas C, Cabezas-Opazo F, Deaton CA, Vergara EH, Johnson GVW, Quintanilla R. 2018. It's all about tau. Prog Neurobiol. pii: S0301-0082(17)30237-X.

48. Mietelska-Porowska A, Wasik U, Goras M, Filipek A, Niewiadomska G. 2014. Tau protein modifications and interactions: their role in function and dysfunction. Int J Mol Sci. 15(3):4671-713.

49. Hanger DP, Anderton BH, Noble W. 2009. Tau phosphorylation: the therapeutic challenge for neurodegenerative disease. Trends Mol Med. 15(3):112-9.

50. Yamaguchi H, Ishiguro K, Uchida T, Takashima A, Lemere CA, Imahori K.1996. Preferential labeling of Alzheimer neurofibrillary tangles with antisera for tau protein

kinase (TPK) I/glycogen synthase kinase-3 beta and cyclin-dependent kinase 5, a component of TPK II. Acta Neuropathol. 92(3):232-41.

51. Pei JJ, Tanaka T, Tung YC, Braak E, Iqbal K, Grundke-Iqbal I. 1997. Distribution, levels, and activity of glycogen synthase kinase-3 in the Alzheimer disease brain. J Neuropathol Exp Neurol. 56(1):70-8.

52. Leroy K, Yilmaz Z, Brion JP. 2007. Increased level of active GSK-3beta in Alzheimer's disease and accumulation in argyrophilic grains and in neurones at different stages of neurofibrillary degeneration. Neuropathol Appl Neurobiol. 33(1):43-55.

53. Leroy K, Boutajangout A, Authelet M, Woodgett JR, Anderton BH, Brion JP. 2002. The active form of glycogen synthase kinase-3beta is associated with granulovacuolar degeneration in neurons in Alzheimer's disease. Acta Neuropathol. 103(2):91-9.

54. Lucas JJ, Hernández F, Gómez-Ramos P, Morán MA, Hen R, Avila J. 2001. Decreased nuclear beta-catenin, tau hyperphosphorylation and neurodegeneration in GSK-3beta conditional transgenic mice. EMBO J. 20(1-2):27-39.

55. Noble W, Planel E, Zehr C, Olm V, Meyerson J, Suleman F, Gaynor K, Wang L, LaFrancois J, Feinstein B, Burns M, Krishnamurthy P, Wen Y, Bhat R, Lewis J, Dickson D, Duff K. 2005. Inhibition of glycogen synthase kinase-3 by lithium correlates with reduced tauopathy and degeneration in vivo. Proc Natl Acad Sci U S A. 102(19):6990-5.

56. Tan WF, Cao XZ, Wang JK, Lv HW, Wu BY, Ma H. 2010. Protective effects of lithium treatment for spatial memory deficits induced by tau hyperphosphorylation in splenectomized rats. Clin Exp Pharmacol Physiol. 37(10):1010-5.

57. Matsunagg S, Kishi T, Annas P, Basun H, Hampel H, Iwata N. Lithium as a Treatment for Alzheimer’s Disease: A Systematic Review and Meta-Analysis. J Alzheimers Dis. 48(2):403-10.

58. Noble W, Olm V, Takata K, Casey E, Mary O, Meyerson J, Gaynor K, LaFrancois J, Wang L, Kondo T, Davies P, Burns M, Veeranna, Nixon R, Dickson D, Matsuoka Y, Ahlijanian M, Lau LF, Duff K. 2003. Cdk5 is a key factor in tau aggregation and tangle formation in vivo. Neuron. 38(4):555-65.

59. Cruz JC, Tseng HC, Goldman JA, Shih H, Tsai LH. 2003. Aberrant Cdk5 activation by p25 triggers pathological events leading to neurodegeneration and neurofibrillary tangles. Neuron. 40(3):471-83.

60. Piedrahita D, Hernández I, López-Tobón A, Fedorov D, Obara B, Manjunath BS, Boudreau RL, Davidson B, Laferla F, Gallego-Gómez JC, Kosik KS, Cardona-Gómez GP. 2010. Silencing of CDK5 reduces neurofibrillary tangles in transgenic alzheimer’s mice. J Neurosci. 30(42):13966-76.

61. Sengupta A, Wu Q, Grundke-Iqbal I, Iqbal K, Singh TJ. 1997. Potentiation of GSK-3-catalyzed Alzheimer-like phosphorylation of human tau by cdk5. Mol Cell Biochem. 167(1-2):99-105.

62. Li T, Hawkes C, Qureshi HY, Kar S, Paudel HK. 2006. Cyclin-dependent protein kinase 5 primes microtubule-associated protein tau site-specifically for glycogen synthase kinase 3beta. Biochemistry. 45(10):3134-45.

63. Vogelsberg-Ragaglia V, Schuck T, Trojanowski JQ, Lee VM. 2001. PP2A mRNA expression is quantitatively decreased in Alzheimer's disease hippocampus. Exp Neurol. 168(2):402-12.

64. Gong CX, Singh TJ, Grundke-Iqbal I, Iqbal K. 1993. Phosphoprotein phosphatase activities in Alzheimer disease brain. J Neurochem. 61(3):921-7.

65. Min SW, Chen X, Tracy TE, Li Y, Zhou Y, Wang C, Shirakawa K, Minami SS , Defensor E, Mok SA, Sohn PD, Schilling B, Cong X, Ellerby L, Gibson BW, Johnson J, Krogan N, Shamloo M, Gestwicki J, Masliah E, Verdin E, Gan L. 2015. Critical role of acetylation in tau-mediated neurodegeneration and cognitive deficits. Nat Med. 21(10):1154-62. doi: 10.1038/nm.3951.

66. Trzeciakiewicz H, Tseng JH, Wander CM, Madden V, Tripathy A, Yuan CX, Cohen TJ. 2017. A Dual Pathogenic Mechanism Links Tau Acetylation to Sporadic Tauopathy. Sci Rep. 7:44102.

67. Cohen TJ, Guo JL, Hurtado DE, Kwong LK, Mills IP, Trojanowski JQ, Lee VM. 2011. The acetylation of tau inhibits its function and promotes pathological tau aggregation. Nat Commun. 2:252.

68. Van den Steen P, Rudd PM, Dwek RA, Opdenakker G. 1998. Concepts and principles of O-linked glycosylation. Crit Rev Biochem Mol Biol. 33(3):151-208.

69. Lima VV, Rigsby CS, Hardy DM, Webb RC, Tostes RC. 2009. O-GlcNAcylation: a novel post-translational mechanism to alter vascular cellular signaling in health and disease: focus on hypertension. J Am Soc Hypertens. 3(6):374-87.

70. Arnold CS, Johnson GV, Cole RN, Dong DL, Lee M, Hart GW. 1996. The microtubule-associated protein tau is extensively modified with O-linked N-acetylglucosamine. J Biol Chem. 271(46):28741-4.

71. Yuzwa SA, Yadav AK, Skorobogatko Y, Clark T, Vosseller K, Vocadlo DJ. 2011. Mapping O-GlcNAc modification sites on tau and generation of a site-specific O-GlcNAc tau antibody. Amino Acids. 40(3):857-68.

72. Smet-Nocca C, Broncel M, Wieruszeski JM, Tokarski C, Hanoulle X, Leroy A, Landrieu I, Rolando C, Lippens G, Hackenberger CP. 2011. Identification of O-GlcNAc

sites within peptides of the Tau protein and their impact on phosphorylation. Mol Biosyst. 7(5):1420-9.

73. Wang Z, Udeshi ND, O'Malley M, Shabanowitz J, Hunt DF, Hart GW. 2010. Enrichment and site mapping of O-linked N-acetylglucosamine by a combination of chemical/enzymatic tagging, photochemical cleavage, and electron transfer dissociation mass spectrometry. Mol Cell Proteomics. 9(1):153-60.

74. Nelson PT, Alafuzoff I, Bigio EH, Bouras C, Braak H, Cairns NJ, Castellani RJ, Crain BJ, Davies P, Del Tredici K, Duyckaerts C, Frosch MP, Haroutunian V, Hof PR, Hulette CM, Hyman BT, Iwatsubo T, Jellinger KA, Jicha GA, Kövari E, Kukull WA, Leverenz JB, Love S, Mackenzie IR, Mann DM, Masliah E, McKee AC, Montine TJ, Morris JC, Schneider JA, Sonnen JA, Thal DR, Trojanowski JQ, Troncoso JC, Wisniewski T, Woltjer RL, Beach TG. 2012. Correlation of Alzheimer disease neuropathologic changes with cognitive status: a review of the literature. *J Neuropathol Exp Neurol* 71(5):362-381. J Neuropathol Exp Neurol. 71(5):362-81.

75. Augustinack JC, Schneider A, Mandelkow EM, Hyman BT. 2002. Specific tau phosphorylation sites correlate with severity of neuronal cytopathology in Alzheimer's disease. Acta Neuropathol. 103(1):26-35.

76. Liu F, Shi J, Tanimukai H, Gu J, Gu J, Grundke-Iqbal I, Iqbal K, Gong CX. 2009. Reduced O-GlcNAcylation links lower brain glucose metabolism and tau pathology in Alzheimer's disease. Brain. 132(Pt 7):1820-32.

77. Robertson LA, Moya KL, Breen KC. 2004. The potential role of tau protein O-glycosylation in Alzheimer's disease. J Alzheimers Dis. 6(5):489-95.

78. Yuzwa SA, Macauley MS, Heinonen JE, Shan X, Dennis RJ, He Y, Whitworth GE, Stubbs KA, McEachern EJ, Davies GJ, Vocadlo DJ. 2008. A potent mechanism-inspired O-GlcNAcase inhibitor that blocks phosphorylation of tau in vivo. Nat Chem Biol. 4(8):483-90.

79. Yu CH, Si T, Wu WH, Hu J, Du JT, Zhao YF, Li YM. 2008. O-GlcNAcylation modulates the self-aggregation ability of the fourth microtubule-binding repeat of tau. Biochem Biophys Res Commun. 375(1):59-62.

80. Reynolds MR, Berry RW, Binder LI. 2005. Site-specific nitration differentially influences tau assembly in vitro. Biochemistry. 44(42):13997-4009.

81. Reynolds MR, Reyes JF, Fu Y, Bigio EH, Guillozet-Bongaarts AL, Berry RW, Binder LI.2006. Tau nitration occurs at tyrosine 29 in the fibrillar lesions of Alzheimer's disease and other tauopathies. J Neurosci.26(42):10636-45.

82. Reyes JF, Fu Y, Vana L, Kanaan NM, Binder LI. 2011. Tyrosine nitration within the proline-rich region of Tau in Alzheimer's disease. Am J Pathol. 178(5):2275-85.

83. Petrucelli L, Dickson D, Kehoe K, Taylor J, Snyder H, Grover A, De Lucia M, McGowan E, Lewis J, Prihar G, Kim J, Dillmann WH, Browne SE, Hall A, Voellmy R, Tsuboi Y, Dawson TM, Wolozin B, Hardy J, Hutton M. 2004. CHIP and Hsp70 regulate tau ubiquitination, degradation and aggregation. Hum Mol Genet.13(7):703-14.

84. Riederer IM, Schiffrin M, Kövari E, Bouras C, Riederer BM. 2009. Ubiquitination and cysteine nitrosylation during aging and Alzheimer's disease. Brain Res Bull. 80(4-5):233-41.

85. Dorval V, Fraser PE. 2006. Small ubiquitin-like modifier (SUMO) modification of natively unfolded proteins tau and alpha-synuclein. J Biol Chem. 281(15):9919-24.

86. Luo HB, Xia YY, Shu XJ, Liu ZC, Feng Y, Liu XH, Yu G, Yin G, Xiong YS, Zeng K, Jiang J, Ye K, Wang XC, Wang JZ. 2015. SUMOylation at K340 inhibits tau degradation through deregulating its phosphorylation and ubiquitination. Proc Natl Acad Sci U S A. 2014 Nov 18;111(46):16586-91.

87. Funk KE, Thomas SN, Schafer KN, Cooper GL, Liao Z, Clark DJ, Yang AJ, Kuret J. 2014. Lysine methylation is an endogenous post-translational modification of tau protein in human brain and a modulator of aggregation propensity. Biochem J. 462(1):77-88.

88. Thomas SN, Funk KE, Wan Y, Liao Z, Davies P, Kuret J, Yang AJ. 2012. Dual modification of Alzheimer's disease PHF-tau protein by lysine methylation and ubiquitylation: a mass spectrometry approach. Acta Neuropathol. 123(1):105-17.

89. Zhou XZ, Kops O, Werner A, Lu PJ, Shen M, Stoller G, Küllertz G, Stark M, Fischer G, Lu KP. 2000. Pin1-dependent prolyl isomerization regulates dephosphorylation of Cdc25C and tau proteins. Mol Cell. 6(4):873-83.

90. Nakamura K, Greenwood A, Binder L, Bigio EH, Denial S, Nicholson L, Zhou XZ, Lu KP. 2012. Proline isomer-specific antibodies reveal the early pathogenic tau conformation in Alzheimer's disease. Cell. 149(1):232-44.

91. Braak H, Braak E. 1991. Neuropathological stageing of Alzheimer-related changes. Acta Neuropathol. 82(4):239-59.

92. Braak H, Alafuzoff I, Arzberger T, Kretzschmar H, Del Tredici K. 2006. Staging of Alzheimer disease-associated neurofibrillary pathology using paraffin sections and immunocytochemistry. Acta Neuropathol. 112(4):389-404.

93. Arriagada PV, Marzloff K, Hyman BT. 1992. Distribution of Alzheimer-type pathologic changes in nondemented elderly individuals matches the pattern in Alzheimer's disease. Neurology. 42(9):1681-8.

94. Bancher C, Braak H, Fischer P, Jellinger KA. 1993. Neuropathological staging of Alzheimer lesions and intellectual status in Alzheimer's and Parkinson's disease patients. Neurosci Lett. 162(1-2):179-82.

95. Guillozet AL, Weintraub S, Mash DC, Mesulam MM. 2003. Neurofibrillary tangles, amyloid, and memory in aging and mild cognitive impairment. Arch Neurol. 60(5):729-36.

96. Cowan CM, Mudher A. 2013. Are tau aggregates toxic or protective in tauopathies? Front Neurol. 4:114.

97. Skrabana R, Sevcik J, Novak M. 2006. Intrinsically disordered proteins in the neurodegenerative processes: formation of tau protein paired helical filaments and their analysis. Cell Mol Neurobiol. 26(7-8):1085-97.

98. Schweers O, Schönbrunn-Hanebeck E, Marx A, Mandelkow E. 1994. Structural studies of tau protein and Alzheimer paired helical filaments show no evidence for beta-structure. J Biol Chem. 269(39):24290-7.

99. Maeda S, Sahara N, Saito Y, Murayama M, Yoshiike Y, Kim H, Miyasaka T, Murayama S, Ikai A, Takashima A. 2007. Granular tau oligomers as intermediates of tau filaments. Biochemistry. 46(12):3856-61.

100. Maeda S, Sahara N, Saito Y, Murayama S, Ikai A, Takashima A. 2006. Increased levels of granular tau oligomers: an early sign of brain aging and Alzheimer's disease. Neurosci Res. 54(3):197-201.

101. Bibow S, Ozenne V, Biernat J, Blackledge M, Mandelkow E, Zweckstetter M. 2011. Structural impact of proline-directed pseudophosphorylation at AT8, AT100, and PHF1 epitopes on 441-residue tau. J Am Chem Soc. 133(40):15842-5.

102. Chirita CN, Congdon EE, Yin H, Kuret J. 2005. Triggers of full-length tau aggregation: a role for partially folded intermediates. Biochemistry. 44(15):5862-72.

103. von Bergen M, Friedhoff P, Biernat J, Heberle J, Mandelkow EM, Mandelkow E. 2000. Assembly of tau protein into Alzheimer paired helical filaments depends on a local sequence motif ((306)VQIVYK(311)) forming beta structure. Proc Natl Acad Sci U S A. 97(10):5129-34.

104. Goedert M. 1997. The Neurofibrillary Pathology of Alzheimer's Disease. The neuroscientist. 3(2): 131-141.

105. Rankin CA, Sun Q, Gamblin TC. Tau phosphorylation by GSK-3beta promotes tangle-like filament morphology. Mol Neurodegener. 2:12.

106. Alonso A, Zaidi T, Novak M, Grundke-Iqbal I, Iqbal K. 2001.

Hyperphosphorylation induces self-assembly of tau into tangles of paired helical filaments/straight filaments. Proc Natl Acad Sci U S A. 98(12):6923-8.

107. Baker S, Götz J. 2016. A local insult of okadaic acid in wild-type mice induces tau phosphorylation and protein aggregation in anatomically distinct brain regions. Acta Neuropathol Commun. 4:32.

108. Sundaram JR, Poore CP, Sulaimee NH, Pareek T, Asad AB, Rajkumar R, Cheong WF, Wenk MR, Dawe GS, Chuang KH, Pant HC, Kesavapany S. 2013. Specific inhibition of p25/Cdk5 activity by the Cdk5 inhibitory peptide reduces neurodegeneration in vivo. J Neurosci. 33(1):334-43.

109. D'Souza I, Schellenberg GD. 2005. Regulation of tau isoform expression and dementia.Biochim Biophys Acta. 1739(2-3):104-15.

110. Park SA, Ahn SI, Gallo JM. 2016. Tau mis-splicing in the pathogenesis of neurodegenerative disorders. BMB Rep. 49(8):405-13.

111. Ke YD, Suchowerska AK, van der Hoven J, De Silva DM, Wu CW, van Eersel J, Ittner A, Ittner LM. 2012. Lessons from tau-deficient mice. Int J Alzheimers Dis. 2012:873270.

112. Drechsel DN, Hyman AA, Cobb MH, Kirschner MW. 1992. Modulation of the Dynamic Instability of Tubulin Assembly by the Microtubule-Associated Protein Tau. Mol Biol Cell. 3(10):1141-54.

113. Breuzard G, Hubert P, Nouar R, De Bessa T, Devred F, Barbier P, Sturgis JN, Peyrot V. 2013. Molecular mechanisms of Tau binding to microtubules and its role in microtubule dynamics in live cells. J Cell Sci. 126(Pt 13):2810-9.

114. Dixit R, Ross JL, Goldman YE, Holzbaur EL. 2008. Differential Regulation of Dynein and Kinesin Motor Proteins by Tau. Science. 319(5866):1086-9.

115. Tai HC, Serrano-Pozo A, Hashimoto T, Frosch MP, Spires-Jones TL, Hyman BT. 2012. The synaptic accumulation of hyperphosphorylated tau oligomers in Alzheimer disease is associated with dysfunction of the ubiquitin-proteasome system. Am J Pathol. 181(4):1426-35.

116. Tracy TE, Gan L. 2018. Tau-mediated synaptic and neuronal dysfunction in neurodegenerative disease. Curr Opin Neurobiol. 51:134-138.

117. Pooler AM, Noble W, Hanger DP. 2014. A role for tau at the synapse in Alzheimer's disease pathogenesis. Neuropharmacology. 76 Pt A:1-8.

118. Cowan CM, Quraishe S, Mudher A. 2012. What is the pathological significance of tau oligomers? Biochem Soc Trans. 40(4):693-7.

119. Spires-Jones TL, Kopeikina KJ, Koffie RM, de Calignon A, Hyman BT. 2011. Are tangles as toxic as they look? J Mol Neurosci. 45(3):438-44.

120. Nagy Z, Esiri MM, Jobst KA, Morris JH, King EM, McDonald B, Litchfield S, Smith A, Barnetson L, Smith AD. 1995. Relative roles of plaques and tangles in the dementia of Alzheimer's disease: correlations using three sets of neuropathological criteria. Dementia. 6(1):21-31.

121. Arriagada PV, Growdon JH, Hedley-Whyte ET, Hyman BT. 1992. Neurofibrillary tangles but not senile plaques parallel duration and severity of Alzheimer's disease. Neurology. 42(3 Pt 1):631-9.

122. Gómez-Isla T, Hollister R, West H, Mui S, Growdon JH, Petersen RC, Parisi JE, Hyman BT. 1997. Neuronal loss correlates with but exceeds neurofibrillary tangles in Alzheimer's disease. Ann Neurol. 41(1):17-24.

123. Rudinskiy N, Hawkes JM, Wegmann S, Kuchibhotla KV, Muzikansky A, Betensky RA, Spires-Jones TL, Hyman BT. 2014. Tau pathology does not affect experience-driven single-neuron and network-wide Arc/Arg3.1 responses. Acta Neuropathol Commun. 2:63.

124. Kuchibhotla KV, Wegmann S, Kopeikina KJ, Hawkes J, Rudinskiy N, Andermann ML, Spires-Jones TL, Bacskai BJ, Hyman BT. 2014. Neurofibrillary tangle-bearing neurons are functionally integrated in cortical circuits in vivo. Proc Natl Acad Sci U S A. 111(1):510-4.

125. Santacruz K, Lewis J, Spires T, Paulson J, Kotilinek L, Ingelsson M, Guimaraes A, DeTure M, Ramsden M, McGowan E, Forster C, Yue M, Orne J, Janus C, Mariash A, Kuskowski M, Hyman B, Hutton M, Ashe KH. 2005. Tau suppression in a neurodegenerative mouse model improves memory function. Science. 309(5733):476-81.

126. Wittmann CW, Wszolek MF, Shulman JM, Salvaterra PM, Lewis J, Hutton M, Feany MB. 2001. Tauopathy in Drosophila: neurodegeneration without neurofibrillary tangles. Science. 293(5530):711-4.

127. Flach K, Hilbrich I, Schiffmann A, Gärtner U, Krüger M, Leonhardt M, Waschipky H, Wick L, Arendt T, Holzer M. 2012. Tau oligomers impair artificial membrane integrity and cellular viability. J Biol Chem. 287(52):43223-33.

128. Götz J, Probst A, Spillantini MG, Schäfer T, Jakes R, Bürki K, Goedert M. 1995. Somatodendritic localization and hyperphosphorylation of tau protein in transgenic mice expressing the longest human brain tau isoform. EMBO J. 14(7):1304-13.

129. Götz J, Chen F, van Dorpe J, Nitsch RM. 2001. Formation of neurofibrillary tangles in P301l tau transgenic mice induced by Abeta 42 fibrils. Science. 293(5534):1491-5.

130. Ramsden M, Kotilinek L, Forster C, Paulson J, McGowan E, SantaCruz K, Guimaraes A, Yue M, Lewis J, Carlson G, Hutton M, Ashe KH. 2005. Age-dependent neurofibrillary tangle formation, neuron loss, and memory impairment in a mouse model of human tauopathy (P301L). J Neurosci. 25(46):10637-47.

131. Yoshiyama Y, Higuchi M, Zhang B, Huang SM, Iwata N, Saido TC, Maeda J, Suhara T, Trojanowski JQ, Lee VM. 2007. Synapse loss and microglial activation precede tangles in a P301S tauopathy mouse model. Neuron. 53(3):337-51.

132. Berger Z, Roder H, Hanna A, Carlson A, Rangachari V, Yue M, Wszolek Z, Ashe K, Knight J, Dickson D, Andorfer C, Rosenberry TL, Lewis J, Hutton M, Janus C. 2007. Accumulation of pathological tau species and memory loss in a conditional model of tauopathy. J Neurosci. 27(14):3650-62.

133. Lasagna-Reeves CA, Castillo-Carranza DL, Sengupta U, Clos AL, Jackson GR, Kayed R. 2011. Tau oligomers impair memory and induce synaptic and mitochondrial dysfunction in wild-type mice. Mol Neurodegener. 6:39.

134. Castillo-Carranza DL, Gerson JE, Sengupta U, Guerrero-Muñoz MJ, Lasagna-Reeves CA, Kayed R. 2014. Specific targeting of tau oligomers in Htau mice prevents cognitive impairment and tau toxicity following injection with brain-derived tau oligomeric seeds. J Alzheimers Dis. 40 Suppl 1:S97-S111.

135. Gerson JE, Kayed R. 2013. Formation and propagation of tau oligomeric seeds. Front Neurol. 4:93.

136. Wu JW, Hussaini SA, Bastille IM, Rodriguez GA, Mrejeru A, Rilett K, Sanders DW, Cook C, Fu H, Boonen RA, Herman M, Nahmani E, Emrani S, Figueroa YH, Diamond MI, Clelland CL, Wray S, Duff KE. 2016. Neuronal activity enhances tau propagation and tau pathology in vivo. Nat Neurosci. 19(8):1085-92.

137. Kfoury N, Holmes BB, Jiang H, Holtzman DM, Diamond MI. 2012. Trans-cellular propagation of Tau aggregation by fibrillar species. J Biol Chem. 287(23):19440-51.

138. Frost B, Jacks RL, Diamond MI. 2009. Propagation of tau misfolding from the outside to the inside of a cell. J Biol Chem. 284(19):12845-52.

139. Clavaguera F, Bolmont T, Crowther RA, Abramowski D, Frank S, Probst A, Fraser G, Stalder AK, Beibel M, Staufenbiel M, Jucker M, Goedert M, Tolnay M. 2009. Transmission and spreading of tauopathy in transgenic mouse brain. Nat Cell Biol. 11(7):909-13.

140. Pooler AM, Polydoro M, Wegmann S, Nicholls SB, Spires-Jones TL, Hyman BT. 2013. Propagation of tau pathology in Alzheimer's disease: identification of novel therapeutic targets. Alzheimers Res Ther. 5(5):49.

141. Rustom A, Saffrich R, Markovic I, Walther P, Gerdes HH. 2004. Nanotubular Highways for Intercellular Organelle Transport. Science. 303(5660):1007-10.

142. Tardivel M, Bégard S, Bousset L, Dujardin S, Coens A, Melki R, Buée L, Colin M. 2016. Tunneling nanotube (TNT)-mediated neuron-to neuron transfer of pathological Tau protein assemblies. Acta Neuropathol Commun. 4(1):117.

143. Abounit S, Wu JW, Duff K, Victoria GS, Zurzolo C. 2016. Tunneling nanotubes: A possible highway in the spreading of tau and other prion-like proteins in neurodegenerative diseases. Prion. 10(5):344-351.

144. Arai H, Terajima M, Miura M, Higuchi S, Muramatsu T, Machida N, Seiki H, Takase S, Clark CM, Lee VM, et al. 1995. Tau in cerebrospinal fluid: a potential diagnostic marker in Alzheimer's disease. Ann Neurol. 38(4):649-52.

145. Yamada K, Cirrito JR, Stewart FR, Jiang H, Finn MB, Holmes BB, Binder LI, Mandelkow EM, Diamond MI, Lee VM, Holtzman DM. 2011. In vivo microdialysis reveals age-dependent decrease of brain interstitial fluid tau levels in P301S human tau transgenic mice. J Neurosci. 31(37):13110-7.

146. Karch CM, Jeng AT, Goate AM. 2012. Extracellular Tau levels are influenced by variability in Tau that is associated with tauopathies. J Biol Chem. 287(51):42751-62.

147. Chai X, Dage JL, Citron M. 2012. Constitutive secretion of tau protein by an unconventional mechanism. Neurobiol Dis. 48(3):356-66.

148. Pooler AM, Phillips EC, Lau DH, Noble W, Hanger DP. 2013. Physiological release of endogenous tau is stimulated by neuronal activity. EMBO Rep. 14(4):389-94.

149. Yamada K, Holth JK, Liao F, Stewart FR, Mahan TE, Jiang H, Cirrito JR, Patel TK, Hochgräfe K, Mandelkow EM, Holtzman DM. 2014. Neuronal activity regulates extracellular tau in vivo. J Exp Med. 211(3):387-93.

150. Santa-Maria I, Varghese M, Ksiezak-Reding H, Dzhun A, Wang J, Pasinetti GM. 2012. Paired helical filaments from Alzheimer disease brain induce intracellular accumulation of Tau protein in aggresomes. J Biol Chem. 287(24):20522-33.

151. Wu JW, Herman M, Liu L, Simoes S, Acker CM, Figueroa H, Steinberg JI, Margittai M, Kayed R, Zurzolo C, Di Paolo G, Duff KE. 2013. Small Misfolded Tau Species Are Internalized via Bulk Endocytosis and Anterogradely and Retrogradely Transported in Neurons. J Biol Chem. 288(3):1856-70.

152. Guo JL, Lee VM. 2011. Seeding of normal Tau by pathological Tau conformers drives pathogenesis of Alzheimer-like tangles. J Biol Chem. 286(17):15317-31.

153. Ahmed Z, Cooper J, Murray TK, Garn K, McNaughton E, Clarke H, Parhizkar S, Ward MA, Cavallini A, Jackson S, Bose S, Clavaguera F, Tolnay M, Lavenir I, Goedert M, Hutton ML, O'Neill MJ. 2014. A novel in vivo model of tau propagation with rapid and progressive neurofibrillary tangle pathology: the pattern of spread is determined by connectivity, not proximity. Acta Neuropathol. 127(5):667-83.

154. de Calignon A, Polydoro M, Suárez-Calvet M, William C, Adamowicz DH, Kopeikina KJ, Pitstick R, Sahara N, Ashe KH, Carlson GA, Spires-Jones TL, Hyman BT. 2012. Propagation of tau pathology in a model of early Alzheimer's disease. Neuron. 73(4):685-97.

155. Liu L, Drouet V, Wu JW, Witter MP, Small SA, Clelland C, Duff K. 2012. Trans-synaptic spread of tau pathology in vivo. PLoS One. 7(2):e31302.

156. DeVos SL, Corjuc BT, Oakley DH, Nobuhara CK, Bannon RN, Chase A, Commins C, Gonzalez JA, Dooley PM, Frosch MP, Hyman BT. 2018. Synaptic Tau Seeding Precedes Tau Pathology in Human Alzheimer's Disease Brain. Front Neurosci. 12:267.

157. Calafate S, Buist A, Miskiewicz K, Vijayan V, Daneels G, de Strooper B, de Wit J, Verstreken P, Moechars D. 2015. Synaptic Contacts Enhance Cell-to-Cell Tau Pathology Propagation. Cell Rep. 11(8):1176-83.

158. Wang Y, Balaji V, Kaniyappan S, Krüger L, Irsen S, Tepper K, Chandupatla R, Maetzler W, Schneider A, Mandelkow E, Mandelkow EM. 2017. The release and trans-synaptic transmission of Tau via exosomes. Mol Neurodegener. 12(1):5.

159. Graham WV, Bonito-Oliva A, Sakmar TP.2017. Update on Alzheimer's Disease Therapy and Prevention Strategies. Annu Rev Med. 68:413-430.

160. Massoulié J, Pezzementi L, Bon S, Krejci E, Vallette FM. 1993. Molecular and cellular biology of cholinesterases. Prog Neurobiol. 41(1):31-91.

161. Bartus RT, Dean RL 3rd, Beer B, Lippa AS. 1982. The cholinergic hypothesis of geriatric memory dysfunction. Science. 217(4558):408-14.

162. Rountree SD, Chan W, Pavlik VN, Darby EJ, Siddiqui S, Doody RS. 2009. Persistent treatment with cholinesterase inhibitors and/or memantine slows clinical progression of Alzheimer disease. Alzheimers Res Ther. 1(2):7.

163. Li F, Tsien JZ. 2009. Memory and the NMDA receptors. N Engl J Med. 361(3):302-3.

164. Winblad B, Poritis N. 1999. Memantine in severe dementia: results of the 9M-Best Study (Benefit and efficacy in severely demented patients during treatment with memantine). Int J Geriatr Psychiatry. 14(2):135-46.

165. Selkoe DJ, Hardy J. 2016. The amyloid hypothesis of Alzheimer's disease at 25 years. EMBO Mol Med. 8(6):595-608.

166. Schenk D, Basi GS, Pangalos MN. 2012. Treatment strategies targeting amyloid β-protein. Cold Spring Harb Perspect Med. 2(9):a006387.

167. Muchowski PJ. 2002. Protein misfolding, amyloid formation, and neurodegeneration: a critical role for molecular chaperones? Neuron. 35(1):9-12.

168. Roher AE, Palmer KC, Yurewicz EC, Ball MJ, Greenberg BD. 1993. Morphological and biochemical analyses of amyloid plaque core proteins purified from Alzheimer disease brain tissue. J Neurochem. 61(5):1916-26.

169. Calamai M, Chiti F, Dobson CM. 2005. Amyloid fibril formation can proceed from different conformations of a partially unfolded protein. Biophys J.89(6):4201-10.

170. Schenk D, Barbour R, Dunn W, Gordon G, Grajeda H, Guido T, Hu K, Huang J, Johnson-Wood K, Khan K, Kholodenko D, Lee M, Liao Z, Lieberburg I, Motter R, Mutter L, Soriano F, Shopp G, Vasquez N, Vandevert C, Walker S, Wogulis M, Yednock T, Games D, Seubert P. 1999. Immunization with amyloid-beta attenuates Alzheimer-disease-like pathology in the PDAPP mouse. Nature. 400(6740):173-7.

171. Panza F, Lozupone M, Seripa D, Imbimbo BP. 2019. Amyloid-β Immunotherapy for Alzheimer's Disease - Is It Now A Long Shot…? Ann Neurol.

172. Sevigny J, Chiao P, Bussière T, Weinreb PH, Williams L, Maier M, Dunstan R, Salloway S, Chen T, Ling Y, O'Gorman J, Qian F, Arastu M, Li M, Chollate S, Brennan MS, Quintero-Monzon O, Scannevin RH, Arnold HM, Engber T, Rhodes K, Ferrero J, Hang Y, Mikulskis A, Grimm 2, Hock C, Nitsch RM, Sandrock A. 2016. The antibody aducanumab reduces Aβ plaques in Alzheimer's disease. Nature. 537(7618):50-6.

173. Budd Haeberlein S, O'Gorman J, Chiao P, Bussière T, von Rosenstiel P, Tian Y, Zhu Y, von Hehn C, Gheuens S, Skordos L, Chen T, Sandrock A. 2017. Clinical Development of Aducanumab, an Anti-Aβ Human Monoclonal Antibody Being Investigated for the Treatment of Early Alzheimer's Disease. J Prev Alzheimers Dis. 4(4):255-263.

174. Biogen/Eisai Halt Phase 3 Aducanumab Trials. Tom Fagan. Alzforum. March 21, 2019. From https://www.alzforum.org/news/research-news/biogeneisai-halt-phase-3-aducanumab-trials.

175. Cheng C, Zandi P, Stuart E, Lin CH, Su PY, Alexander GC, Lan TH. 2017. Association Between Lithium Use and Risk of Alzheimer's Disease. J Clin Psychiatry. 78(2):e139-e145.

176. Forlenza OV, Diniz BS, Radanovic M, Santos FS, Talib LL, Gattaz WF. 2011. Disease-modifying properties of long-term lithium treatment for amnestic mild cognitive impairment: randomised controlled trial. Br J Psychiatry. 198(5):351-6.

177. Lahmy V, Meunier J, Malmström S, Naert G, Givalois L, Kim SH, Villard V, Vamvakides A, Maurice T. 2013. Blockade of Tau hyperphosphorylation and $A\beta_{1-42}$ generation by the aminotetrahydrofuran derivative ANAVEX2-73, a mixed muscarinic and σ_1 receptor agonist, in a nontransgenic mouse model of Alzheimer's disease. Neuropsychopharmacology. 38(9):1706-23.

178. ClinicalTrials.gov [Internet]. Anavex Life Sciences Corp. (NY). 2019 Jan 1 - . Identifier NCT03790709, ANAVEX2-73 for Treatment of Early Alzheimer's Disease; Available from: https://clinicaltrials.gov/ct2/show/NCT03790709

179. Martinez A, Gil C, Perez D. 2011. Glycogen synthase kinase 3 inhibitors in the next horizon for Alzheimer's disease treatment. Int J Alzheimers Dis. 2011:280502.
180. Nygaard HB. 2018. Targeting Fyn Kinase in Alzheimer's Disease. Biol Psychiatry. 83(4):369-376.

181. Hennequin LF, Allen J, Breed J, Curwen J, Fennell M, Green TP, Lambert-van der Brempt C, Morgentin R, Norman RA, Olivier A, Otterbein L, Plé PA, Warin N, Costello G. 2006. N-(5-chloro-1,3-benzodioxol-4-yl)-7-[2-(4-methylpiperazin-1-yl)ethoxy]-5- (tetrahydro-2H-pyran-4-yloxy)quinazolin-4-amine, a novel, highly selective, orally available, dual-specific c-Src/Abl kinase inhibitor. J Med Chem. 49(22):6465-88.

182. Lau DH, Hogseth M, Phillips EC, O'Neill MJ, Pooler AM, Noble W, Hanger DP. 2016. Critical residues involved in tau binding to fyn: implications for tau phosphorylation in Alzheimer's disease. Acta Neuropathol Commun. 4(1):49.

183. Kaufman AC, Salazar SV, Haas LT, Yang J, Kostylev MA, Jeng AT, Robinson SA, Gunther EC, van Dyck CH, Nygaard HB, Strittmatter SM. 2015. Fyn Inhibition Rescues Established Memory and Synapse Loss in Alzheimer Mice. Ann Neurol. 77(6):953-71.

184. Baskaran R, Velmurugan BK. 2018. Protein phosphatase 2A as therapeutic targets in various disease models. Life Sci. 210:40-46.

185. Corcoran NM, Martin D, Hutter-Paier B, Windisch M, Nguyen T, Nheu L, Sundstrom LE, Costello AJ, Hovens CM. 2010. Sodium selenate specifically activates PP2A phosphatase, dephosphorylates tau and reverses memory deficits in an Alzheimer's disease model. J Clin Neurosci. 17(8):1025-33.

186. van Eersel J, Ke YD, Liu X, Delerue F, Kril JJ, Götz J, Ittner LM. 2010. Sodium selenate mitigates tau pathology, neurodegeneration, and functional deficits in Alzheimer's disease models. Proc Natl Acad Sci U S A. 107(31):13888-93.

187. Liu SJ, Zheng P, Wright DK, Dezsi G, Braine E, Nguyen T, Corcoran NM, Johnston LA, Hovens CM, Mayo JN, Hudson M, Shultz SR, Jones NC, O'Brien TJ. 2016. Sodium selenate retards epileptogenesis in acquired epilepsy models reversing changes in protein phosphatase 2A and hyperphosphorylated tau. Brain. 139(Pt 7):1919-38.

188. Shultz SR, Wright DK, Zheng P, Stuchbery R, Liu SJ, Sashindranath M, Medcalf RL, Johnston LA, Hovens CM, Jones NC, O'Brien TJ. 2015. Sodium selenate reduces hyperphosphorylated tau and improves outcomes after traumatic brain injury. Brain. 138(Pt 5):1297-313.

189. Sandhu, P., Lee, J., Ballard, J., Walker, B., Ellis, J., Marcus, J., Toolan, D., Dreyer, D., McAvoy, T., Duffy, J., et al. 2016. Pharmacokinetics and pharmacodynamics to support clinical studies of MK-8719: An *O*-GlcNAcase inhibitor for Progressive Supranuclear palsy. *Alzheimers Dement. 12*, P1028.

190. Matsuoka Y, Jouroukhin Y, Gray AJ, Ma L, Hirata-Fukae C, Li HF, Feng L, Lecanu L, Walker BR, Planel E, Arancio O, Gozes I, Aisen PS. 2008. A neuronal microtubule-interacting agent, NAPVSIPQ, reduces tau pathology and enhances cognitive function in a mouse model of Alzheimer's disease. J Pharmacol Exp Ther. 325(1):146-53.

191. Quraishe S, Cowan CM, Mudher A. 2013. NAP (davunetide) rescues neuronal dysfunction in a Drosophila model of tauopathy. Mol Psychiatry. 18(7):834-42.

192. Morimoto BH, Schmechel D, Hirman J, Blackwell A, Keith J, Gold M; AL-108-211 Study. 2013. A double-blind, placebo-controlled, ascending-dose, randomized study to evaluate the safety, tolerability and effects on cognition of AL-108 after 12 weeks of intranasal administration in subjects with mild cognitive impairment. Dement Geriatr Cogn Disord. 35(5-6):325-36.

193. Boxer AL, Lang AE, Grossman M, Knopman DS, Miller BL, Schneider LS, Doody RS, Lees A, Golbe LI, Williams DR, Corvol JC, Ludolph A, Burn D, Lorenzl S, Litvan I, Roberson ED, Höglinger GU, Koestler M, Jack CR Jr, Van Deerlin V, Randolph C, Lobach IV, Heuer HW, Gozes I, Parker L, Whitaker S, Hirman J, Stewart AJ, Gold M, Morimoto BH; AL-108-231 Investigators. 2014. Davunetide in patients with progressive supranuclear palsy: a randomised, double-blind, placebo-controlled phase 2/3 trial. Lancet Neurol. 13(7):676-85.

194. Chiorazzi A, Nicolini G, Canta A, Oggioni N, Rigolio R, Cossa G, Lombardi R, Roglio I, Cervellini I, Lauria G, Melcangi RC, Bianchi R, Crippa D, Cavaletti G. 2009. Experimental epothilone B neurotoxicity: results of in vitro and in vivo studies. Neurobiol

Dis. 35(2):270-7.

195. Alves RC, Fernandes RP, Eloy JO, Salgado HRN, Chorilli M. 2018. Characteristics, Properties and Analytical Methods of Paclitaxel: A Review. Crit Rev Anal Chem. 48(2):110-118.

196. Golovyashkina N, Penazzi L, Ballatore C, Smith AB 3rd, Bakota L, Brandt R. 2015. Region-specific dendritic simplification induced by Aβ, mediated by tau via dysregulation of microtubule dynamics: a mechanistic distinct event from other neurodegenerative processes. Mol Neurodegener. 10:60.

197. Ilschner S, Brandt R. 1996. The transition of microglia to a ramified phenotype is associated with the formation of stable acetylated and detyrosinated microtubules. Glia. 18(2):129-40.

198. Cisek K, Cooper GL, Huseby CJ, Kuret J. 2014. Structure and mechanism of action of tau aggregation inhibitors. Curr Alzheimer Res. 11(10):918-27.

199. Crowe A, Huang W, Ballatore C, Johnson RL, Hogan AM, Huang R, Wichterman J, McCoy J, Huryn D, Auld DS, Smith AB 3rd, Inglese J, Trojanowski JQ, Austin CP, Brunden KR, Lee VM. 2009. Identification of aminothienopyridazine inhibitors of tau assembly by quantitative high-throughput screening. Biochemistry. 48(32):7732-45.

200. Crowe A, James MJ, Lee VM, Smith AB 3rd, Trojanowski JQ, Ballatore C, Brunden KR. 2013. Aminothienopyridazines and methylene blue affect Tau fibrillization via cysteine oxidation. J Biol Chem. 288(16):11024-37.

201. Wischik CM, Edwards PC, Lai RY, Roth M, Harrington CR. 1996. Selective inhibition of Alzheimer disease-like tau aggregation by phenothiazines. Proc Natl Acad Sci U S A. 93(20):11213-8.

202. Taniguchi S, Suzuki N, Masuda M, Hisanaga S, Iwatsubo T, Goedert M, Hasegawa M. 2005. Inhibition of heparin-induced tau filament formation by phenothiazines, polyphenols, and porphyrins. J Biol Chem. 280(9):7614-23.

203. Pickhardt M, Gazova Z, von Bergen M, Khlistunova I, Wang Y, Hascher A, Mandelkow EM, Biernat J, Mandelkow E. 2005. Anthraquinones inhibit tau aggregation and dissolve Alzheimer's paired helical filaments in vitro and in cells. J Biol Chem. 280(5):3628-35.

204. Pickhardt M, Biernat J, Khlistunova I, Wang YP, Gazova Z, Mandelkow EM, Mandelkow E. 2007. N-phenylamine derivatives as aggregation inhibitors in cell models of tauopathy. Curr Alzheimer Res. 4(4):397-402.

205. Pickhardt M, Larbig G, Khlistunova I, Coksezen A, Meyer B, Mandelkow EM, Schmidt B, Mandelkow E. 2007. Phenylthiazolyl-hydrazide and its derivatives are potent inhibitors of tau aggregation and toxicity in vitro and in cells. Biochemistry. 46(35):10016-23.

206. Chang E, Congdon EE, Honson NS, Duff KE, Kuret J. 2009. Structure-activity relationship of cyanine tau aggregation inhibitors. J Med Chem. 52(11):3539-47.

207. Bulic B, Pickhardt M, Khlistunova I, Biernat J, Mandelkow EM, Mandelkow E, Waldmann H. 2007. Rhodanine-based tau aggregation inhibitors in cell models of tauopathy. Angew Chem Int Ed Engl. 46(48):9215-9.

208. Schirmer RH, Adler H, Pickhardt M, Mandelkow E. 2011. "Lest we forget you--methylene blue...". Neurobiol Aging. 32(12):2325.e7-16.

209. Congdon EE, Wu JW, Myeku N, Figueroa YH, Herman M, Marinec PS, Gestwicki JE, Dickey CA, Yu WH, Duff KE. 2012. Methylthioninium chloride (methylene blue) induces autophagy and attenuates tauopathy in vitro and in vivo. Autophagy. 8(4):609-22.

210. Stack C, Jainuddin S, Elipenahli C, Gerges M, Starkova N, Starkov AA, Jové M, Portero-Otin M, Launay N, Pujol A, Kaidery NA, Thomas B, Tampellini D, Beal MF, Dumont M. 2014. Methylene blue upregulates Nrf2/ARE genes and prevents tau-related neurotoxicity. Hum Mol Genet. 23(14):3716-32.

211. Hochgräfe K, Sydow A, Matenia D, Cadinu D, Könen S, Petrova O, Pickhardt M, Goll P, Morellini F, Mandelkow E, Mandelkow EM. 2015. Preventive methylene blue treatment preserves cognition in mice expressing full-length pro-aggregant human Tau. Acta Neuropathol Commun. 3:25.

212. Wischik CM, Staff RT, Wischik DJ, Bentham P, Murray AD, Storey JM, Kook KA, Harrington CR. 2015. Tau aggregation inhibitor therapy: an exploratory phase 2 study in mild or moderate Alzheimer's disease. J Alzheimers Dis. 44(2):705-20.

213. Tucker D, Lu Y, Zhang Q. 2018. From Mitochondrial Function to Neuroprotection-an Emerging Role for Methylene Blue. Mol Neurobiol. 55(6):5137-5153.

214. Baddeley TC, McCaffrey J, Storey JM, Cheung JK, Melis V, Horsley D, Harrington CR, Wischik CM. 2015. Complex disposition of methylthioninium redox forms determines efficacy in tau aggregation inhibitor therapy for Alzheimer's disease. J Pharmacol Exp Ther. 352(1):110-8.

215. Gauthier S, Feldman HH, Schneider LS, Wilcock GK, Frisoni GB, Hardlund JH, Moebius HJ, Bentham P, Kook KA, Wischik DJ, Schelter BO, Davis CS, Staff RT, Bracoud L, Shamsi K, Storey JM, Harrington CR, Wischik CM. 2016. Efficacy and safety of tau-aggregation inhibitor therapy in patients with mild or moderate Alzheimer's

disease: a randomised, controlled, double-blind, parallel-arm, phase 3 trial. Lancet. 388(10062):2873-2884.

216. Pedersen JT, Sigurdsson EM. 2015. Tau immunotherapy for Alzheimer's disease. Trends Mol Med. 21(6):394-402.

217. Asuni AA, Boutajangout A, Quartermain D, Sigurdsson EM. 2007. Immunotherapy targeting pathological tau conformers in a tangle mouse model reduces brain pathology with associated functional improvements. J Neurosci. 27(34):9115-29.

218. Troquier L, Caillierez R, Burnouf S, Fernandez-Gomez FJ, Grosjean ME, Zommer N, Sergeant N, Schraen-Maschke S, Blum D, Buee L. 2012. Targeting phospho-Ser422 by active Tau Immunotherapy in the THYTau22 mouse model: a suitable therapeutic approach. Curr Alzheimer Res. 9(4):397-405.

219. Boutajangout A, Ingadottir J, Davies P, Sigurdsson EM. 2011. Passive immunization targeting pathological phospho-tau protein in a mouse model reduces functional decline and clears tau aggregates from the brain. J Neurochem. 118(4):658-67.

220. Novak P, Schmidt R, Kontsekova E, Zilka N, Kovacech B, Skrabana R, Vince-Kazmerova Z, Katina S, Fialova L, Prcina M, Parrak V, Dal-Bianco P, Brunner M, Staffen W, Rainer M, Ondrus M, Ropele S, Smisek M, Sivak R, Winblad B, Novak M. 2017. Safety and immunogenicity of the tau vaccine AADvac1 in patients with Alzheimer's disease: a randomised, double-blind, placebo-controlled, phase 1 trial. Lancet Neurol. 16(2):123-134.

221. Novak P, Schmidt R, Kontsekova E, Kovacech B, Smolek T, Katina S, Fialova L, Prcina M, Parrak V, Dal-Bianco P, Brunner M, Staffen W, Rainer M, Ondrus M, Ropele S, Smisek M, Sivak R, Zilka N, Winblad B, Novak M. 2018. FUNDAMANT: an interventional 72-week phase 1 follow-up study of AADvac1, an active immunotherapy against tau protein pathology in Alzheimer's disease. Alzheimers Res Ther.10(1):108.

222. Theunis C, Crespo-Biel N, Gafner V, Pihlgren M, López-Deber MP, Reis P, Hickman DT, Adolfsson O, Chuard N, Ndao DM, Borghgraef P, Devijver H, Van Leuven F, Pfeifer A, Muhs A. 2013. Efficacy and safety of a liposome-based vaccine against protein Tau, assessed in tau.P301L mice that model tauopathy. PLoS One. 8(8):e72301.

223. Wisniewski HM, Wegiel J. 1991. Spatial relationships between astrocytes and classical plaque components. Neurobiol Aging. 12(5):593-600.

224. McGeer PL, Itagaki S, Tago H, McGeer EG. 1987. Reactive microglia in patients with senile dementia of the Alzheimer type are positive for the histocompatibility glycoprotein HLA-DR. Neurosci Lett. 79(1-2):195-200.

225. Padmanabhan J, Levy M, Dickson DW, Potter H. 2006. Alpha1-antichymotrypsin, an inflammatory protein overexpressed in Alzheimer's disease brain, induces tau phosphorylation in neurons. Brain. 129(Pt 11):3020-34.

226. Mucke L, Yu GQ, McConlogue L, Rockenstein EM, Abraham CR, Masliah E. 2000. Astroglial expression of human alpha(1)-antichymotrypsin enhances alzheimer-like pathology in amyloid protein precursor transgenic mice. Am J Pathol. 157(6):2003-10.

227. Nilsson LN, Bales KR, DiCarlo G, Gordon MN, Morgan D, Paul SM, Potter H. 2001. Alpha-1-antichymotrypsin promotes beta-sheet amyloid plaque deposition in a transgenic mouse model of Alzheimer's disease. J Neurosci. 21(5):1444-51.

228. Qiao X, Cummins DJ, Paul SM. 2001. Neuroinflammation-induced acceleration of amyloid deposition in the APPV717F transgenic mouse. Eur J Neurosci. 14(3):474-82.
229. Wang J, Tan L, Wang HF, Tan CC, Meng XF, Wang C, Tang SW, Yu JT. 2015. Anti-inflammatory drugs and risk of Alzheimer's disease: an updated systematic review and meta-analysis. J Alzheimers Dis. 44(2):385-96.

230. Miguel-Álvarez M, Santos-Lozano A, Sanchis-Gomar F, Fiuza-Luces C, Pareja-Galeano H, Garatachea N, Lucia A. 2015. Non-steroidal anti-inflammatory drugs as a treatment for Alzheimer's disease: a systematic review and meta-analysis of treatment effect. Drugs Aging.32(2):139-47.

231. Shih-Ya Hung, Wen-Mei Fu. 2017. Drug candidates in clinical trials for Alzheimer’s disease. J Biomed Sci. 24: 47.

232. Breitner JC, Baker LD, Montine TJ, Meinert CL, Lyketsos CG, Ashe KH, Brandt J, Craft S, Evans DE, Green RC, Ismail MS, Martin BK, Mullan MJ, Sabbagh M, Tariot PN; ADAPT Research Group. 2011. Extended results of the Alzheimer's disease anti-inflammatory prevention trial. Alzheimers Dement.7(4):402-11.

233. Sui D, Xu X, Ye X, Liu M, Mianecki M, Rattanasinchai C, Buehl C, Deng X, Kuo MH. 2015. Protein interaction module-assisted function X (PIMAX) approach to producing challenging proteins including hyperphosphorylated tau and active CDK5/p25 kinase complex. Mol Cell Proteomics. 14(1):251-62.

234. George RC, Lew J, Graves DJ. 2013. Interaction of cinnamaldehyde and epicatechin with tau: implications of beneficial effects in modulating Alzheimer's disease pathogenesis. J Alzheimers Dis. 36(1):21-40.

235. Barghorn S, Mandelkow E. 2002. Toward a unified scheme for the aggregation of tau into Alzheimer paired helical filaments. Biochemistry. 41(50):14885-96.

CHAPTER II

RECOMBINANT HYPERPHOSPHORYLATED TAU (P-TAU) GENERATED VIA THE PIMAX SYSTEM EXHIBITS ANTICIPATED PATHOGENIC ACTIVITIES

ABSTRACT

Alzheimer's disease (AD) is an irreversible neurodegenerative disease that has no cure or prevention to date. One defining feature of AD is neurofibrillary tangles (NFTs) composed of fibrils of hyperphosphorylated tau. The spatiotemporal distribution and the density of NFTs predict the progression and severity of cognitive impairments. Accumulating evidence suggests that the oligomeric, pre-tangle hyperphosphorylated tau aggregates are an underlying cause for neuronal loss. Accordingly, small-molecule compounds that inhibit or revert the aggregation of hyperphosphorylated tau hold the promise to be AD therapeutics. To date, all tangle-centric drug discovery attempts used heparin-induced, unmodified tau aggregation as the primary screening assay. Without the defining character of hyperphosphorylation, the pathophysiological relevance of these drug screens is therefore of concern. Here I show that hyperphosphorylated tau (p-tau) expressed by the PIMAX approach possesses clinically relevant sites of phosphorylation, fibrillizes autonomously, triggers apoptosis and superoxide production, and induces cell death at sub-micromolar concentrations. These results suggest p-tau produced by PIMAX system is a proper target for high-throughput screening to search for tau aggregation modulators as AD therapeutics.

INTRODUCTION

Neurofibrillary tangles (NFTs) composed of fibrils of hyperphosphorylated tau (p-tau) are one of the defining markers of Alzheimer's disease (AD) [1]. Aggregation of p-tau in selective neurons is a common pathological character shared by more than a dozen neurodegenerative tauopathies that include AD, frontotemporal dementia with parkinsonism linked to chromosome 17 (FTDP-17), Pick's disease, chronic traumatic encephalopathy, and others [2]. Tau protein contains 2 – 4 phospates per molecule and binds to microtubules in the normal brain [3]. In AD, hyperphosphorylation results in the detachment of tau protein from microtubules and promotes the formation of NFTs [4, 5]. Prion-like, inter-neuronal propagation of cytotoxic hyperphosphorylated tau oligomers is considered an underlying cause for neurodegeneration, and therefore affords a promising target for treatment [60].

Efforts have been made to search for agents that can inhibit tau aggregation pathway or disaggregate tau fibrils. The tau aggregation process can be replicated in vitro by adding polyanionic substrates like arachidonic acid (ARA) [6] and heparin [7], while the protein alone shows modest or no aggregation at physiological concentrations [8]. Alternative tau derivatives, such as the K18 fragment containing the four repeat domains [9] and tau bearing selective mutations seen in FTDP-17 [10], have been used in a number of compound library screens, but these screens have yet to yield promising drug candidates [11, 12]. The weak pathophysiological relevance between unmodified tau and AD may have contributed to the slow progress of AD drug discovery targeting NFT genesis. To overcome this hurdle, our lab developed the PIMAX system (Protein Interaction Modules-Assisted function X) that produced recombinant p-tau with GSK-3β

or CDK5/p25 kinase [13]. I chose GSK-3β, one of the most likely tau kinases for AD [14], to phosphorylate tau in the system. The overarching goal of my thesis research is to develop a novel, hyperphosphorylated tau aggregation-based AD drug discovery system for effective therapeutics for this devastating neurodegenerative disease. In this chapter, evidence supporting the validity of p-tau for AD drug discovery is presented.

MATERIALS AND METHODS

Materials. Fluorescein diacetate, propidium iodide and thioflavin S and Amicon Centrifugal Filter Unit were purchased from Sigma Aldrich (St. Louis, MO). Gibco Dulbecco's Modified Eagle Medium (DMEM), HyClone^{TM} Fetal Bovine Serum, Optical Adhesive Film, fluorescein isothiocyanate (FITC)-conjugated Annexin V and MitoSOX were purchased from Thermo Fisher Scientific (Waltham, MA). Small volume, black, flat-bottom, 384-well plate was purchased from Griner Bio-One (Monroe, NC). Malachite Green Phosphate Assay Kit was purchased from Cayman Chemical (Ann Arbor, MI).All other chemicals for common buffers and solutions were purchased from Sigma Aldrich (St. Louis, MO).

Plasmids and Recombinant Genes. The plasmids and primers used in this work are listed in Tables 2.1 and 2.2. Plasmid and expression procedures for the 1N4R tau and p-tau were previously described [13]. Residue 291 Cys-to-Ser mutations were generated using C291S S and C291S AS oligos, Residue 322 Cys-to-Ser mutation were generated using C322S S and C322S AS oligos by QuikChange mutagenesis. All constructs were verified by DNA sequencing.

Table 2.1 Plasmid constructs used in this study

Plasmid	Main features	Source or reference
pMK1013	His6-Fos-thrombin + Jun-TEV	13
pMK1013-tau 1N4R	His6-Fos-thrombin + Jun-TEV-tau 1N4R	13
pMK1013-GSK-3β-tau 1N4R	His6-Fos-thrombin-GSK-3β + Jun-TEV-tau 1N4R	13
pMK1013-GSK-3β-tau (1N4R) C291S C322S	His6-Fos-thrombin-GSK-3β + Jun-TEV-tau (1N4R) C291S C322S	This study

Table 2.2 Oligos used in this study

Oligo	Sequence
C291S S	CTTAGCAACGTCCAGTCCAAGGCTGGCTCAAAGGATAATATCAAA
C291S AS	TTTGATATTATCCTTTGAGCCAGCCTTGGACTGGACGTTGCTAAG
C322S S	CTGAGCAAGGTGACCTCCAAGGCTGGCTCATTAGGCAACATCCAT
C322S AS	ATGGATGTTGCCTAATGAGCCAGCCTTGGAGGTCACCTTGCTCAG

Recombinant Protein Expression and Purification. P-tau and tau were expressed as previously described [13]. For tau and p-tau purification, bacterial pellets from 1 L of cultures were suspended in 10-ml cold purification buffer (20 mM Tris-HCl pH 5.8, 100 mM NaCl, 1 mM PMSF, 0.2 mM orthovanadate) and treated with 1 mg/ml lysozyme at 30°C for 30 min. The mixture was then sonicated (Branson Digital Sonifier 450; 30% amplitude; total process time 3 min; pulse-ON time 5 sec; pulse-OFF time 5 sec) and centrifuged at 17,000 x g for 40 min at 4°C. The supernatant was left in a boiling water bath for 30 min and left on ice for 30 min with occasional and gentle shaking in both steps. After centrifugation at 17,000 x g for 50 min at 4°C, the supernatant was transferred to another tube before 0.5 mM DTT and 1 mM EDTA were supplied. One OD_{280} of purified recombinant TEV protease was added to digest each 100 OD_{280} of the sample, and the reaction was incubated at 4°C for overnight. The digestion mixture was then centrifuged at 17,000 x g for 30 min at 4°C, and the supernatant was transferred to another tube. The buffer was adjusted to gel filtration buffer (20 mM Tris-HCl pH 7.4, 100 mM NaCl) by the use of a spin column (Amicon Centrifugal Filter Unit, Ultra-15, 10K) at 5,000 x g at 4°C until the volume was reduced to less than 1 ml. Three ml of gel filtration buffer was added to the column. The centrifugation and buffer supply were repeated twice. The final gel filtration buffer equilibrated solution was injected to a Superdex 200 10/300 GL column. Size exclusion chromatography was done on an AKTA explorer FPLC unit at 4°C. The flow rate was set at 0.3 ml/min, and the fractions containing the desired protein were pooled and concentrated by a spin column. After the concentration was completed, the protein solution was collected and supplemented with 10% glycerol (v/v) before – 80°C storage.

Malachite Green Phosphate Assay. P-tau was diluted to 4 µM using 50 mM Tris (pH 7.4) buffer. Phosphate standard of 0, 0.08, 0.16, 0.31, 0.63 and 1.25 nmoles of phosphates in 50 µl were diluted from the MG phosphate standard in the Cayman Malachite Green kit. 10 µl of p-tau or standard was mixed with 10 µl of 2M NaOH and boiled for 15 min. 10 µl of 4.7 M HCl was then added to neutralize the solution. After cooling to room temperature, 10 µl of the mixture was transferred into 96-well plate. 1 µl of MG Acidic Solution was added and incubated for 10 min, followed by the treatment of 3 µl of MG Blue Solution for 20 min at room temperature. The absorbance was read at 620 nm using a BioTek plate reader.

Mapping p-tau phosphorylation sites by LC-MS/MS. The four MS were done by Cayman Chemical (Ann Arbor, MI), Dr. Yeou-Guang Tsay's group (at National Yang Ming University, Taiwan), MSU Mass Spectrometry and Metabolomics Core and Dr. Philip C. Andrews' group at MSU. Below is the protocol used by Dr. Yeou-Guang Tsay's group.

For in-gel digestion, the protein band of interest was excised from the gel for digestion with endoproteinase trypsin, Lys-C, Arg-C or AspN (Roche, USA). The gel piece was soaked in 1 mL of 25 mM NH_4HCO_3 for 10 min and dehydrated with 1 mL of 25 mM NH_4HCO_3/50% acetonitrile for 10 min. After dried in a Speed-Vac (Savant, USA), the gel was incubated in 100 mL of 1% β mercaptoethanol/25 mM NH_4HCO_3 for 20 min at room temperature and at dark. An equal volume of 5% 4-vinylpyridine in 25 mM NH_4HCO_3/50% acetonitrile was added for cysteine alkylation. After a 20-min

incubation, the gel piece was washed in 1 mL of 25 mM NH_4HCO_3 for 10 min and in 1 mL of 25 mM NH_4HCO_3/50% acetonitrile for another 10 min. The gel piece was dried and then incubated with 25 mM NH_4HCO_3 containing 500 ng of endoproteinase at 37°C or at room temperature overnight (~18 h). After the digest was saved, the peptides remaining in gel piece were extracted sequentially with 300 mL of 25 mM NH_4HCO_3 and 300 mL of 25 mM NH_4HCO_3/50% acetonitrile. The digest and the two extracts were combined together and then dried in a Speed-Vac. The dried sample was kept at 20°C for storage and resuspended in 0.1% formic acid immediately before use.

For phosphorylation site mapping by LC-MS/MS, electrospray mass spectrometry was performed using LTQ-Orbitrap hybrid tandem mass spectrometer (ThermoFisher, USA) in-lined with Agilent 1200 nanoflow HPLC system. The HPLC system was equipped with LC packing C18 PepMap100 (length: 5 mm; internal diameter: 300 mm; bead size 5 mm) as the trap column and in house-made capillary column packed with C18 beads (length: 105 mm; internal diameter: 75 mm; bead size: 5 mm) as the separating column. The mobile phase consisted of (A) 0.1% formic acid in water and (B) 0.1% formic acid in acetonitrile. Mass spectra for the elute were acquired as successive sets of scan modes. For the setting of LTQ-Orbitrap, full scans with Orbitrap analyses were collected in the range of 200~2000. The Dynamic Exclusion function in Data Dependent Settings was activated, with the Repeat Count as 1, Exclusion Duration as 180 s and Exclusion List Size as 50. While those with +1 or unassigned charge state were rejected, the top three ions in the survey scan fulfilling the above criteria Were examined for their MS/MS with LTQ mass analyzer.

For informatics analysis, File Converter in Xcalibur 2.0.7 (ThermoFisher, USA) and a set of our in-house programs [15] were used to process the LC-MS/MS data. The mass spectra (MS) and tandem mass spectra (MS/MS) were first extracted and separated using our OutputPlus computer program. The MS spectra became segmental average MS using our SegAveMS algorithm. MS/MS Were interpreted using Sequest/TurboSequest to find the bested matched peptide with human protein FASTA database (release 2016_06) downloaded from UniProt website. Our GetOUT macro found peptide sequences with XCorr score ≥ 2.5 and a mass error ≤ 15 ppm. The GetOUT and SegAveMS results were queried using our FindPTM algorithm, which produced a list of candidates modified peptides. The MS/MS spectra were eventually verified using our MS2Display and MS2Graph programs [15].

Transmission electron microscopy. 72-hr incubated 10 µM of p-tau aggregation samples were diluted 50 fold with water. Ten µl of diluted sample was applied to the grid and sit for one minute. The excessive liquid on the grid was then removed by filter paper. Negative staining was done by applying 1% uranyl acetate on the grid for one minute. Stained grids were viewed with a JEOL 100CXII transmission electron microscope.

Cytotoxicity of p-tau. Cell viability assays were conducted in 96-well plates. 2,000 SH-SY5Y cells or HEK 293T in 100 µL media (DMEM, 10% FBS, pen/strep) were seeded to a well and cultured for 40 – 48 hours at 37°C, 5% CO_2. The confluency of cells may affect their sensitivity to p-tau. Values of LD_{50} can therefore only be compared

among experiments done at the same time. To prepare pre-aggregated p-tau for cytotoxicity test, p-tau at 2, 6, 8 µM were incubated in a dye-free aggregation (20 mM Tris, pH 7.4, 1 mM DTT) buffer for 0, 24, 48, 72, 96 or 120 hrs at 37°C. At the time of cell treatment, 10 µl of the pre-aggregated protein was added to each well of cells. 16 hrs (for SH-SY5Y) or 24 hrs (for HEK 293T) after the addition of protein, cells were trypsinized and transferred to microcentrifuge tubes, and pelleted at 1,000 x g for 5 min at room temperature. Cell pellets were resuspended in phosphate-buffered saline (PBS, 137 mM NaCl, 2.7 mM KCl, 10 mM Na_2HPO_4, 1.8 mM KH_2PO_4) and incubated with 5 µg/ml fluorescein diacetate (FDA) for 5 min at room temperature. 5 µg/ml propidium iodide (PI) was then added to the mixture. Cells stained by FDA or PI were examined using an Olympus BX51 Fluorescence Microscope. Cells from randomly chosen fields were counted for FDA or PI stainability. At least fifty cells from multiple fields were counted for each treatment well. Viability was calculated using the equation:

Relative viability = FDA stained cells / (FDA stained cells + PI stained cells).

For thioflavin S (ThS) and PI double staining, HEK 293T cells were harvested after 5-hr 0.6 µM p-tau treatment. The cell pellets were resuspended in PBS buffer and incubated with 100 µM ThS for 5 min at room temperature. 5 µg/ml PI was then added to the mixture. The cells were examined using an Olympus BX51 Fluorescence Microscope.

To examine apoptosis, SH-SY5Y or HEK 293T cells were treated by 0.3 – 0.8 µM of p-tau, or 2 mM velcade, a known apoptosis inducer [33] as control for 12 hrs. The harvested cells were respuspended in annexin V binding buffer (0.1 M HEPES, pH 7.4; 0.1 M NaCl; 25 mM $CaCl_2$). 5 µL of cell suspension was stained with 0.5 µL of FITC-

conjugated annexin V at room temperature for 15 min in the dark, followed by addition of PI to final concentration of 5 µg/ml. The cells were examined using an Olympus BX51 Fluorescence Microscope.

For MitoSOX and ThS double staining, HEK 293T cells were harvested after 5-hr 0.6 µM of p-tau treatment. Cell pellets were resuspended in 20 mM Tris, pH7.4 buffer and incubated with 100 µM ThS for 5 min at room temperature. The cell suspension was then stained with 5 µM MitoSOX at 37°C for 10 min in the dark and examined using an Olympus BX51 Fluorescence Microscope. To analyze the production of superoxide by flow cytometry, SH-SY5Y cells after 5-hr 0.6 µM of p-tau treatment was only stained by MitoSOX, and then examined at Excitation 510 nm, Emission 580 nm using the BD^{TM} LSR II flow cytometer.

Seeding assay. 9 µM of tau or buffer as control was mixed with 0, 1, 3, 6 or 9 µM of p-tau in a dye-free aggregation buffer (20 mM Tris, pH 7.4; 1 mM DTT). The mixture was used for either thioflavin S (ThS) aggregation assay or cytotoxicity test. For ThS assay, 20 µM ThS was supplied and the mixture was transferred to a 384-well low-volume plate. The plate was covered by an Optical Adhesive Film to minimize evaporation during the assay. The plate was set at 37°C briefly before placing to a BioTek Synergy Neo Plate reader. ThS fluorescence was measured every 10 min (excitation 440 nm, emission 490 nm) for 16 hrs and collected using Gen5 software bundled with the BioTek plate reader. For cytotoxicity test, 10 µl of the mixture of p-tau and tau or p-tau and buffer was added to HEK 293T cells, which was cultured under the same conditions as

the cytotoxicity assay. After 24 hrs incubation, the cell viability was examined by FDA/PI staining.

RESULTS

Hyperphosphorylated tau (p-tau) generated via PIMAX fibrillizes efficiently

To produce sufficient quantities of hyperphosphorylated tau (p-tau) and avoid the high cost of in vitro kinase assays, I used the PIMAX method [13, Fig 2.1A], which fuses the Fos and Jun leucine zipper domains to the GSK-3β kinase and the 1N4R isoform of tau respectively. A TEV-protease digestion sequence was inserted between Jun and tau. Upon bacterial co-expression, Fos-Jun heterodimerization [16] brought the kinase and tau to close proximity, resulting in efficient phosphorylation of tau. P-tau was then liberated from the complex via TEV-protease digestion. Tau phosphorylation was verified by retarded SDS-PAGE gel mobility and by western blots using antibodies against tau phospho-epitopes [13]. Following this approach with protocols optimized for p-tau purification, I produced GSK-3β-modified p-tau at a yield of 800 – 1000 µg per liter of bacterial culture. SDS-PAGE shows significant kinase-dependent mobility shift of tau (Fig 2.1B). The stoichiometry of p-tau phosphorylation in different protein batches was determined by the malachite green phosphate quantification assays [17] to be 3.6 – 5.3 moles of phosphate per mole of p-tau (Fig 2.1C). Transmission electron microscopy (TEM) of 72 hr-aggregated p-tau fibrils revealed multiple fibrillization intermediates (Figure 2.1D). These intermediates were reminiscent of a model depicting the pathway of NFT formation (discussed in Chapter I), and the reports of granular cytotoxic oligomers of disease tau [18, 19].

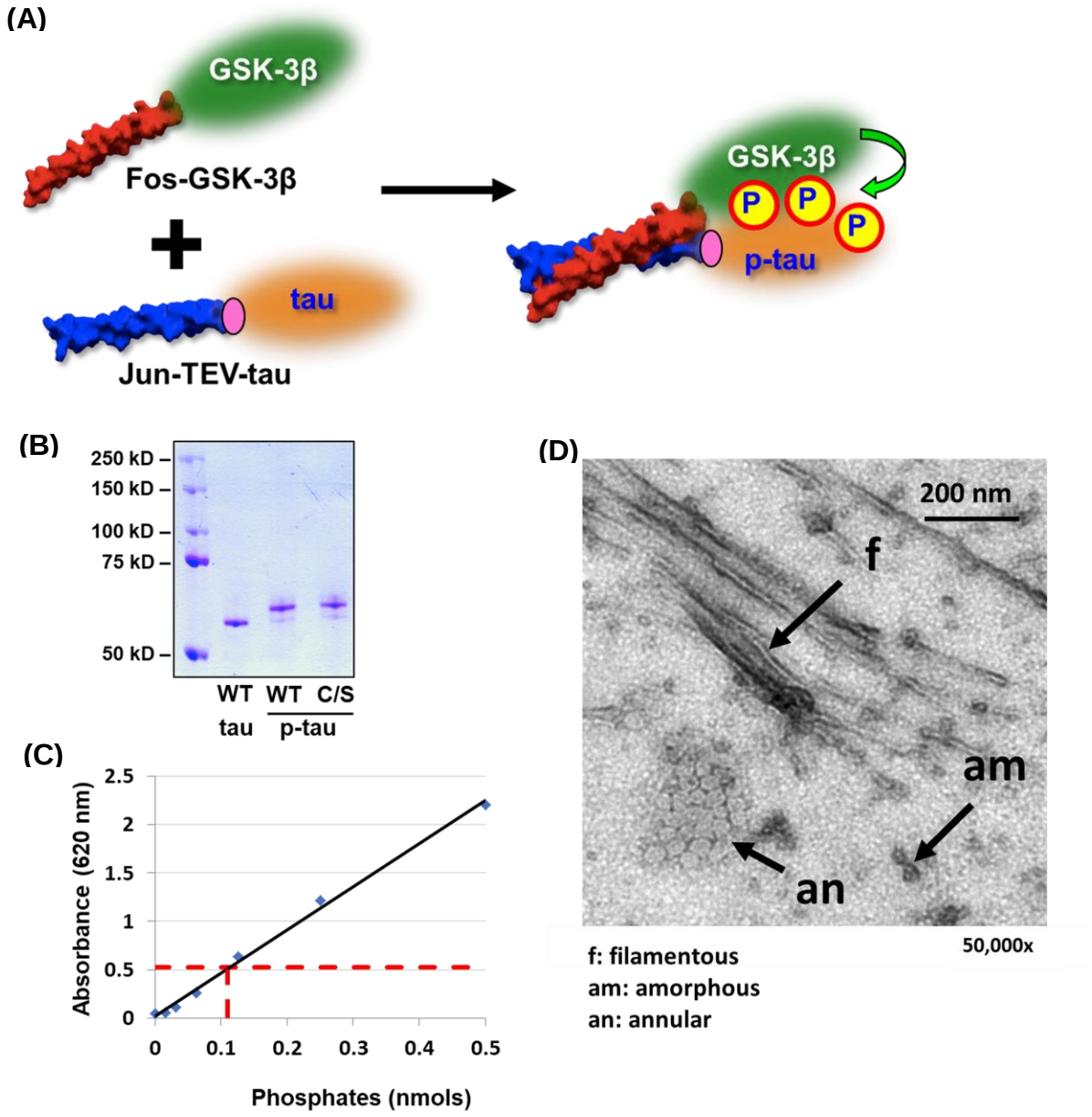

Figure 2.1 Hyperphosphorylated tau (p-tau) produced via PIMAX forms fibrils.

Figure 2.1 (cont'd)

(A) Schematic mechanism of PIMAX [13]. The interaction between the leucine zipper domains of Fos and Jun facilitates the modification of a substrate (tau) by the cognate enzyme (GSK-3β). (B) Purified tau 1N4R, p-tau (phosphorylated by GSK-3β) and p-tau bearing Cys-to-Ser mutations (detailed in chapter III) were resolved by an 8% SDS-PAGE gel. (C) The number of phosphates in each tau molecule identified by malachite green phosphate assays. The black line is the linear fitting curve for standard. The intersection point of red dotted line and the standard curve indicates the absorbance and number of phosphates in p-tau sample. (D) Transmission electron micrograph of p-tau aggregation intermediates. Filamentous (f), amorphous (am), and an annular (an) hexagonal structure ~ 30 nm in diameter are seen. (D) was done by Xiexong Deng.

Mapping PIMAX p-tau phosphorylation pattern

To map the phosphorylation sites, I submitted p-tau to different collaborators and facilities for mass spectrometry (MS) analysis. Phosphorylation sites found in these MS assays are listed in Table 2.3. These residues are grouped into 4 classes based on their detection frequency among the four independent MS assays: eight sites were positive in all four MS assays (“4-hitters”, green), eight were positive in 3 out of 4 attempts (“3-hitters”, light green), fifteen were positive in 2 out of 4 attempts (“2-hitters”, light orange), and fourteen were found in only 1 attempt (“1-hitters”, light blue). The 16 high-confidence sites (4-hitters and 3-hitters) are shown in Fig 2.2. The p-tau phosphorylation patterns were further compared with sites phosphorylated by GSK-3β, found in paired helical filament (PHF) samples, and to those used for NFT staging [20, 21]. The frequency distribution of each class is shown in Table 2.4. Overall, 31 PIMAX p-tau phosphorylation sites are also phosphorylated residues in PHFs. Nine high-confidence sites are phospho-markers for NFT staging, suggesting disease relevance of PIMAX p-tau. Moreover, there is a strong correlation between high-confidence PIMAX p-tau phosphorylation and the reported GSK-3β targets. Seven 4-hitters (88%) and six 3-hitters (75%) were previously shown to be substrates of the GSK-3β kinase [22]. Overall, these independently identified p-tau phosphorylation sites exhibit substantial overlapping with clinical markers and documented GSK-3β substrates.

Table 2.3 Summary of PIMAX p-tau phosphorylation sites mapping by mass spectrometry. The four MS attempts were done by Cayman Chemical (Ann Arbor, MI), Dr. Yeou-Guang Tsay's group (at National Yang Ming University, Taiwan), MSU Mass Spectrometry and Metabolomics Core and Dr. Philip C. Andrews' group at MSU. The first column shows all serine, threonine, and tyrosine residues of the longest tau isoform, 2N4R. Phosphorylated residues are shaded according to the number of repetitions among the four assays. The last column marks phosphorylated residues used for NFT staging in reference [20] or [21].

Ser/Thr/Tyr	MS #1	MS #2	MS #3	MS #4	Reported GSK-3β sites	PHF sites	AD staging*
T17							
Y18						√	
Y29			+				
T30			+				
T39			+				
S46	+		+		√	√	
T50	+	+	+		√		
T52		+	+				
S56							
S61							
T63							
S64							
S68						√	
T69				+	√	√	
T71						√	
T76							
T95							
T101							
T102							
T111	+	+		+			
S113						√	
T123						√	
S129							
S131							
T135							
S137							
T149	+				√	√	
T153	+				√	√	√Ref[20]

Table 2.3 (cont'd)

S162						√	
S169	+		+			√	
T175	+	+	+	+	√	√	√ Ref[20]
T181	+	+	+	+	√	√	√ Ref[20]
S184					√	√	
S185						√	
S191			+	+			
S195			+	+	√	√	
Y197			+	+		√	
S198			+	+	√	√	
S199	+	+	+		√	√	√ Ref[20, 21]
S202	+		+	+	√	√	√ Ref[20, 21]
T205		+	+	+	√	√	√ Ref[20, 21]
S208				+		√	
S210					√	√	
T212	+		+		√	√	√ Ref[20]
S214			+		√	√	√ Ref[20]
T217	+	+	+	+	√		
T220	+	+			√	√	
T231	+		+	+	√	√	√ Ref[20]
S235	+		+		√	√	
S237					√	√	
S238				+			
S241					√		
T245	+				√	√	
S258					√	√	
S262					√		√ Ref[20]
T263							
S285					√	√	
S289	+		+		√		
S292							
S305	+		+		√		
S316							
T319							
S320	+						
S324	+			+	√		
S341							
S352					√		
S356	+				√	√	√ Ref[20]
S361							
T373	+		+		√		
T377							
T386							
Y394	+					√	
S396	+	+	+	+	√	√	√ Ref[20]
S400	+	+	+	+	√	√	

Table 2.3 (cont'd)

T403	+	+	+	+		√	
S404	+	+	+	+	√	√	√ **Ref[20]**
S409	+		+	+	√	√	
S412	+					√	
S413			+	+	√	√	
T414						√	
S416	+	+	+			√	
S422	+	+	+		√	√	√ **Ref[20]**
T427						√	
S433						√	
S435						√	
peptide coverage	**98%**	**92.7%**	**49%**	**85%**			
# p-tau phos. sites	**31**	**16**	**32**	**21**			

Table 2.4 Strong correlations between high-confidence p-tau phosphorylation sites and those reported GSK-3β target residues, the phosphorylation sites found in PHFs in AD and the sites used for NFT staging.

		Overlap with…			
	# sites	GSK	PHF	GSK+PHF	staging
4-hitters	8	7	7	6	5
3-hitters	8	6	6	5	4
2-hitters	15	12	10	8	2
1-hitters	14	5	8	5	2
	45	30	31	24	13

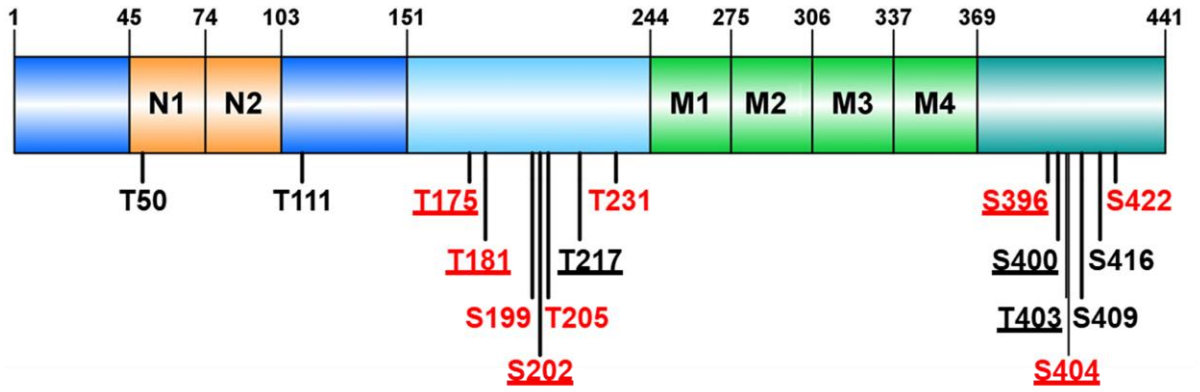

Figure 2.2 Hyperphosphorylated tau (p-tau) produced via PIMAX system bears disease-relevant phosphorylation sites. Mass spectrometry (MS) assays were done in four biological replicates of different batches of 1N4R p-tau. The sixteen high-confidence phosphorylation sites that are detected in at least 3 out of 4 attempts are shown. Phosphoepitopes used for NFT staging [20, 21] are marked by red color. Underlined sites are “4-hitters”.

P-tau elicits cytotoxicity, triggers apoptosis and raises cytoplasmic superoxide levels

Neuron loss underlies irreversible neurodegeneration. An anticipated trait for a disease-relevant AD screen subject would be the ability to cause dysfunction or even death to cells. To test whether p-tau and its aggregation intermediates affected cell viability, p-tau harvested from 0, 24-, 48-, 72-, 96- and 120-hr inducer-free aggregation reactions were added to SH-SY5Y neuroblastoma cells at final concentrations of 0.2, 0.6 or 0.8 μM. Sixteen hours later cells were collected for simultaneous staining of fluorescein diacetate (FDA) and propidium iodide (PI). FDA is converted by cellular esterases into a fluorogenic fluorescein, therefore revealing live cells [23]. PI is excluded by living cells, but diffuses into dead cells and binds nucleic acid [24]. FDA/PI differential staining thus provides a quantitative assessment of cellular viability. The cell viability loss was proportional to p-tau concentration and the duration of aggregation up to 48 hours of pre-aggregation (Fig 2.3A). Remarkably, the 72 – 120 hr p-tau aggregates became progressively less toxic than the 24- and 48-hr samples. The aggregation duration-dependent decreases of p-tau cytotoxicity are consistent with the notion that the oligomeric p-tau aggregates confer toxicity to cells, but larger species are less damaging, probably because larger molecular ensembles are too massive to diffuse effectively [126]. The human embryonic kidney (HEK) 293T cells were also susceptible to p-tau toxicity, but were slightly less sensitive compared to SH-SY5Y cells (Fig 2.3B). In stark contrast to the potent cell killing activity, 1 μM of unmodified tau did not have a discernible effect on cell survival (Fig 2.3B, gray bar) [25].

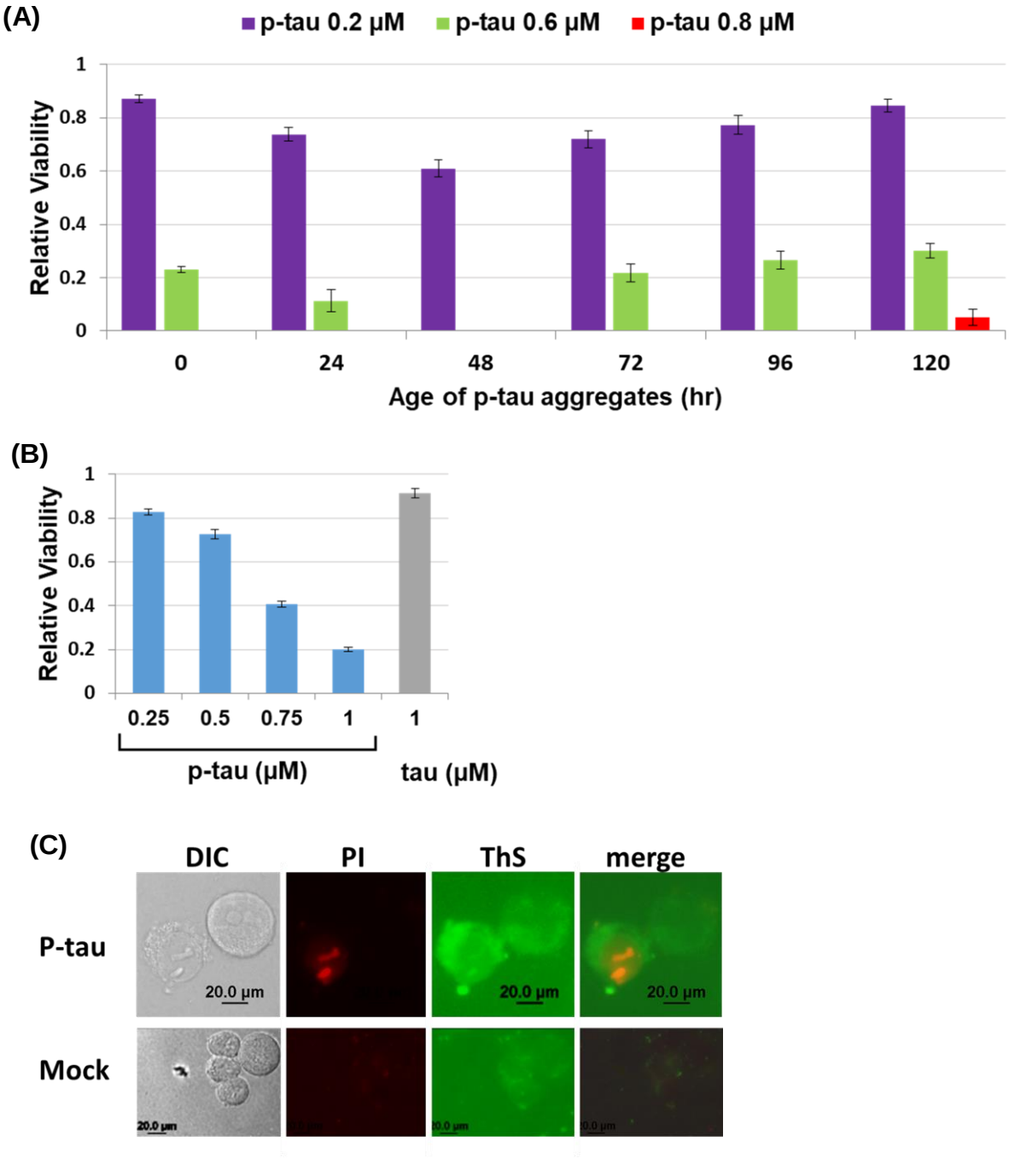

Figure 2.3 P-tau triggers cell death.

Figure 2.3 (cont'd)

(A) Monitoring SH-SY5Y cell survival as a function of p-tau concentration and extent of aggregation. The viability of cells after 16-hr treatment of 0.2 – 0.8 μM of p-tau pre-aggregated for 0 – 120 hrs was quantified by fluorescein diacetate (FDA) and propidium iodide (PI) differential staining. (B) The viability of HEK 293T cells after 24-hr treatment of 0.25 – 1 μM of p-tau or 1 μM of tau pre-aggregated for 24 hrs. Error bars are standard deviation; n = 3. (C) P-tau treated cells can be stained by ThS. 5-hr 0.6 μM of p-tau or buffer mock-treated HEK 293T cells were harvested for ThS and PI staining and visualized microscopically.

To understand the molecular basis for p-tau mediated cell death, I first tested whether p-tau entered cells by staining cells with thioflavin S (ThS) for microscopic scrunity. ThS displays enhanced fluorescence when binding to β sheet-rich fibrillar structures in amyloid aggregates [58], thus its signal indicates the location of p-tau aggregates. HEK 293T cells treated with 0.6 μM of p-tau for 5 hours were stained by ThS and PI (Fig 2.3C). ThS fluorescence was readily detectable in the cytoplasm of dead cells (PI positive) after p-tau treatment, suggesting uptake of p-tau fibrils by cells or diffusion of p-tau into dying cells with disintegrated membrane.

I then tested whether the p-tau-elicited cell death was associated with apoptosis. To this end, I performed annexin V staining. Apoptosis is a regulated and energy-dependent process of cell death, and dysregulated apoptosis is linked to disease conditions including cancer and neurodegenerative diseases [26]. Annexin V is a cytoplasmic membrane marker that stains phosphatidylserine [27]. Phosphatidylserine normally exists at the inner leaflet of the membrane, whereas it’s exposed at the surface of apoptotic cells due to a loss of membrane phospholipid asymmetry [27]. The staining ability of fluorescein isothiocyanate (FITC)-conjugated Annexin V was verified by cells after the treatment of velcade, a known cell apoptosis inducer [33] (Fig 2.4 C, rightmost bar). SH-SY5Y or HEK 293T cells after 24-hr p-tau treatment were doubled stained by FITC-conjugated Annexin V and PI. Early apoptotic cells were stained by Annexin V but not by PI, while cells in late apoptosis or already dead were stained by both. Fig 2.4 A and B show that both SH-SY5Y and HEK 293T cells were susceptible to p-tau's apoptosis-inducing activity. The total amount of apoptotic cells (Annexin positive) is propotional to the concentration of p-tau added to the cells (Fig 2.4C).

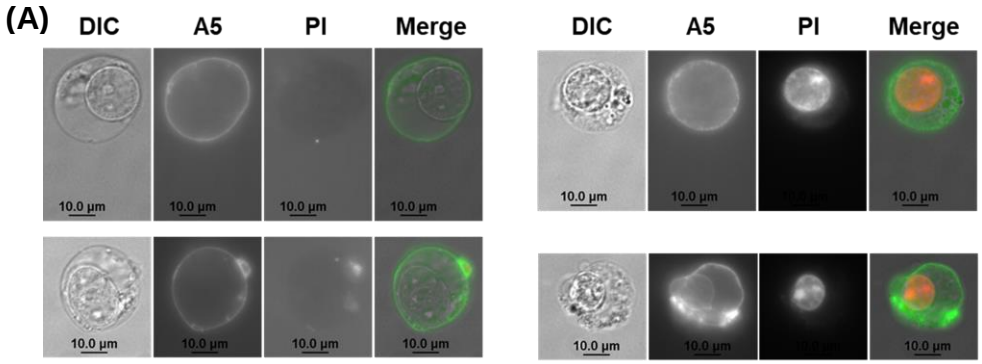
(A)
DIC
A5
PI
Merge
DIC
A5
PI
Merge
10.0 µm

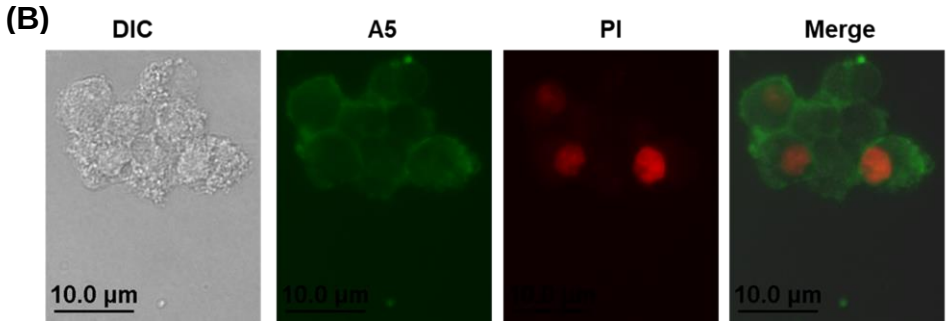
(B)
DIC
A5
PI
Merge
10.0 µm

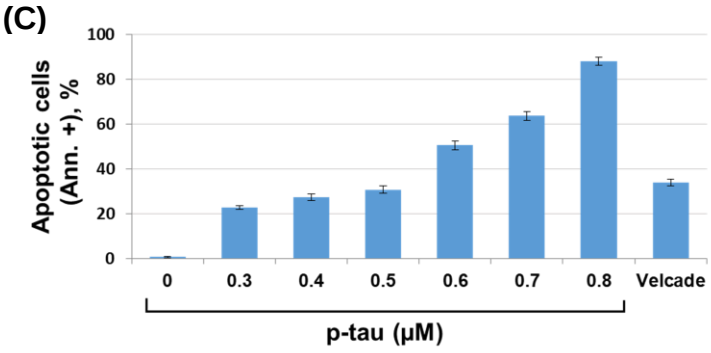
(C)
Apoptotic cells (Ann. +), %
100
80
60
40
20
0
0
0.3
0.4
0.5
0.6
0.7
0.8
Velcade
p-tau (µM)

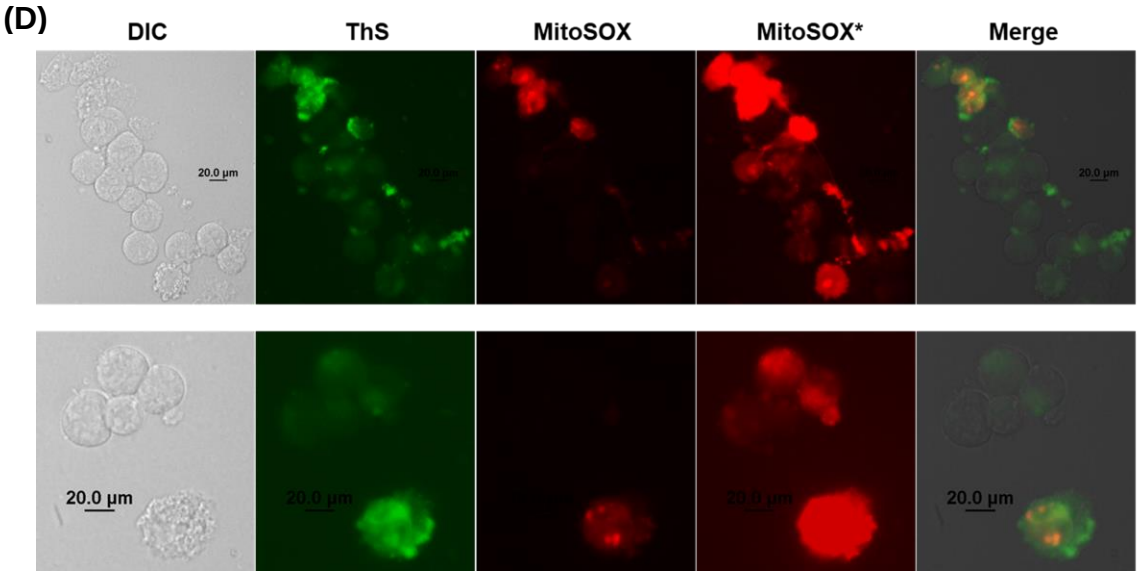
(D)
DIC
ThS
MitoSOX
MitoSOX*
Merge
20.0 µm

Figure 2.4 (cont'd)

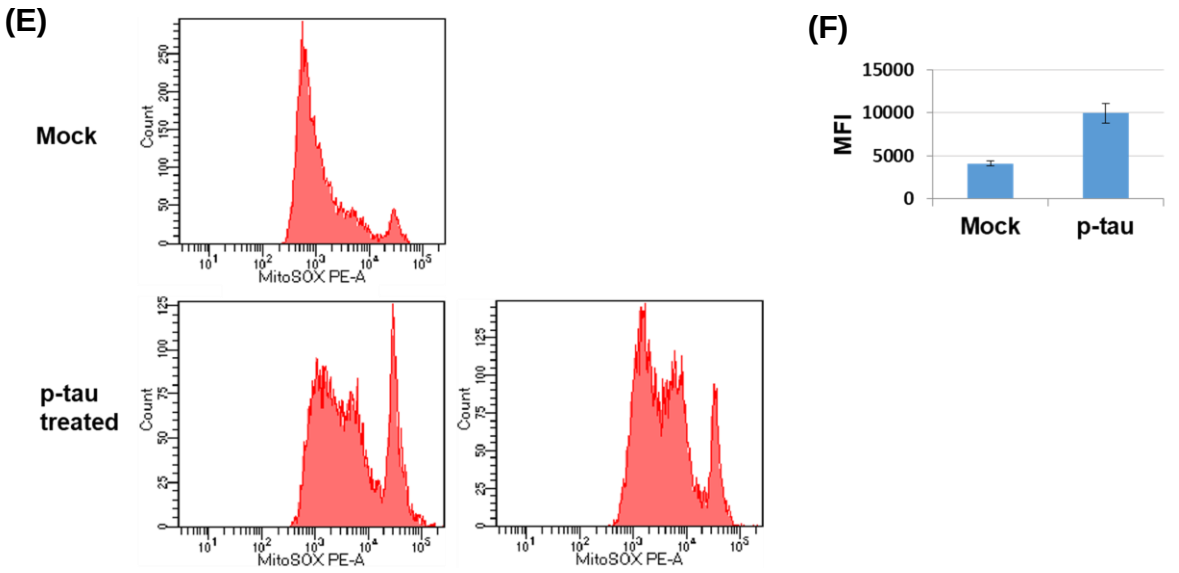

Figure 2.4 P-tau triggers apoptosis and mitochondrial superoxide production. (A) SH-SY5Y or (B) HEK 293T cells after p-tau treatment were examined by FITC-Annexin V and PI double staning. Here shows the existence of both early apoptotic (Annexin V positive and PI negative) and late apoptotic or already dead (Annexin V and PI both positive) cells. (C) Percentage of apoptotic HEK 293T cells (Annexin V positive) after 12-hr treatment of 0.3 – 0.8 µM p-tau or 2 mM Velcade, an apoptosis inducer [33]. Error bars are standard deviation; n = 3. (D) P-tau treated HEK 293T cells were examined by MitoSOX and ThS double staining. MitoSOX*, longer exposure of MitoSOX staining images to see "normal cells". DIC: differential interference contract. (E) Flow cytometry analysis of MitoSOX stained p-tau treated SH-SY5Y cells. 20 mM Tris (pH7.4) buffer was used as mock treatment. The mean fluorescence intensity (MFI) is shown in (F). Error bars show range. Flow cytometry was done by Stacy Hovde.

Tau protein, especially tau oligomers are involved in the mitochondrial dysfunction at synapses [28, 29], which may further trigger apoptosis [29-31]. The amount of mitochondrial superoxide was monitored by MitoSOX staining. MitoSOX selectively targets mitochondria, where it is oxidized and assumes high affinity for mitochondrial DNA as indicated by red fluorescence [32]. Most cells were weakly stained by MitoSOX, consistent with the constant production of small amounts of superoxide by mitochondria [59]. However, among the ThS positive stained cells, which most likely absorbed p-tau from the medium, the MitoSOX signal was elevated dramatically (Fig 2.4D, with “normal” exposure and overexposure *). To gain a more quantitative assessment of superoxide production after p-tau treatment, flow cytometry was performed to quantify the MitoSOX fluorescence, which shows a significant elevation in the mitochondrial superoxide production in SH-SY5Y cells after p-tau treatment (Fig 2.4E, F). Together, these results suggest that internalized p-tau contributes to raising superoxide level and mitonchondria damage, which further results in apoptosis.

Seeding activity of p-tau potentiates tau aggregation and cytotoxicity

Another feature of disease-linked tau is the ability to nucleate aggregation of normal tau [34]. To examine the seeding activity of PIMAX p-tau on unmodified tau aggregation, 9 µM of tau was mixed with 0, 1, 3, 6, 9 µM of p-tau and applied for ThS aggregation assessment (Fig 2.5A). At 9 µM, tau by itself did not show detectable fibrillization. Adding p-tau to tau without any inducer resulted in net increases of ThS signals greater than the sum of tau and p-tau aggregation if performed separately. To see whether the unphosphorylated tau assumed cytotoxicity in the presence of p-tau as anticipated from AD pathogenesis, HEK 293T cells were treated with tau (0.9 µM, without pre-incubation) supplemented with 0 – 0.9 µM of p-tau (also without pre-aggregation) (Fig 2.5B). 0.9 µM of tau alone caused less than 5% of cell death. The percentage of live cells decreased steadily with p-tau supplement. At 0.6 µM, p-tau alone caused 17% of cell death, but the combined action of tau and p-tau reached 60% killing. The simplest explanation for Fig. 2.5 would be that p-tau nucleated the conversion of the otherwise benign tau into cytotoxic aggregates. P-tau produced by PIMAX exhibits a seeding activity that augments both tau aggregation and cell killing.

In conclusion, in vitro data showed clearly that p-tau produced by the PIMAX approach possessed disease-relevant sites of phosphorylation, and was toxic to tissue culture cells. The cytotoxicity was likely due to damages to mitochondria, thus resulting in a burst of superoxide, which may in turn activate the apoptosis pathway.

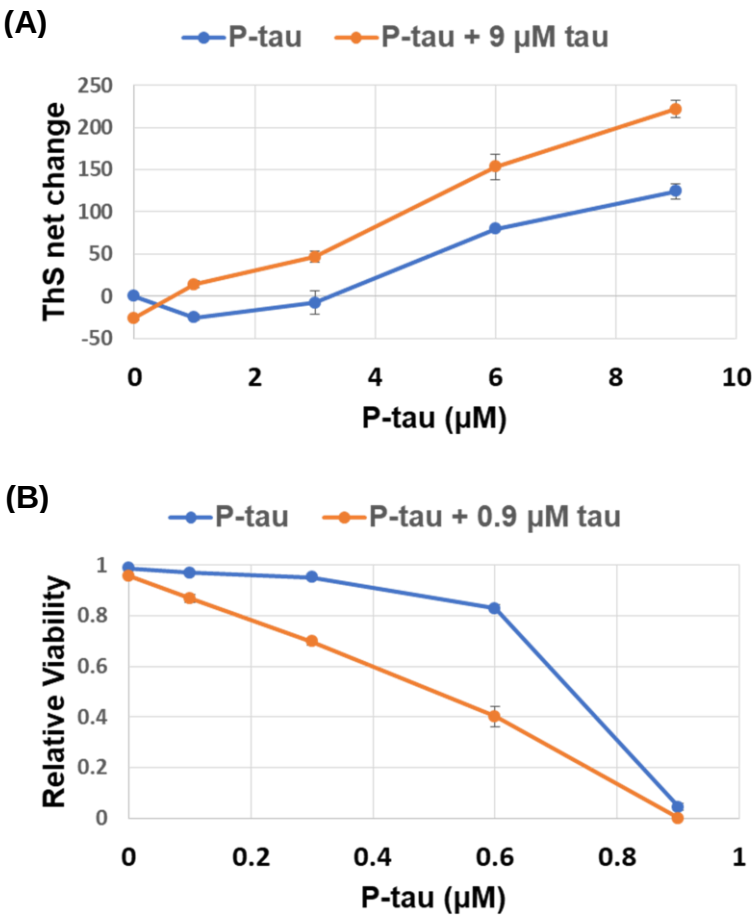

Figure 2.5 Seeding activity of p-tau potentiates tau aggregation and cytotoxicity. (A) Inducer-free aggregation reactions with tau, p-tau, or a mixture of these two proteins were monitored for 16 hrs. Comparison of ThS net changes is shown. (B) P-tau converts tau into a cytotoxic species. HEK 293T cells were treated with 0.9 µM of unaggregated tau supplemented with 0 – 0.9 µM of p-tau (no pre-aggregation) for 24 hours before FDA and PI staining. Error bars are standard deviation; n = 3.

DISCUSSION

Here I show that hyperphosphorylated tau (p-tau) generated by PIMAX exhibits anticipated pathogenic activities that render this protein a proper subject for large-scale AD drug screening. PIMAX p-tau possesses phosphorylation sites that significantly overlap with AD-related phosphorylation sites. Unlike the unmodified tau that typically requires an inducer such as heparin and arachidonic acid for fibrillization, no inducer is required for p-tau aggregation. This provides a significant advantage in that p-tau aggregation-based drug screen (see Chapter III) is not subjected to the interference of compounds that act on the inducer or the p-tau-inducer interaction interface.

Given the relevance of hyperphosphorylation to neurodegeneration, different means have been used to prepare phosphorylated tau. Phosphorylated tau has been made previously by incubating tau protein with recombinant GSK-3β kinase in vitro for 20 hours [35]. The phosphorylated tau in this work contained 3 moles of phosphates per mole of tau. The pattern of phosphorylation or whether this tau was able to form cytotoxic aggregates without an inducer was not reported, therefore the pathophysiological relevance was not substantiated. An alternative kinase source was the use of a 100,000 x g rat brain crude extract to phosphorylate recombinant tau in vitro. This method produced a stoicheometry of 12-15 moles phosphate per mole of tau after 24-hr incubation, and the [^{32}P] incorporation to tau continuted to increase even after 24 hours [38]. This non-saturating nature of labelling raises a concern of non-enzymatic phospho-labelling. There were no data on the kinetics of fibrillzation. A rather stunning result was that this phosphorylated tau formed micrometer-long fibrils within 90 minutes (10 - 20 nm thick). This incredibly fast fibril formation suggested strongly that

during the hour-long phosphorylation reaction, fibrillzation has already proceeded significantly. Overall, this method was "dirty" and inappropriate for high-throughput screening. Another baculoviral expression system produced a tau containing up to 20 phosphates (P20) per molecule after the treatment of okadaic acid, a potent phosphatase inhibitor [39]. This P20-tau did not form the canonical fibrils that were quantifiable by dyes such as thioflavin S, and has a negligible effect on cell survival. Lastly, biochemical purification of hyperphosphorylated tau from the disease brain, though feasible, is faced with the challenge of heterogeneity in tau isoforms and additional post-translational modifications [40], as well as molecules co-purified from neurofibrillary tangles [41].

PIMAX p-tau triggers cell death in both SH-SY5Y neuroblastoma and human embryonic kidney (HEK) 293T cells. Unphosphorylated tau has no effect on the viability under the same assay conditions, which is consistent with the failure of detecting the cytotoxicity of tau monomer and fibrils in cell-based assays in the literature [43]. Two kinds of tau species, 2N4R wild-type and tauRDΔK280 have been used for cell survival tests using SH-SY5Y cells [43]. TauRDΔK280 is the four repeat domains (RD) containing an FTDP-17 mutation ΔK280, which facilitates tau aggregation [42]. Pre-incubating this mutant core of tau for 48 hours resulted in 20% reduction in cell viability when as much as 10 μM of the protein was used [43]. Unphosphorylated tau therefore is deemed as non-toxic to cells under typical growth conditions.

The detection of live (PI negative) cells with a sign of apoptosis (Annexin V positive) in both HEK 293T and SH-SY5Y cells indicates that PIMAX p-tau triggers apoptosis before massive cell death. Tau expression in HEK 293T is negligible [49], but

transfected tau can be phosphorylated in HEK 293T cells [50]. Undifferentiated SH-SY5Y cells express a single tau 3R isoform that predominantly locates in the nucleus [51]. SH-SY5Y-expressed tau is phosphorylated at Ser199/202 [52, 53], both are disease-related, but the proportaion of this species among the entire population is not clear. However, this discovery suggested that SH-SY5Y may offer its native tau if invated by a cytotoxic, prion-like tau, such as the PIMAX p-tau under the current study. Indeed, we consistently saw that the SH-SY5Y cells were more sensitive to p-tau than HEK 293T cells. Using the tau-deficient HEK 293T cells, cytoplasmic staining by ThS was readily observable after p-tau treatment, suggesting the p-tau entered cells. However, whether this was due to an active uptake mechanism remains to be delineated. Futhermore, ThS and MitoSOX co-staining showed clear overlap of cytoplasmic ThS and strongly elevated MitoSOX signals, suggesting an intriguing possibility of chain events that includes cellular active uptake or diffusion of p-tau, followed by superoxide elevation via mitochondrial disfunction or cytoplasmic calcium surge [54], increased mitochondrial membrane permeability [55] and eventually caspase activation and apoptosis [56, 57] (Fig 2.6). Detailed tests of this model will be one of the future research focuses.

In conclusion, hyperphosphorylated tau (p-tau) expressed by the PIMAX approach possesses clinically relevant sites of phosphorylation, fibrillizes efficiently, and triggers apoptosis, superoxide production and cell death at sub-micromolar concentrations. All these indicate PIMAX p-tau has higher AD disease relevance and therapeutic value as a target for AD drug screening.

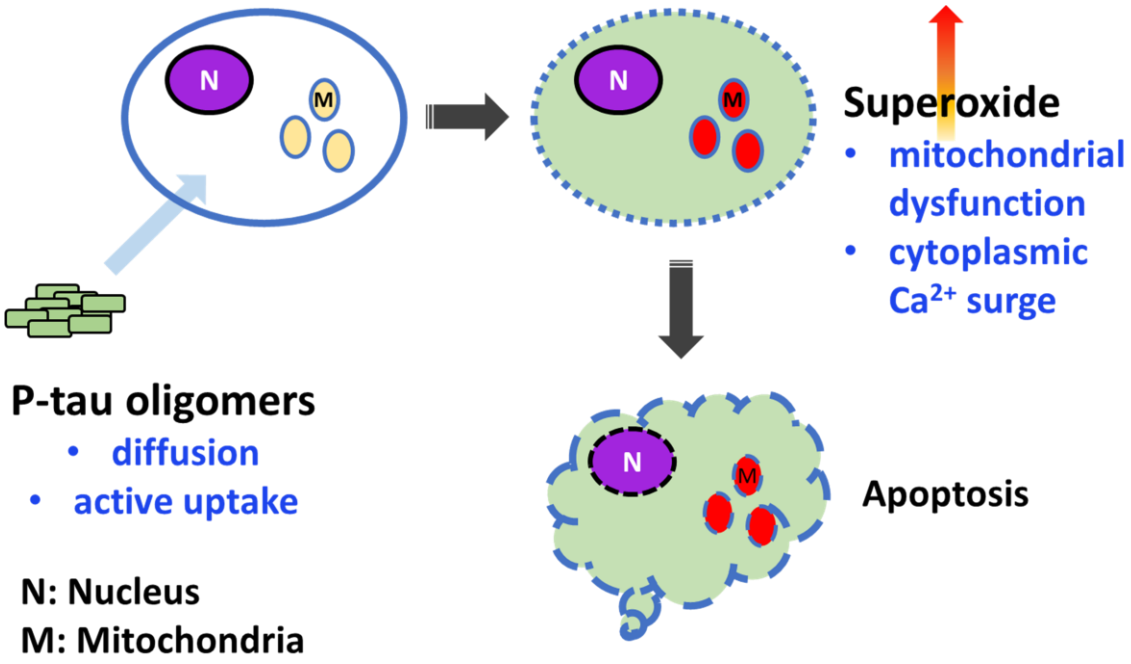

Figure 2.6 Schematic model of p-tau cytotoxicity. P-tau aggregates entered cells by either diffusion or active uptake. P-tau in the cells induced enhanced superoxide production by causing mitochondrial dysfunction or cytoplasmic calcium surge. Elevated superoxide further triggers apoptosis.

REFERENCES

REFERENCES

1. Bancher C, Brunner C, Lassmann H, Budka H, Jellinger K, Wiche G, Seitelberger F, Grundke-Iqbal I, Iqbal K, Wisniewski HM. 1989. Accumulation of abnormally phosphorylated tau precedes the formation of neurofibrillary tangles in Alzheimer's disease. Brain Res. 477(1-2):90-9.

2. Arendt T, Stieler JT, Holzer M. 2016. Tau and tauopathies. Brain Res Bull. 126(Pt 3):238-292.

3. Köpke E, Tung YC, Shaikh S, Alonso AC, Iqbal K, Grundke-Iqbal I. 1993. Microtubule-associated protein tau. Abnormal phosphorylation of a non-paired helical filament pool in Alzheimer disease. J Biol Chem. 268(32):24374-84.

4. Martin L, Latypova X, Wilson CM, Magnaudeix A, Perrin ML, Yardin C, Terro F. 2013. Tau protein kinases: involvement in Alzheimer's disease. Ageing Res Rev. 12(1):289-309.

5. Ihara Y, Nukina N, Miura R, Ogawara M. 1986. Phosphorylated tau protein is integrated into paired helical filaments in Alzheimer’s disease. J Biochem. 99(6):1807-10.

6. Chirita CN, Necula M, Kuret J. 2003. Anionic micelles and vesicles induce tau fibrillization in vitro. J Biol Chem. 278(28):25644-50.

7. Goedert M, Jakes R, Spillantini MG, Hasegawa M, Smith MJ, Crowther RA. 1996. Assembly of microtubule-associated protein tau into Alzheimer-like filaments induced by sulphated glycosaminoglycans. Nature. 383(6600):550-3.

8. Schweers O, Mandelkow EM, Biernat J, Mandelkow E. 1995. Oxidation of cysteine-322 in the repeat domain of microtubule-associated protein tau controls the in vitro assembly of paired helical filaments. Proc Natl Acad Sci U S A. 92(18):8463-7.

9. Barghorn S, Biernat J, Mandelkow E. 2005. Purification of recombinant tau protein and preparation of Alzheimer-paired helical filaments in vitro. Methods Mol Biol. 299:35-51.

10. Crowe A, Huang W, Ballatore C, Johnson RL, Hogan AM, Huang R, Wichterman J, McCoy J, Huryn D, Auld DS, Smith AB 3rd, Inglese J, Trojanowski JQ, Austin CP, Brunden KR, Lee VM. 2009. Identification of aminothienopyridazine inhibitors of tau assembly by quantitative high-throughput screening. Biochemistry. 48(32):7732-45.

11. Wischik CM, Staff RT, Wischik DJ, Bentham P, Murray AD, Storey JM, Kook KA,

Harrington CR. 2015. Tau aggregation inhibitor therapy: an exploratory phase 2 study in mild or moderate Alzheimer's disease. J Alzheimers Dis. 44(2):705-20.

12. Gauthier S, Feldman HH, Schneider LS, Wilcock GK, Frisoni GB, Hardlund JH, Moebius HJ, Bentham P, Kook KA, Wischik DJ, Schelter BO, Davis CS, Staff RT, Bracoud L, Shamsi K, Storey JM, Harrington CR, Wischik CM. 2016. Efficacy and safety of tau-aggregation inhibitor therapy in patients with mild or moderate Alzheimer's disease: a randomised, controlled, double-blind, parallel-arm, phase 3 trial. Lancet. 388(10062):2873-2884.

13. Sui D, Xu X, Ye X, Liu M, Mianecki M, Rattanasinchai C, Buehl C, Deng X, Kuo MH. 2015. Protein interaction module-assisted function X (PIMAX) approach to producing challenging proteins including hyperphosphorylated tau and active CDK5/p25 kinase complex. Mol Cell Proteomics. 14(1):251-62.

14. Hanger DP, Anderton BH, Noble W. 2009. Tau phosphorylation: the therapeutic challenge for neurodegenerative disease. Trends Mol Med. 15(3):112-9.

15. Liu NY, Lee HH, Chang ZF, Tsay YG. 2015. Examination of segmental average mass spectra from liquid chromatography-tandem mass spectrometric (LC-MS/MS) data enables screening of multiple types of protein modifications. Anal Chim Acta. 892:115-22.

16. Ransone LJ1, Visvader J, Sassone-Corsi P, Verma IM. 1989. Fos-Jun interaction: mutational analysis of the leucine zipper domain of both proteins. Genes Dev. 3(6):770-81.

17. Ekman P, Jäger O. 1993. Quantification of subnanomolar amounts of phosphate bound to seryl and threonyl residues in phosphoproteins using alkaline hydrolysis and malachite green. Anal Biochem. 214(1):138-41.

18. Maeda S, Sahara N, Saito Y, Murayama M, Yoshiike Y, Kim H, Miyasaka T, Murayama S, Ikai A, Takashima A. 2007. Granular tau oligomers as intermediates of tau filaments. Biochemistry. 46(12):3856-61.

19. Lasagna-Reeves CA, Sengupta U, Castillo-Carranza D, Gerson JE, Guerrero-Munoz M, Troncoso JC, Jackson GR, Kayed R. 2014. The formation of tau pore-like structures is prevalent and cell specific: possible implications for the disease phenotypes. Acta Neuropathol Commun. 2:56.

20. Nelson PT, Alafuzoff I, Bigio EH, Bouras C, Braak H, Cairns NJ, Castellani RJ, Crain BJ, Davies P, Del Tredici K, Duyckaerts C, Frosch MP, Haroutunian V, Hof PR, Hulette CM, Hyman BT, Iwatsubo T, Jellinger KA, Jicha GA, Kövari E, Kukull WA, Leverenz JB, Love S, Mackenzie IR, Mann DM, Masliah E, McKee AC, Montine TJ, Morris JC, Schneider JA, Sonnen JA, Thal DR, Trojanowski JQ, Troncoso JC, Wisniewski T, Woltjer RL, Beach TG. 2012. Correlation of Alzheimer disease

neuropathologic changes with cognitive status: a review of the literature. *J Neuropathol Exp Neurol* 71(5):362-381. J Neuropathol Exp Neurol. 71(5):362-81.

21. Augustinack JC, Schneider A, Mandelkow EM, Hyman BT. 2002. Specific tau phosphorylation sites correlate with severity of neuronal cytopathology in Alzheimer's disease. Acta Neuropathol. 103(1):26-35.

22. Hanger DP, Anderton BH, Noble W. 2009. Tau phosphorylation: the therapeutic challenge for neurodegenerative disease. Trends Mol Med. 15(3):112-9.

23. D. A. Fontvieille, A. Outaguerouine, Daniel Thevenot. 1992. Fluorescein diacetate hydrolysis as a measureof microbial activity in aquatic systems: Application to activated sludges. Environmental Technology. 13 (6): 531-540.

24. Suzuki T, Fujikura K, Higashiyama T, Takata K. 1997. DNA staining for fluorescence and laser confocal microscopy. J Histochem Cytochem. 45(1):49-53.

25. Kumar S, Tepper K, Kaniyappan S, Biernat J, Wegmann S, Mandelkow EM, Müller DJ, Mandelkow E. 2014. Stages and conformations of the Tau repeat domain during aggregation and its effect on neuronal toxicity. J Biol Chem. 289(29):20318-32.

26. Elmore S. 2007. Apoptosis: A Review of Programmed Cell Death. Toxicol Pathol. 35(4):495-516.

27. Koopman G, Reutelingsperger CP, Kuijten GA, Keehnen RM, Pals ST, van Oers MH. 1994. Annexin V for flow cytometric detection of phosphatidylserine expression on B cells undergoing apoptosis. Blood. 84(5):1415-20.

28. Pérez MJ, Jara C, Quintanilla RA. 2018. Contribution of Tau Pathology to Mitochondrial Impairment in Neurodegeneration. Front Neurosci. 12:441.

29. Lasagna-Reeves CA, Castillo-Carranza DL, Sengupta U, Clos AL, Jackson GR, Kayed R. 2011. Tau oligomers impair memory and induce synaptic and mitochondrial dysfunction in wild-type mice. Mol Neurodegener. 6:39.

30. Zilkova M, Zilka N, Kovac A, Kovacech B, Skrabana R, Skrabanova M, Novak M. 2011. Hyperphosphorylated truncated protein tau induces caspase-3 independent apoptosis-like pathway in the Alzheimer's disease cellular model. J Alzheimers Dis. 23(1):161-9.

31. Shafiei SS, Guerrero-Muñoz MJ, Castillo-Carranza DL. 2017. Tau Oligomers: Cytotoxicity, Propagation, and Mitochondrial Damage. Front Aging Neurosci. 9:83.

32. Partha Mukhopadhyay, Mohanraj Rajesh, György Haskó, Brian J Hawkins, Muniswamy Madesh, and Pál Pacher. 2007. Simultaneous detection of apoptosis and

mitochondrial superoxide production in live cells by flow cytometry and confocal microscopy. Nat Protoc. 2007; 2(9): 2295–2301.

33. Poulaki V, Mitsiades CS, Kotoula V, Negri J, McMillin D, Miller JW, Mitsiades N. 2007. The proteasome inhibitor bortezomib induces apoptosis in human retinoblastoma cell lines in vitro. Invest Ophthalmol Vis Sci. 48(10):4706-19.

34. Falcon B, Cavallini A, Angers R, Glover S, Murray TK, Barnham L, Jackson S, O'Neill MJ, Isaacs AM, Hutton ML, Szekeres PG, Goedert M, Bose S. 2015. Conformation determines the seeding potencies of native and recombinant Tau aggregates. J Biol Chem. 290(2):1049-65.

35. Rankin CA, Sun Q, Gamblin TC. 2007. Tau phosphorylation by GSK-3beta promotes tangle-like filament morphology. Mol Neurodegener. 2:12.

36. Zhu HL, Fernández C, Fan JB, Shewmaker F, Chen J, Minton AP, Liang Y. 2010. Quantitative characterization of heparin binding to Tau protein: implication for inducer-mediated Tau filament formation. J Biol Chem. 285(6):3592-9.

37. Pickhardt M, Neumann T, Schwizer D, Callaway K, Vendruscolo M, Schenk D, St George-Hyslop P, Mandelkow EM, Dobson CM, McConlogue L, Mandelkow E, Tóth G. Identification of Small Molecule Inhibitors of Tau Aggregation by Targeting Monomeric Tau As a Potential Therapeutic Approach for Tauopathies. Curr Alzheimer Res. 12(9):814-28.

38. Alonso A, Zaidi T, Novak M, Grundke-Iqbal I, Iqbal K. 2001. Hyperphosphorylation induces self-assembly of tau into tangles of paired helical filaments/straight filaments. Proc Natl Acad Sci U S A. 98(12):6923-8.

39. Tepper K, Biernat J, Kumar S, Wegmann S, Timm T, Hübschmann S, Redecke L, Mandelkow EM, Müller DJ, Mandelkow E. 2014. Oligomer formation of tau protein hyperphosphorylated in cells. J Biol Chem. 289(49):34389-407.

40. Russell CL, Koncarevic S, Ward MA. 2014. Post-translational modifications in Alzheimer's disease and the potential for new biomarkers. J Alzheimers Dis. 41(2):345-64.

41. Wang Q, Woltjer RL, Cimino PJ, Pan C, Montine KS, Zhang J, Montine TJ. 2005. Proteomic analysis of neurofibrillary tangles in Alzheimer disease identifies GAPDH as a detergent-insoluble paired helical filament tau binding protein. FASEB J. 19(7):869-71.

42. Khlistunova I, Biernat J, Wang Y, Pickhardt M, von Bergen M, Gazova Z, Mandelkow E, Mandelkow EM. 2006. Inducible expression of Tau repeat domain in cell models of tauopathy: aggregation is toxic to cells but can be reversed by inhibitor drugs. J Biol Chem. 281(2):1205-14.

43. Kumar S, Tepper K, Kaniyappan S, Biernat J, Wegmann S, Mandelkow EM, Müller DJ, Mandelkow E. 2014. Stages and conformations of the Tau repeat domain during aggregation and its effect on neuronal toxicity. J Biol Chem. 289(29):20318-32.

44. Bandyopadhyay B, Li G, Yin H, Kuret J. 2007. Tau aggregation and toxicity in a cell culture model of tauopathy. J Biol Chem. 282(22):16454-64.

45. Khatoon S, Grundke-Iqbal I, Iqbal K. 1992. Brain levels of microtubule-associated protein tau are elevated in Alzheimer's disease: a radioimmuno-slot-blot assay for nanograms of the protein. J Neurochem.59(2):750-3.

46. Butner KA, Kirschner MW. 1991. Tau protein binds to microtubules through a flexible array of distributed weak sites. J Cell Biol. 115(3):717-30.

47. Pickhardt M, Biernat J, Hübschmann S, Dennissen FJA, Timm T, Aho A, Mandelkow EM, Mandelkow E. 2017. Time course of Tau toxicity and pharmacologic prevention in a cell model of Tauopathy. Neurobiol Aging. 57:47-63.

48. Schneider A, Biernat J, von Bergen M, Mandelkow E, Mandelkow EM. 1999. Phosphorylation that detaches tau protein from microtubules (Ser262, Ser214) also protects it against aggregation into Alzheimer paired helical filaments. Biochemistry. 38(12):3549-58.

49. Santa-Maria I, Hernández F, Del Rio J, Moreno FJ, Avila J. 2007. Tramiprosate, a drug of potential interest for the treatment of Alzheimer's disease, promotes an abnormal aggregation of tau. Mol Neurodegener. 2:17.

50. Houck AL, Hernández F, Ávila J. 2016. A Simple Model to Study Tau Pathology. J Exp Neurosci. 10:31-8.

51. Uberti D, Rizzini C, Spano PF, Memo M. 1997. Characterization of tau proteins in human neuroblastoma SH-SY5Y cell line. Neurosci Lett. 235(3):149-53.

52. Smith CJ, Anderton BH, Davis DR, Gallo JM. 1995. Tau isoform expression and phosphorylation state during differentiation of cultured neuronal cells. FEBS Lett. 375(3):243-8.

53. Boban M, Babić Leko M, Miškić T, Hof PR, Šimić G. 2018. Human neuroblastoma SH-SY5Y cells treated with okadaic acid express phosphorylated high molecular weight tau-immunoreactive protein species. J Neurosci Methods. pii: S0165-0270(18)30297-8.

54. Görlach A, Bertram K, Hudecova S, Krizanova O. 2015. Calcium and ROS: A mutual interplay. Redox Biol. 6:260-271.

55. Guo C, Sun L, Chen X, Zhang D. 2013. Oxidative stress, mitochondrial damage and neurodegenerative diseases. Neural Regen Res. 8(21):2003-14.

56. Liu X, Kim CN, Yang J, Jemmerson R, Wang X. 1996. Induction of apoptotic program in cell-free extracts: requirement for dATP and cytochrome c. Cell. 86(1):147-57.

57. Jiang X, Wang X. 2004. Cytochrome C-mediated apoptosis. Annu Rev Biochem. 73:87-106.

58. Biancalana M, Koide S. 2010. Molecular mechanism of Thioflavin-T binding to amyloid fibrils. Biochim Biophys Acta. 1804(7):1405-12.

59. Mukhopadhyay P, Rajesh M, Yoshihiro K, Haskó G, Pacher P. 2007. Simple quantitative detection of mitochondrial superoxide production in live cells. Biochem Biophys Res Commun. 358(1):203-8.

60. Walker LC, Jucker M. 2015. Neurodegenerative diseases: expanding the prion concept. Annu Rev Neurosci. 38:87-103.

CHAPTER III

IDENTIFICATION OF POTENTIAL ALZHEIMER'S DISEASE THERAPEUTICS BASED ON THE ABILITY TO INHIBIT AGGREGATION AND CYTOTOXICITY OF HYPERPHOSPHORYLATED TAU

ABSTRACT

Hyperphosphorylated tau (p-tau) expressed by the PIMAX approach possesses disease-relevant sites of phosphorylation, fibrillizes autonomously, and triggers apoptosis and cell death at sub-micromolar concentrations. Using the inducer-free p-tau aggregation assay and cell-based experiment as the primary and secondary assays for a 1,280-compound screen, I identified two brain permeant prescription drugs, R-(–)-apomorphine and raloxifene as potent p-tau aggregation inhibitors that also antagonized p-tau cytotoxicity. Both compounds were previously shown to preserve cognitive function in model animals and in humans. These results pave the way for high-throughput screening for therapeutics for the development of Alzheimer's disease.

INTRODUCTION

Based on the strong correlation between the spatiotemporal distribution of neurofibrillary tangles (NFTs) and the progression of cognitive impairment and disease severity [1], tau is accepeted as a legitimate target for AD therapeutics development. Current tangle-centric therapeutic strategies include: modulating tau post-translational modification especially hyperphosphorylation, maintaining microtubule stability, preventing tau aggregation, and clearance of tau tangles by anti-tau immunotherapy [2]. Identifying the exact responsible kinases in different stages of AD development and the multifunctional nature of kinases and phosphatases are mainjor challenges in controlling the enzyme activities to modulate tau phosphorylation [3]. Tau-mediated neurodegeneration likely results from gain-of-function cytotoxicty, thus microtubule stabilizers do not actually tackle the source of the problem [4, 5]. Accumulating evidence suggests that tau oligomer rather than monomer or fibril is the most toxic species [6, 7] and mediates tau propagation in AD brain [8, 9]. Therefore, modulating tau aggregation assumes the center stage of tau-based AD therapy development.

Thus far, all tau-targeting drug screening used unmodified tau as the subject. The concentration of p-tau in the frontal cortex of AD brain is 8 – 10 μM [24, 73]. In vitro experiments show that tau fibrillates rather inefficiently without phosphorylation [10-12]. It may take 3 days for 20-μM tau to form aggregates in the presence of heparin [11], and the duration extends to 10 days at the concentration of 10 μM [12]. Using the four repeat domains (K18) accelerates the process [13], but there's no such a species in the brain. Two tau mutations, P301L [14] and ΔK280 [15] are frequently used for drug screening but they lack the disease-relevant phosphorylation [14 - 17]. A method to

reduce the required tau concentration to as low as 0.5 μM requires the addition of 18.5 μM of arachidonic acid as an inducer [18]. Many compounds found by large-scale drug screening targeting unphosphorylated tau turned out to be non-specific redox modulators [14], including methylene blue, which has been tested in clinical trials [19, 20]. It failed to show benefit to cognitive functions [20]. These shortcomings of unmodified tau may have contributed to the slow progress of AD drug discovery targeting NFT genesis.

The deficiency of the current unmodified tau-based high-throughput screening prompted me to use our PIMAX p-tau for AD drug discovery. Chapter II shows that p-tau aggregation intermediates are toxic to cells. However, cell-based drug screen can be costly and inefficient. Instead, I chose to first screen for compounds that effectively inhibited p-tau aggregation then used cell-based assays as a functional secondary screen. This chapter describes my pilot screen results, and the identification of two brain permeant prescription drugs, R-(–)-apomorphine and raloxifene as potent p-tau aggregation inhibitors that also antagonized p-tau cytotoxicity.

MATERIALS AND METHODS

Materials. Prestwick FDA Approved Chemical Library was provided by MSU Assay Development and Drug Repurposing Core (ADDRC). R-(–)-apomorphine hydrochloride, raloxifene hydrochloride, fosinopril, nifedipine, nisoldipine, idebenone, itraconazole, prednicarbate and carmofur were from Cayman Chemical (Ann Arbor, MI). Fluorescein diacetate, propidium iodide, clofazimine, hexachlorophene, hydralazine hydrochloride, thioflavin S and Amicon Centrifugal Filter Unit were purchased from Sigma Aldrich (St. Louis, MO). Gibco Dulbecco's Modified Eagle Medium (DMEM), HyClone^{TM} Fetal Bovine Serum, Optical Adhesive Film and FITC-Annexin V were purchased from Thermo Fisher Scientific (Waltham, MA). Small volume, black, flat-bottom, 384-well plate was purchased from Griner Bio-One (Monroe, NC). All other chemicals for common buffers and solutions were from Sigma Aldrich (St. Louis, MO).

Plasmids and Recombinant Genes. The plasmids and primers used in this work are listed in Tables 3.1 and 3.2. Plasmid and expression procedures for the 1N4R tau and p-tau were previously described [71]. Residue 291 Cys-to-Ser mutations were generated using C291S S and C291S AS oligos, Residue 322 Cys-to-Ser mutation were generated using C322S S and C322S AS oligos by QuikChange mutagenesis. All constructs were verified by DNA sequencing.

Table 3.1 Plasmid constructs used in this study

Plasmid	Main features	Source or reference
pMK1013	His6-Fos-thrombin + Jun-TEV	71
pMK1013-tau 1N4R	His6-Fos-thrombin + Jun-TEV-tau 1N4R	71
pMK1013-GSK-3β-tau 1N4R	His6-Fos-thrombin-GSK-3β + Jun-TEV-tau 1N4R	71
pMK1013-GSK-3β-tau (1N4R) C291S C322S	His6-Fos-thrombin-GSK-3β + Jun-TEV-tau (1N4R) C291S C322S	This study

Table 3.2 Oligos used in this study

Oligo	Sequence
C291S S	CTTAGCAACGTCCAGTCCAAGGCTGGCTCAAAGGATAATATCAAA
C291S AS	TTTGATATTATCCTTTGAGCCAGCCTTGGACTGGACGTTGCTAAG
C322S S	CTGAGCAAGGTGACCTCCAAGGCTGGCTCATTAGGCAACATCCAT
C322S AS	ATGGATGTTGCCTAATGAGCCAGCCTTGGAGGTCACCTTGCTCAG

Recombinant Protein Expression and Purification. The detailed purification steps for p-tau and tau 1N4R was described in Chapter II. 1N4R p-tau carrying the Cys-to-Ser mutations was purified using the same protocol.

Aggregation assay. Before aggregation assays, proteins were removed from the freezer and thawed on ice. A typical aggregation reaction contained 6 µM of protein unless otherwise stated. Other components of the reaction included 20 mM Tris (pH 7.4), 0 or 1 mM DTT, 20 µM thioflavin S (ThS), and a compound of interest as the aggregation modulator. Typically, the assays were assembled in a 384-well low-volume plate. The plate was covered by an Optical Adhesive Film to minimize evaporation during the assay. The plate was set at 37°C briefly before placing to a BioTek Synergy Neo Plate reader. ThS fluorescence was measured every 10 min (excitation 440 nm; emission 490 nm) for 16 hrs and collected using Gen5 software bundled with the BioTek plate reader.

High-throughput screening. A common mix of 6 µM p-tau, 20 mM Tris pH 7.4, 1 mM DTT, and 20 µM ThS was assembled and dispensed to 384-well low-volume plates (10 µl per well) using BioTek EL406 Washer, followed by the addition of 150 nl of the Prestwick Library compounds (final concentration of 30 µM per well) or DMSO in a Beckman Coulter Biomek FX^P workstation. Each plate was covered with an Optical Adhesive Film and set at 37°C briefly. ThS fluorescence was measured every 10 min at 440/490 nm for 16 hours by Biotek Synergy Neo Plate Reader. Four plates were used

to cover the 1,280-compound library. The real-time kinetics of ThS signals were collected using Gen5 software. The net change of ThS of each reaction was calculated and was used to assess the standard deviation. The Z'-value of p-tau aggregation reactions was derived by first calculating the ThS net change over 16 hours of no-protein, ThS-only reactions as the negative control (c), and p-tau-containing reactions (with DMSO vehicle) as the positive control (+c). The Z'-value was calculated by the equation:

$$Z' = [1-(3(\sigma_{+c} + \sigma_{-c}) / |\mu_{+c} - \mu_{-c}|)].$$

σ_{+c}, σ_{-c}, μ_{+c}, and μ_{-c} are the standard deviations(s) and the averages (μ) of the positive and negative controls [25]. All compounds showing greater than 3 standard deviations (SDs) from the mean and a small number of compounds deviating 2 SDs from the mean were picked for dose response curves (DRC). Those that showed significant deviation from no-compound controls were purchased from commercial venders and repeated for DRC.

Cytotoxicity of p-tau. Cell viability assays were conducted in 96-well plates. 2,000 HEK 293T or SH-SY5Y cells in 100 μL media (DMEM, 10% FBS, pen/strep) were seeded to a well and cultured for 40 – 48 hrs at 37°C, 5% CO_2. PTAIs were typically added to cells along with p-tau or when cells were treated by p-tau for 24 hrs (Fig 3.7). 24 or 48 hrs after the addition of protein/compound, cells were trypsinized and transferred to microcentrifuge tubes, and pelleted at 1,000 x g for 5 min at room temperature. Cell pellets were resuspended in phosphate-buffered saline (137 mM NaCl,

2.7 mM KCl, 10 mM Na_2HPO_4, 1.8 mM KH_2PO_4) and incubated with 5 µg/ml fluorescein diacetate (FDA) for 5 min at room temperature. 5 µg/ml propidium iodide (PI) was then added to the mixture. Cells stained by FDA or PI were examined using an Olympus BX51 Fluorescence Microscope. Cells from randomly chosen fields were counted for FDA or PI stainability. At least fifty cells from multiple fields were counted for each treatment well. Viability was calculated using the equation:

Relative viability = FDA stained cells / (FDA stained cells + PI stained cells).

To examine apoptosis, cell pellets were resuspended in annexin V binding Buffer (0.1 M HEPES pH7.4, 0.1 M NaCl, 25 mM $CaCl_2$). 5 µL of cell suspension was stained with 0.5 µL of FITC-conjugated annexin V at room temperature for 15 min in the dark and then examined using an Olympus BX51 Fluorescence Microscope.

RESULTS

Recombinant hyperphosphorylated tau aggregates spontaneously and independently of its redox state

To begin to perform p-tau aggregation-based AD drug screen, I first established the feasibility and advantage of using p-tau aggregation as the primary screen. To this end, I compared the aggregation kinetics of p-tau, unmodified tau, and the K18 fragment (the repeat domains) conducted at a concentration of 6 μM, which is close to the estimated abundance of oligomeric hyperphosphorylated tau in the AD brain [24]. Thioflavin S (ThS), which displays enhanced fluorescence when binding to β sheet-rich fibrillar structures in amyloid aggregates [74], was included in the aggregation assay to monitor the level of p-tau aggregates. Hyperphosphorylation alone causes tau to aggregate (Fig 3.1A, orange vs. yellow curves), while tau and K18 show modest or no aggregation. Both tau and p-tau fibrillization can also be stimulated by heparin. Net changes of ThS fluorescence over the course of 17 hours showed stastical significance of the hyperphosphorylation-driven tau aggregation (Fig 3.1B). The additive nature of phosphorylation and heparin in tau fibrillization suggests two separate modes for tau aggregation, and implies that compounds controlling solely the heparin-stimulated tau aggregation may not be effective in combating the action of hyperphosphorylation. Additionally, that p-tau aggregation responded effectively to heparin's stimulation suggested that compounds in this category, i.e., p-tau aggregation enhancers, can also be identified. This is the basis for the identification of potential AD risk factors, and will be described in detail in Chapter IV.

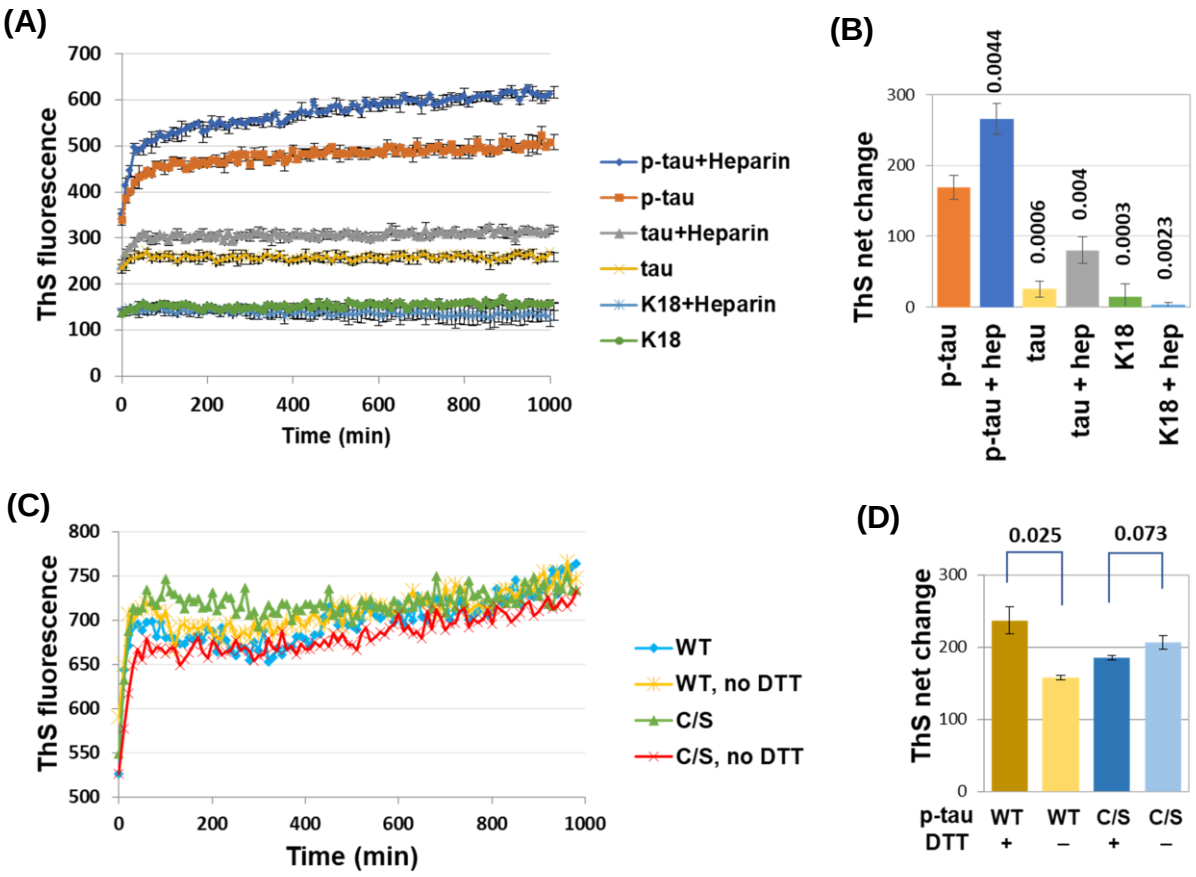

Figure 3.1 Inducer-free and redox-independent aggregation of hyperphosphorylated tau (p-tau). (A) Aggregation of p-tau, tau, and K18 with or without heparin was quantified by real-time thioflavin S (ThS) fluorescence kinetics or (B) by net changes of ThS signal after 17 hours of reaction. Numbers above each bar in panel (B) are the P values for the comparison with p-tau without the use of heparin (leftmost column). (C) Full-course aggregation curves and (D) ThS net changes of p-tau, wildtype or the C291S C322S mutant obtained from reactions with or without 1 mM DTT that kept the reaction in a reduced state. P-tau aggregation does not require the reducing agent DTT and is independent of Cys291 and 322. P values were obtained from two-tailed Student's t tests; n = 3.

Many once-promising tau aggregation inhibitors were later deemed non-specific redox modulators [14]. This discouraging development resulted from the fact that the two cysteine residues of tau control inter- and intra-molecule interaction of tau in vitro [75, 76]. To examine specifically the contribution of the two cysteine residues on the aggregation kinetics of the underlying tau, Cys291 and Cys322 were replaced with serines in the PIMAX p-tau construct. This C/S p-tau was purified using the same protocols and first examined by SDS-PAGE (Chapter 2, Fig 2.1B). The gel mobility of the C/S p-tau was comparable to the wildtype counterpart. The aggregation kinetics of p-tau and C/S p-tau were then compared in the presence or absence of a reducing agent DTT (Fig 3.1C). Unlike the unphosphorylated K18 fragment [13], maintaining a reducing environment was not essential for p-tau or C/S p-tau to form fibrils. C/S p-tau can form fibrils as efficiently as its wildtype counterpart. A moderate reduction of p-tau aggregation efficiency was associated with DTT omission, but the heparin-independent increase of ThS fluorescence remained conspicuous without DTT. Net changes of thioflavin S fluorescence over the course of 17 hours confirmed statistically that the redox state of the two cysteine residues had a minimal effect on PIMAX p-tau aggregation (Fig 3.1D). It is therefore concluded that hyperphosphorylation triggers tau aggregation in an inducer- and redox state-independent fashion.

Pilot screen of a 1,280-compound library uncovered p-tau aggregation modulators

Animal and clinical studies have linked AD neurodegeneration to the aggregation intermediates of p-tau. This premise suggests that small-compounds that modulate the aggregation of p-tau may impact the onset and progression of AD. I hypothesize that p-tau aggregation inhibitors (PTAIs) that stop or revert p-tau aggregation are potential AD therapeutics. On the other hand, p-tau aggregation enhancers (PTAEs) that facilitate p-tau aggregation will be AD risk factors. Fig 3.2 illustrates my working model and research strategy.

To launch the first p-tau aggregation-based AD drug discovery screen, I collaborated with the Dr. Thomas Dexheimer at the Assay Development and Drug Repurposing Core (ADDRC), MSU, to set up a high-throughput (HTS) pilot screen targeting p-tau aggregation via thioflavin S-based fluorescence spectroscopy. The overall drug screen scheme will follow the standard pipeline. The p-tau aggregation inhibitors (PTAIs) identified in the screen, called hits, will be confirmed and evaluated in secondary assays. The promising lead compounds passing the scrutiny of secondary assays will further undergo medicinal chemistry optimization to achieve appropriate physicochemical property, selectivity, and side effect profile in both biochemical and animal models [21], and finally be tested in preclinical and clinical drug development [22, 23]. This chapter focuses on the hits confirmation step which includes confirmatory testing that re-tests the same assay conditions in the HTS with separately purchased powder chemicals, dose response curves, and orthogonal testing which evaluates the hits in different assay conditions.

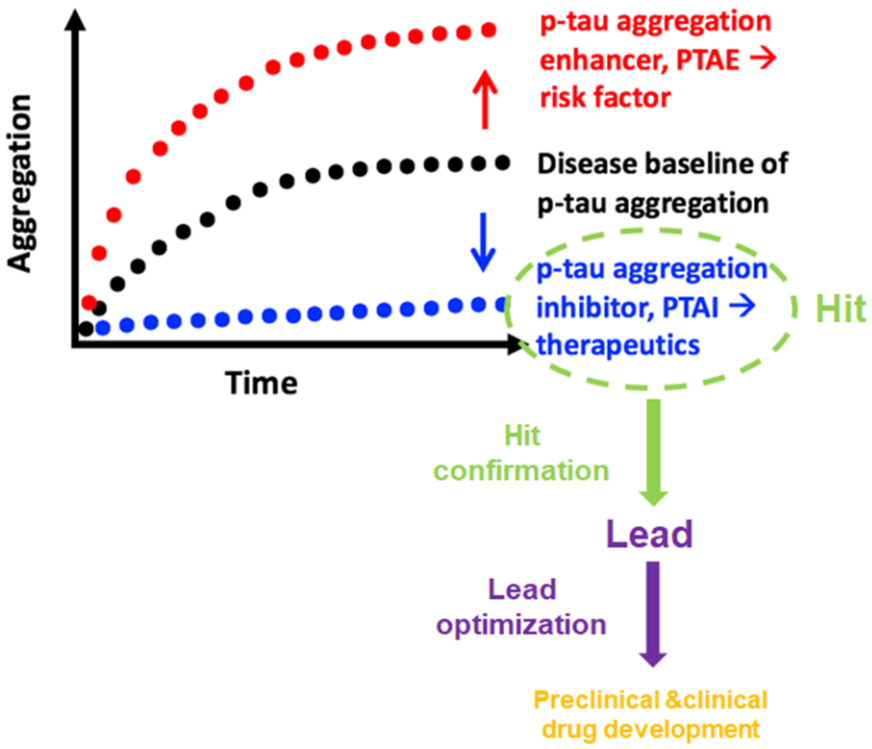

Figure 3.2 Design of high-throughput drug screening targeting p-tau aggregation. The p-tau aggregation based high-throughput screening (HTS) aims at identifying p-tau aggregation enhancers (PTAEs) that may be potential Alzheimer's disease risk factors, and p-tau aggregation inhibitors (PTAIs, hits) that can be developed into therapeutic drugs. Hits need to be confirmed and evaluated to identify promising lead compounds. Lead further undergoes lead optimization and then be tested in preclinical and clinical drug development.

For the primary screen, I used a Prestwick 1,280-compound library (http://www.prestwickchemical.com/libraries-screening-lib-pcl.html). In this library, 95% of the compounds were approved drugs (Food and Drug Administration, European Medicines Agency, and other agencies). The use of this library was primary for obtaining the proof-of-principle evidence demonstrating the robustness and validation of the assay. Aggregation of 6-μM p-tau under the influence of 30 μM of each of the library compound or the DMSO vehicle was monitored every 10 minutes for 16 hours by ThS-based fluorescence assay. The full-course aggregation curves of all reactions are shown in Fig 3.3A. Vehicle-control wells included in this pilot screen had a Z'-factor of 0.699, and a coefficient of variation (CV) of 8.9%, satisfying the criteria for an excellent HTS [25, 26]. The frequency plot (Fig 3.3B) summarizes the distribution of ThS net change (delta) over 16-hr incubation.

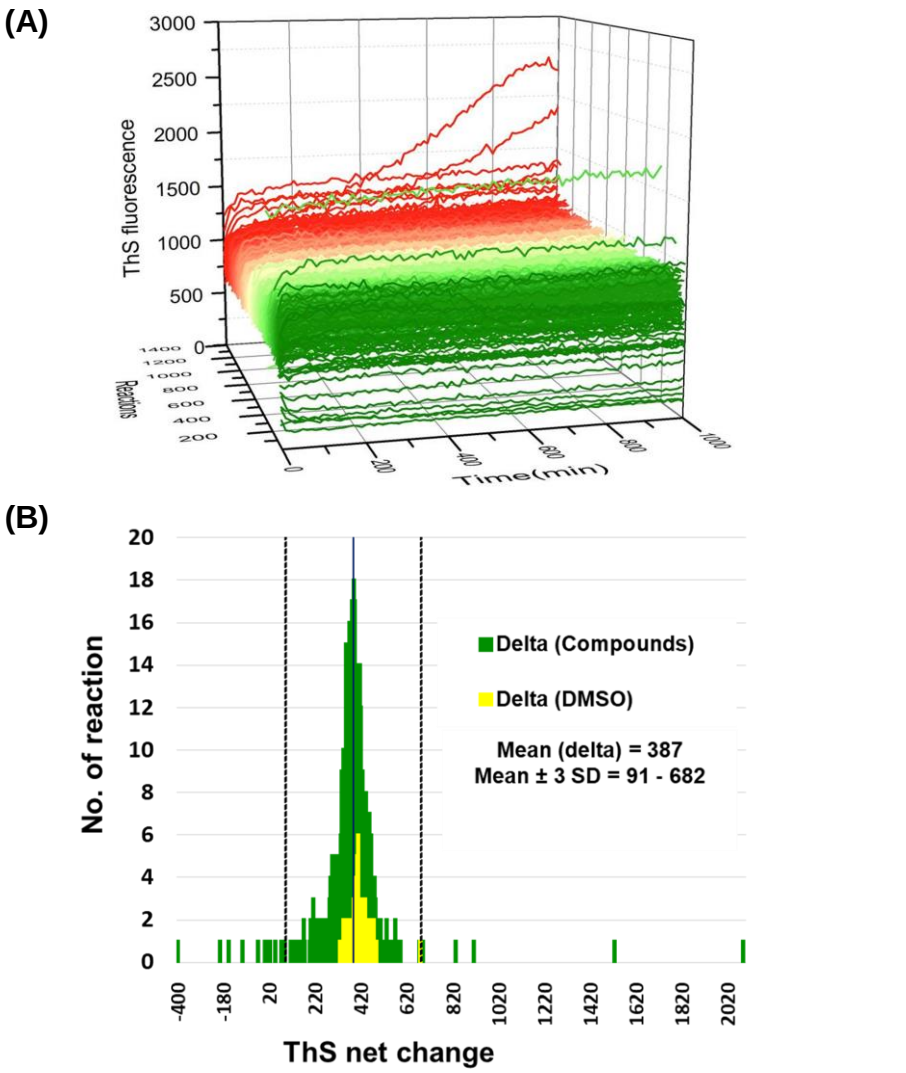

Figure 3.3 Pilot screening of the Prestwick Library for p-tau aggregation modulators. (A) Aggregation curves of 6-µM p-tau with 30 µM of compounds from the library or DMSO vehicle control. (B) Frequency distribution of ThS fluorescence net changes over the course of 16-hr assays. "Delta" in the graph refers to the average net difference of ThS fluorescence of reactions with the library compounds or only the DMSO vehicle control. P-tau with compounds are colored green; DMSO, yellow. The three vertical lines represent the mean and ± 3 SD of all reactions with the compounds.

Confirmation of p-tau aggregation modulation effect by dose-response curve

All compounds deviating 3 standard deviations (SDs) or more from the mean, and a small number of selective ones greater than 2 SDs were subjected to dose-response curve (DRC) tests (1.625 – 100 μM). Those showing p-tau aggregation inhibitor (PTAI) or p-tau aggregation enhancer (PTAE) activity in DRCs were acquired from commercial sources for validation. Compounds that showed consistent PTAI or PTAE behaviors in multiple repeats of DRCs are listed in Fig 3.4. Among the identified PTAIs, R-(–)-apomorphine and raloxifene were selected for further studies. Both are brain permeant prescription drugs that have been implicated in battling AD or dementia in animals or in human epidemiological surveys [27, 28]. I therefore used these two as the model for PTAI studies. The Prestwick library screen also identified carmofur and prednicarbate as apparent PTAEs (Fig 3.4C, D). Prednicarbate is a synthetic corticosteroid for dermatological use, and carmofur (1-hexylcarbamoyl-5-fluorouracil) is an anti-neoplastic pyrimidine analogue treating skin conditions. Neither drug is likely to impose a significant neurodegeneration threat, due to their primary treatment regimens, and therefore was set aside from further studies.

(A)

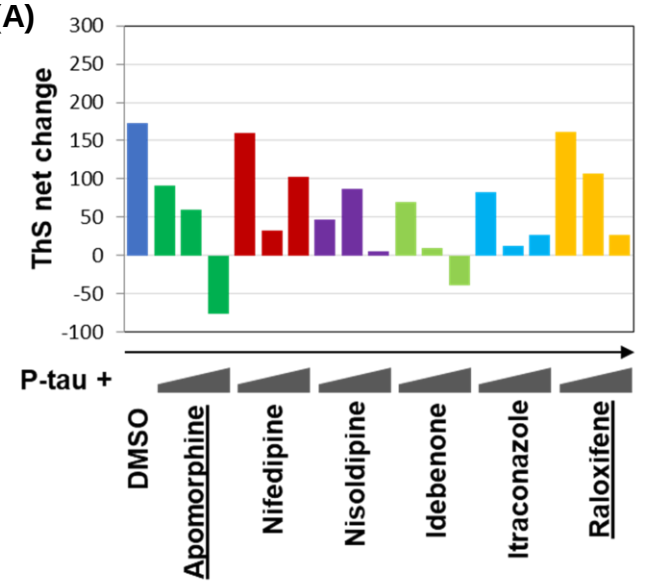

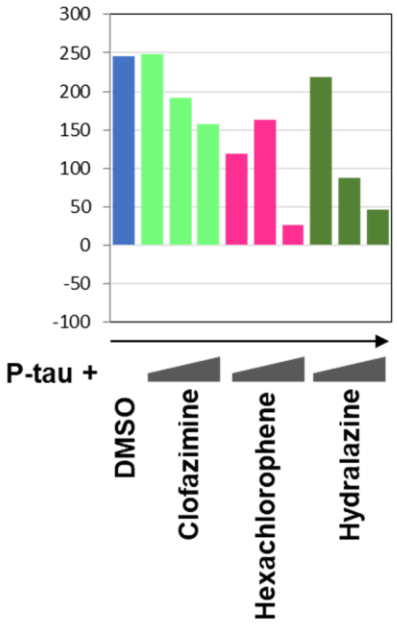

(B)

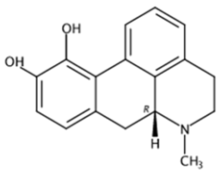

R-(-)-Apomorphine

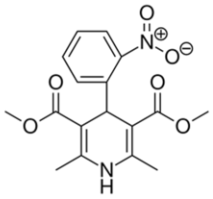

Nifedipine

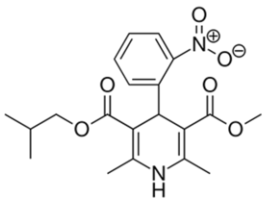

Nisoldipine

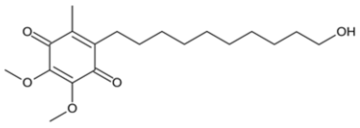

Idebenone

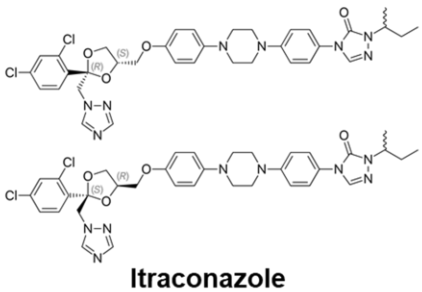

Itraconazole

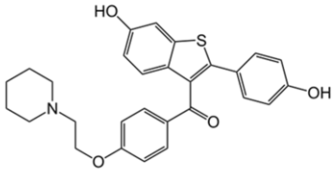

Raloxifene

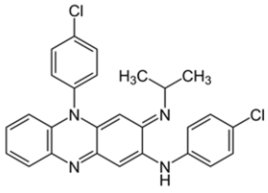

Clofazemine

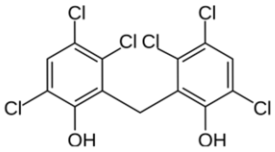

Hexachlorophene

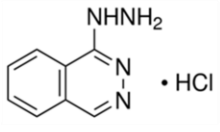

Hydralazine hydrochloride

Figure 3.4 (cont'd)

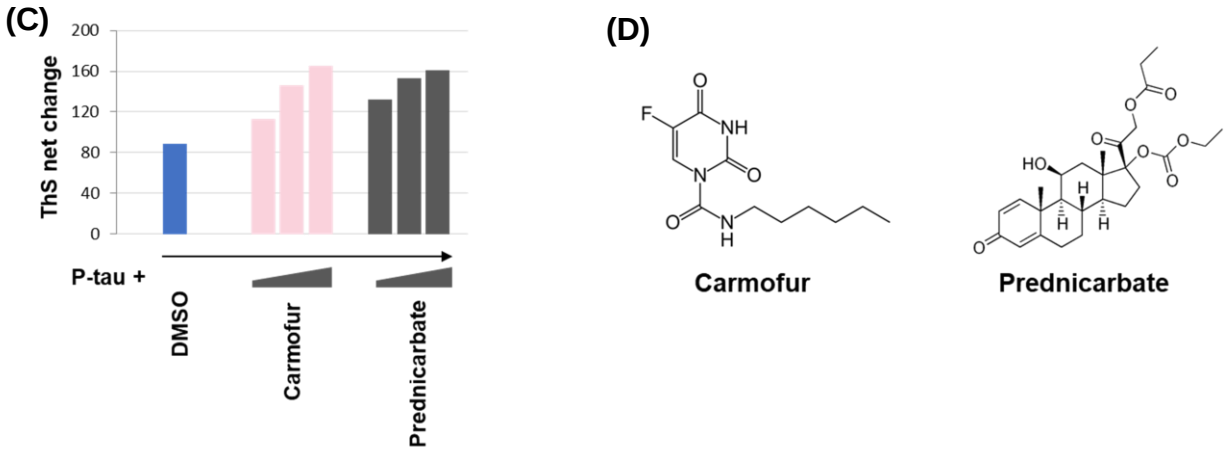

Figure 3.4 Identification of PTAIs and PTAEs by dose-response curve. (A) Dose response curves of candidate PTAIs from separately purchased chemicals. 6 μM of p-tau was assayed against 12.5, 25 or 50 μM of each compound. Shown are representative results of at least three biological repeats. (B) Structures of candidate PTAIs. (C) Dose response curves of candidate PTAEs from purchased chemicals. 6 μM of p-tau was assayed against 12.5, 25 or 50 μM of each compound. Shown are representative results of at least three biological repeats. (D) Structures of candidate PTAEs.

R-(–)-apomorphine and raloxifene inhibit p-tau aggregation and cytotoxicity

Powder chemicals of R-(–)-apomorphine and raloxifene were first acquired from commercial sources for verification. Mass spectrometry confirmed their identity and purity (not shown). Both real-time and net change of ThS fluorescence verified the dose-dependent inhibition of p-tau aggregation (Fig 3.5A, B). To ensure that the two compounds did not act via altering the redox state of p-tau, the aggregation of the C/S p-tau (Fig 3.1 above) was tested in the presence of 0 – 100 μM R-(–)-apomorphine or raloxifene. The inhibition patterns were comparable to that of the wildtype p-tau (Fig 3.5C), affirming that the two PTAIs functioned independently of the redox state of p-tau. The negative values of ThS net change suggested the ability to dissolve existing fibrils. To test this possibility, p-tau was subjected to compound-free aggregation for 24 hrs, followed by binding to the indicator dye ThS. Different doses of R-(–)-apomorphine or raloxifene (0 – 100 μM) were then added to p-tau aggregates. Changes in ThS fluorescence were then measured for 16 hrs. If either compound only stopped p-tau fibril formation and/or growth, the ThS fluorescence would remain unchanged. On the other hand, if these two drugs could disrupt pre-existing p-tau fibrils, the ThS signal was expected to decrease in a compound dose-dependent manner. The latter notion was indeed the case (Fig 3.5D). It is therefore concluded that both R-(–)-apomorphine and raloxifene can disaggregate pre-formed p-tau aggregates.

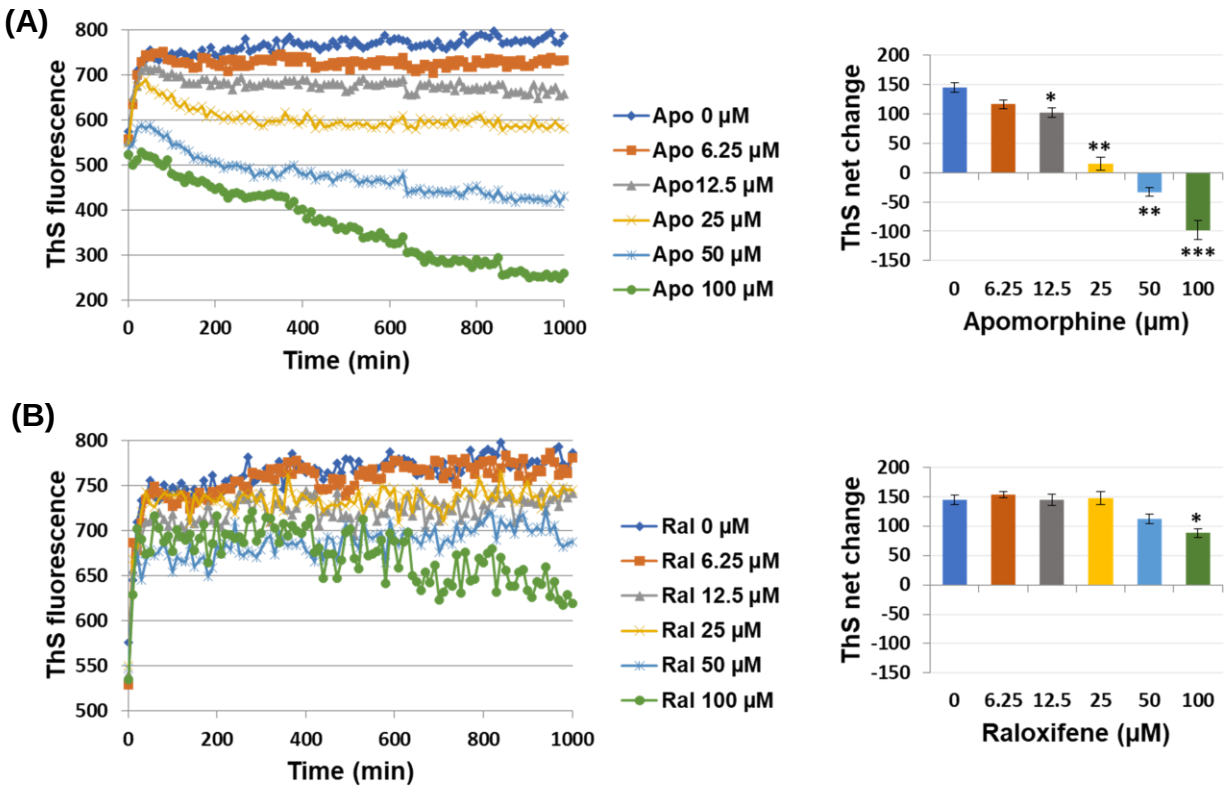
(A)
ThS fluorescence
Time (min)
Apo 0 μM
Apo 6.25 μM
Apo12.5 μM
Apo 25 μM
Apo 50 μM
Apo 100 μM
ThS net change
Apomorphine (μm)
(B)
ThS fluorescence
Time (min)
Ral 0 μM
Ral 6.25 μM
Ral 12.5 μM
Ral 25 μM
Ral 50 μM
Ral 100 μM
ThS net change
Raloxifene (μM)

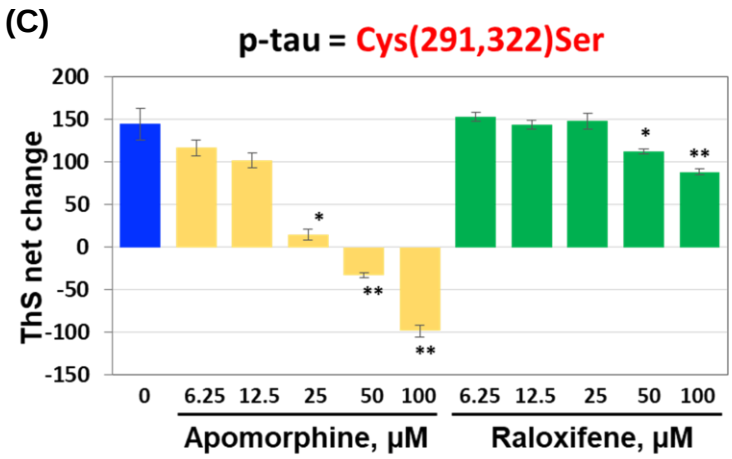
(C)
p-tau = Cys(291,322)Ser
ThS net change
Apomorphine, μM
Raloxifene, μM

Figure 3.5 (cont'd)

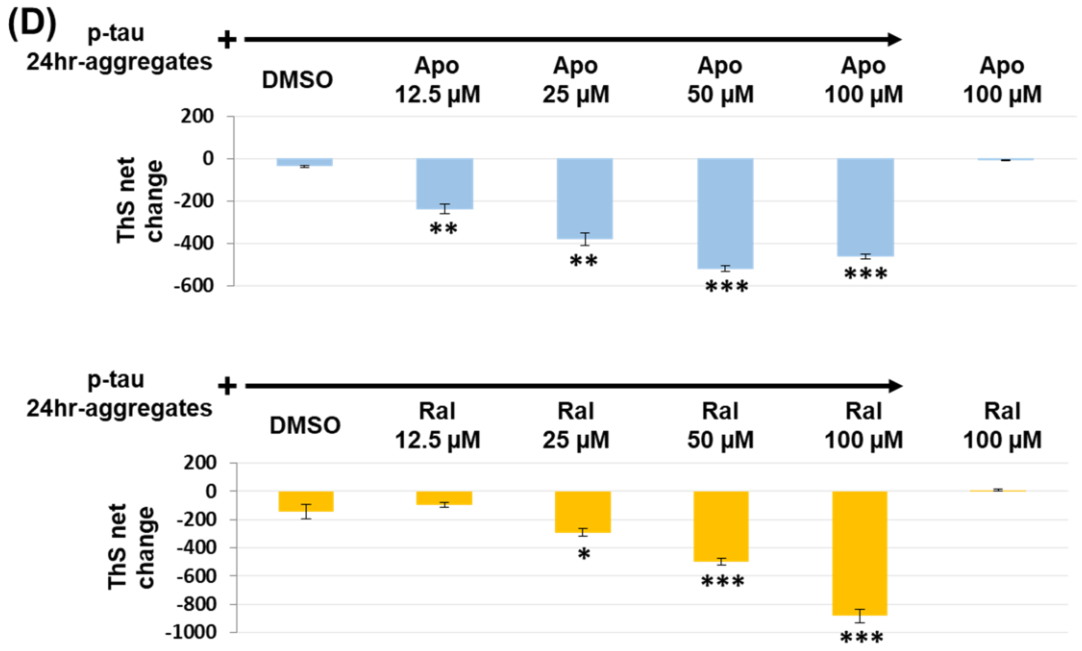

Figure 3.5 R-(–)-apomorphine and raloxifene are p-tau aggregation inhibitors and dissolvers. 0 – 100 μM commercial purchased (A) R-(–)-apomorphine or (B) raloxifene were subjected to the aggregation of 6-μM p-tau. Real-time ThS fluorescence (left) and ThS net change (right) were shown. (C) Both R-(–)-apomorphine and raloxifene act independently of the two cysteine residues of p-tau. P-tau aggregation reactions with the C291S C322S (C/S) mutant p-tau were done in the presence of the indicated amounts of either compound. (D) Both R-(–)-apomorphine and raloxifene are p-tau aggregates dissolvers. ThS and 12.5 – 100 μM compound or DMSO control was added into the 24 hr pre-aggregated p-tau samples, ThS monitor was continued for 16 hrs. Error bars are standard deviation; n = 3. P values were obtained from two-tailed Student's t tests; *: P≤0.05, **: P≤0.01, ***: P≤0.001.

Besides redox- and inducer-independent aggregation, p-tau causes cell death (Chapter II). PTAIs with therapeutic potential are anticipated to quench p-tau cytotoxicity. To test this notion, p-tau cytotoxicity assays were performed with both HEK 293T and SH-SY5Y cells in the presence of increasing amounts of either R-(–)-apomorphine or raloxifene (Fig 3.6A, B). The LD_{50} of p-tau alone (concentration of p-tau causing 50% cell death) was found to be around 0.5 μM for SH-SY5Y cells and 0.8 μM for HEK 293T. Co-incubation with increasing amounts of either compound caused the LD_{50} values of p-tau to increase steadily, suggesting attenuation of cytotoxicity. R-(–)-apomorphine appears to be more potent than raloxifene in both p-tau aggregation and cell killing tests. The EC_{50} of R-(–)-apomorphine (the concentration of the compound that gives half-maximal inhibition effect) against 0.8-μM p-tau cytotoxicity (SH-SY5Y cells) was found to be approximately 3 μM (Fig 3.6C). The p-tau based cell killing was also confirmed to be independent of the redox state, because the C/S p-tau exhibited a similar dose-dependent cytotoxicity on HEK 293T cells that was diminished by 10 μM of R-(–)-apomorphine or raloxifene (Fig 3.6D). Lastly, the pro-apoptosis activity of p-tau was found to be attenuated by R-(–)-apomorphine as well. The number of annexin V-stained apoptotic cells reduced from 50% to 15% if R-(–)-apomorphine was present in the assays (Fig 3.6E).

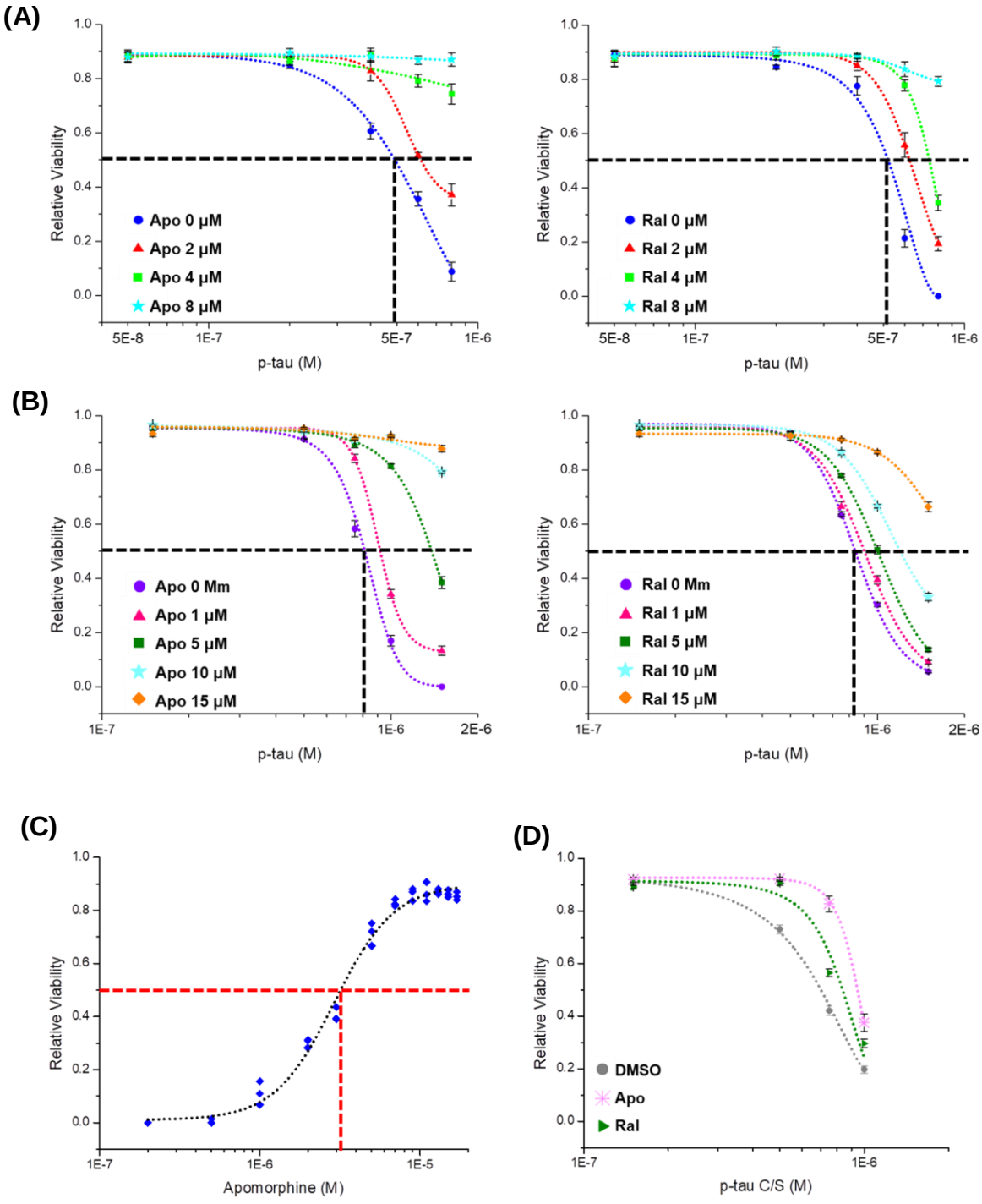
(A)
Relative Viability
p-tau (M)
Apo 0 μM
Apo 2 μM
Apo 4 μM
Apo 8 μM
Ral 0 μM
Ral 2 μM
Ral 4 μM
Ral 8 μM
(B)
Apo 0 Mm
Apo 1 μM
Apo 5 μM
Apo 10 μM
Apo 15 μM
Ral 0 Mm
Ral 1 μM
Ral 5 μM
Ral 10 μM
Ral 15 μM
(C)
Apomorphine (M)
(D)
p-tau C/S (M)
DMSO
Apo
Ral

Figure 3.6 (cont'd)

(E)

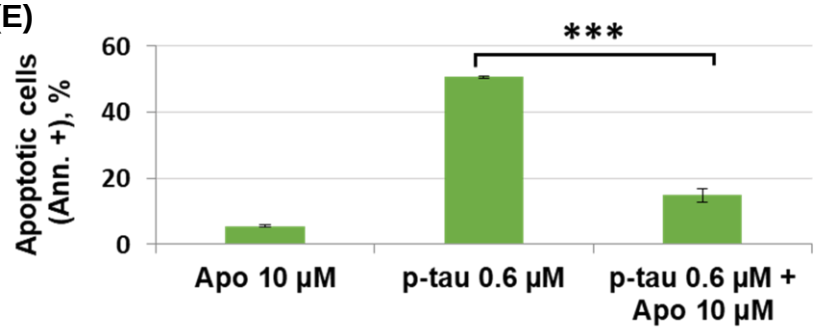

Figure 3.6 R-(–)-apomorphine and raloxifene protect cells from p-tau cytotoxicity. Viability curves of (A) SH-SY5Y or (B) HEK 293T cells treated with varying concentrations of p-tau and R-(–)-apomorphine or raloxifene. P-tau and compounds were added together to cells. Cell viability was quantified by FDA and PI differential staining 24 hrs after the treatment. The black dotted lines indicate 50% viability. (C) Viability curve of SH-SY5Y cells treated by 0.8-µM p-tau in the presence of 0 – 17 µM of R-(–)-apomorphine. The red dotted lines indicate 50% viability. (D) HEK 293T cells treated by 0.5, 0.75 or 1 µM p-tau C/S in the absence/presence of 10-µM R-(–)-apomorphine or raloxifene. (E) Monitoring the percentage of apoptotic cells by annexin V in HEK 293T cells after 12-hr treatment of 10-µM R-(–)-apomorphine, 0.6-µM p-tau or the mixture of 10-µM R-(–)-apomorphine and 0.6-µM p-tau. Error bars are standard deviation; n = 3. P values were obtained from two-tailed Student's t tests; ***: P≤0.001.

P-tau apparently entered cells, evidenced by ThS staining in p-tau-treated HEK 293T cells (Chapter II, Fig 2.3C). To test whether R-(–)-apomorphine blocked p-tau absorption, HEK 293T cells treated with 0.5 or 1 µM of p-tau for 24 hours were then given DMSO or 15 µM of R-(–)-apomorphine. 24 and 48 hours later, cells were harvested for ThS/PI double-staining (Fig 3.7A). Quantitative analysis (Fig 3.7B) shows that the vast majority cells treated with 1 µM p-tau were dead with cytoplasmic ThS staining (red columns). R-(–)-apomorphine effectively reduced the percentage of PI (+) ThS (+) cells ($P = 0.028$ at 24 hr, and 0.001 at 48 hr) even though this compound was given 24 hours after p-tau had started its action. In the viable, PI (-) population of 48-hr treatment wells, half of the cells were free of the ThS signal (dark blue bars; $P = 0.001$ when compared with the DMSO group), suggesting enhanced clearance and/or blocked absorption of p-tau. Live cells bearing ThS fluorescence also were increased in the 48-hr samples (light blue bars; $P = 0.009$), indicating better tolerance to p-tau aggregates. Together, these results showed that R-(–)-apomorphine increased cellular tolerance to p-tau aggregates.

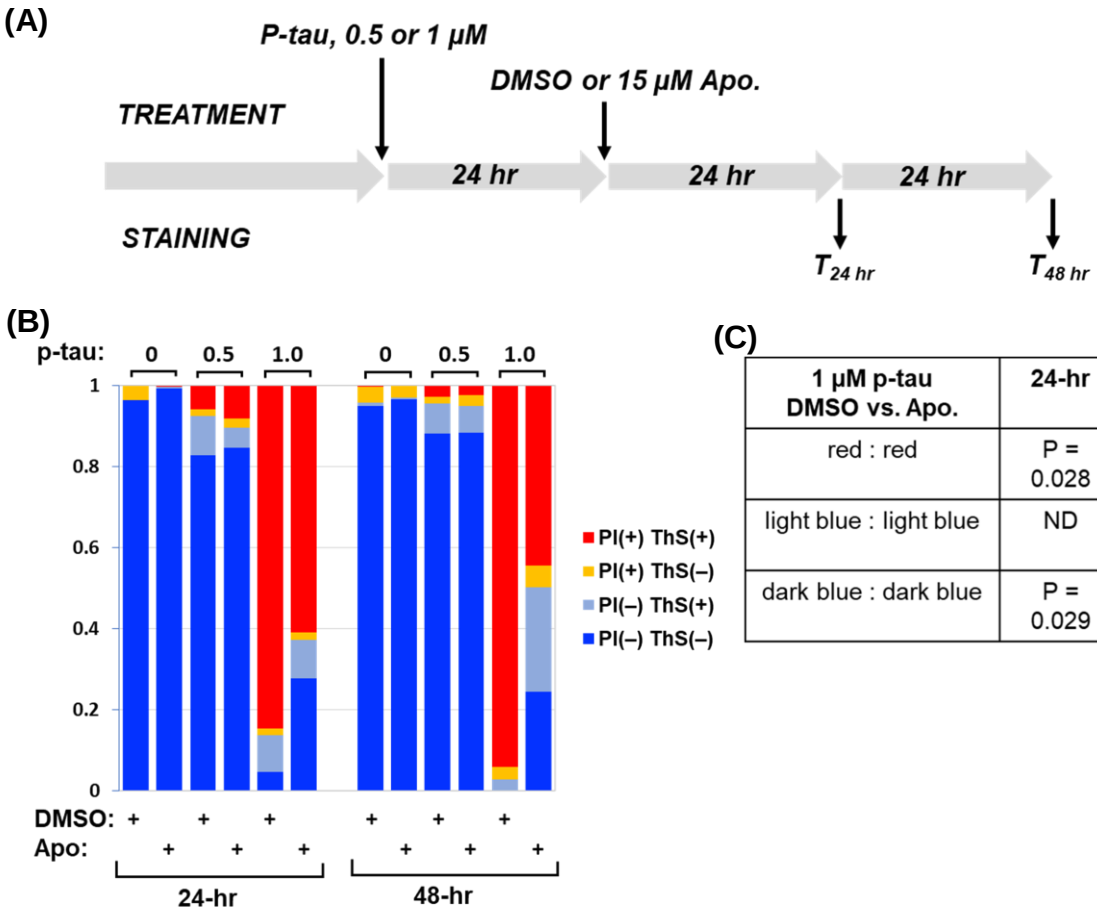

(C)

1 μM p-tau DMSO vs. Apo.	24-hr	48-hr
red : red	P = 0.028	P = 0.001
light blue : light blue	ND	P = 0.009
dark blue : dark blue	P = 0.029	P = 0.001

Figure 3.7 R-(–)-apomorphine increases cell's torelance of p-tau aggregates.

(A) Scheme of experiments that examined the fate of p-tau-induced fibrils in cells after R-(–)-apomorphine treatment. (B) Quantification of ThS and PI stainability among cells. Cells were categorized based on one of the four ThS/PI double-staining patterns. The total number of cells captured microscopically under each treatment was used as the denominator to calculate the percentage of each staining pattern, and expressed in this stacked column chart. (C) The standard deviations from data of panel (B) (n = 3) were used to calculate the P values by one-tailed Student's t tests to compare DMSO and R-(–)-apomorphine treatment under each condition. ND, not different. n = 3.

DISCUSSION

PIMAX p-tau forms aggregates that cause cell death at sub-micromolar concentrations. The low concentration requirement and convenience of PIMAX protein production reduce the cost for a high-throughput screening centering upon hyperphosphorylated tau. In addition, the inducer-free aggregation of PIMAX p-tau also eliminates altogether the likelihood of false hits that act on the tau-inducer interface.

The aggregation assay of PIMAX p-tau is scalable for different throughputs. In a 1,280-compound pilot screen that served as the proof of concept for HTS, I discovered p-tau aggregation inhibitors as the entry candidates for therapeutics development. Two such PTAIs stood out for their ability to pass the blood brain barrier and, importantly, to preserve cognitive functions in animal models or in human trials. Apomorphine has been used as an acute treatment for on-off oscillations in Parkinson's disease (PD) patients since 1988 [33]. The on-off phenomenon refers to a fluctuation of motor function as a result of reduced effectiveness of levodopa in PD patients [34]. Subcutaneous apomorphine efficiently reduces the "off" time with a rapid onset of action [35, 36]. Apomorphine's lipophilic structure leads to its ability to pass the blood-brain-barrier [37]. In addition to PD, apomorphine has been reported to inhibit the fibrillization of amyloid-beta (Aβ) through autoxidation in vitro [38] and improving memory impairment via promoting Aβ degradation in a mouse model [39]. My results suggest a different and pathophysiologically more p-tau-related mechanism for AD drug development.

Raloxifene is a selective estrogen receptor modulator (SERM) that acts as an

agonist on bone and lipid metabolism and as an antagonist in breast and uterine tissues [40]. Postmenopausal women have a higher incidence of AD compared to age-matched men [41, 42], which was postulated, but not proved, to be due to reduced levels of estrogen in the brain [43]. Estrogen can be transferred to the brain by the blood circulation or synthesized in various brain regions [44]. Estrogen manifests its neuroprotective effect through different mechanisms including maintaining the integrity of the blood-brain barrier [45] and mitochondrial function [46]. The decline of estrogen contributes to Aβ accumulation in the AD brain by several pathways including Aβ synthesis, degradation and clearance [47]. Tau is also a target of estrogen, which attenuates tau hyperphosphorylation by upregulating the activity of protein Kinase A in HEK 293T [48], GSK-3β in Neuro2A cells [49], or okadaic acid in SH-SY5Y cells [50]. However, research on hormone therapy (HT) or raloxifene's effect on AD have inconsistent results. Women receiving 120 mg/day of raloxifene have been reported to have reduced risk of AD and mild cognitive impairment in 2005 [28]. Conversely, several reports suggest no change in cognition after treatment with raloxifene among patients already displaying clear cognitive impairments [51, 52]. The timing of HT use appears to be a key factor. HT can reduce the risk of AD by 30% in women who received HT within 5 years of menopause, but has no effect in those who initiated HT 5 or more years after menopause [53]. Thus, the effect of raloxifene on cognition improvement in AD patients needs to be test in a larger and well-designed experiment.

R-(–)-apomorphine is a dopamine receptor agonist, while raloxifene acts through estrogen receptors. Because the PTAI activity of these two compounds was first discovered in a cell-free system, I do not believe that dopamine or estrogen receptor

binding was sufficient to explain their cytoprotective power. Indeed, dopamine and several other SERMs were present in the Prestwick library analyzed above, but none of them affected p-tau aggregation. Structure-activity relationship studies of these two PTAIs and their analogs will help to assess the feasibility of developing AD therapeutics without the off-target receptor affinity.

Besides R-(–)-apomorphine and raloxifene, several other compounds have been identified as PTAIs in the pilot screening, including nifedipine, nisoldipine, idebenone, itraconazole, clofazimine, hexachlorophene and hydralizaine hydrochloride (Fig 3.4A, B). Itraconazole is used to treat fungal infections. Hexachlorophene is a kind of disinfectant. Clofazimine is used to treat leprosy. These compounds have weak relationship with AD or dementia. Among the rest candidates, several are involved in the treatment of high blood pressure and heart failure. Hydralazine has been used to treat hypertension since 1950 [54]. Nifedipine and nisoldipine belong to calcium channel blockers that function as antihypertensive drugs [57], especially in the elderly [58]. Both epidemiological and clinical studies have suggested a relationship between hypertension and AD [59, 60], even though the mechanism is not well understood. Certain antihypertensive drugs including angiotensin-converting enzyme (ACE) and calcium channel blockers can result in reduced risks of cognitive decline and dementia [61 – 63]. The mechanism of antihypertensive drug-based cognition improvement is not clear. However, my data indicate that these drugs may have a role in p-tau aggregation. Idebenone is a man-made analog of Coenzyme Q10 [64] developed for AD therapeutics and it’s an effective antioxidant [65, 66]. Idebenone can easily cross the blood-brain barrier [64] and is well-tolerated in single oral doses up to 1050 mg and in repeated daily doses up to 2250 mg

[67]. However, researches on idebenone’s efficacy in the treatment of AD patients have inconsistent results [68-70].

In conclusion, two prescription drugs, R-(–)-apomorphine and raloxifene were discovered as effective PTAIs from a pilot screening of a 1,280-compound library. These two compounds protect cells from p-tau cytotoxicity, indicating their potential in preventing neuronal loss and neurodegeneration in Alzheimer's disease and other tauopathies.

REFERENCES

REFERENCES

1. Nelson PT, Alafuzoff I, Bigio EH, Bouras C, Braak H, Cairns NJ, Castellani RJ, Crain BJ, Davies P, Del Tredici K, Duyckaerts C, Frosch MP, Haroutunian V, Hof PR, Hulette CM, Hyman BT, Iwatsubo T, Jellinger KA, Jicha GA, Kövari E, Kukull WA, Leverenz JB, Love S, Mackenzie IR, Mann DM, Masliah E, McKee AC, Montine TJ, Morris JC, Schneider JA, Sonnen JA, Thal DR, Trojanowski JQ, Troncoso JC, Wisniewski T, Woltjer RL, Beach TG. 2012. Correlation of Alzheimer disease neuropathologic changes with cognitive status: a review of the literature. J Neuropathol Exp Neurol. 71(5):362-81.

2. Graham WV, Bonito-Oliva A, Sakmar TP.2017. Update on Alzheimer's Disease Therapy and Prevention Strategies. Annu Rev Med. 68:413-430.

3. Hanger DP, Anderton BH, Noble W. 2009. Tau phosphorylation: the therapeutic challenge for neurodegenerative disease. Trends Mol Med. 15(3):112-9.

4. Morimoto BH, Schmechel D, Hirman J, Blackwell A, Keith J, Gold M; AL-108-211 Study. 2013. A double-blind, placebo-controlled, ascending-dose, randomized study to evaluate the safety, tolerability and effects on cognition of AL-108 after 12 weeks of intranasal administration in subjects with mild cognitive impairment. Dement Geriatr Cogn Disord. 35(5-6):325-36.

5. Boxer AL, Lang AE, Grossman M, Knopman DS, Miller BL, Schneider LS, Doody RS, Lees A, Golbe LI, Williams DR, Corvol JC, Ludolph A, Burn D, Lorenzl S, Litvan I, Roberson ED, Höglinger GU, Koestler M, Jack CR Jr, Van Deerlin V, Randolph C, Lobach IV, Heuer HW, Gozes I, Parker L, Whitaker S, Hirman J, Stewart AJ, Gold M, Morimoto BH; AL-108-231 Investigators. 2014. Davunetide in patients with progressive supranuclear palsy: a randomised, double-blind, placebo-controlled phase 2/3 trial. Lancet Neurol. 13(7):676-85.

6. Flach K, Hilbrich I, Schiffmann A, Gärtner U, Krüger M, Leonhardt M, Waschipky H, Wick L, Arendt T, Holzer M. 2012. Tau oligomers impair artificial membrane integrity and cellular viability. J Biol Chem. 287(52):43223-33.

7. Berger Z, Roder H, Hanna A, Carlson A, Rangachari V, Yue M, Wszolek Z, Ashe K, Knight J, Dickson D, Andorfer C, Rosenberry TL, Lewis J, Hutton M, Janus C. 2007. Accumulation of pathological tau species and memory loss in a conditional model of tauopathy. J Neurosci. 27(14):3650-62.

8. Wu JW, Hussaini SA, Bastille IM, Rodriguez GA, Mrejeru A, Rilett K, Sanders DW, Cook C, Fu H, Boonen RA, Herman M, Nahmani E, Emrani S, Figueroa YH, Diamond MI, Clelland CL, Wray S, Duff KE. 2016. Neuronal activity enhances tau

propagation and tau pathology in vivo. Nat Neurosci. 19(8):1085-92.

9. Frost B, Jacks RL, Diamond MI. 2009. Propagation of tau misfolding from the outside to the inside of a cell. J Biol Chem. 284(19):12845-52.

10. Schweers O, Mandelkow EM, Biernat J, Mandelkow E. 1995. Oxidation of cysteine-322 in the repeat domain of microtubule-associated protein tau controls the in vitro assembly of paired helical filaments. Proc Natl Acad Sci U S A. 92(18):8463-7.

11. Taniguchi S, Suzuki N, Masuda M, Hisanaga S, Iwatsubo T, Goedert M, Hasegawa M. 2005. Inhibition of heparin-induced tau filament formation by phenothiazines, polyphenols, and porphyrins. J Biol Chem. 280(9):7614-23.

12. Pickhardt M, Gazova Z, von Bergen M, Khlistunova I, Wang Y, Hascher A, Mandelkow EM, Biernat J, Mandelkow E. 2005. Anthraquinones inhibit tau aggregation and dissolve Alzheimer's paired helical filaments in vitro and in cells. J Biol Chem. 280(5):3628-35.

13. Barghorn S, Biernat J, Mandelkow E. 2005. Purification of recombinant tau protein and preparation of Alzheimer-paired helical filaments in vitro. Methods Mol Biol. 299:35-51.

14. Crowe A, James MJ, Lee VM, Smith AB 3rd, Trojanowski JQ, Ballatore C, Brunden KR. 2013. Aminothienopyridazines and methylene blue affect Tau fibrillization via cysteine oxidation. J Biol Chem. 288(16):11024-37.

15. Pickhardt M, Biernat J, Khlistunova I, Wang YP, Gazova Z, Mandelkow EM, Mandelkow E. 2007. N-phenylamine derivatives as aggregation inhibitors in cell models of tauopathy. Curr Alzheimer Res. 4(4):397-402.

16. Crowe A, Huang W, Ballatore C, Johnson RL, Hogan AM, Huang R, Wichterman J, McCoy J, Huryn D, Auld DS, Smith AB 3rd, Inglese J, Trojanowski JQ, Austin CP, Brunden KR, Lee VM. 2009. Identification of aminothienopyridazine inhibitors of tau assembly by quantitative high-throughput screening. Biochemistry. 48(32):7732-45.

17. Li W, Sperry JB, Crowe A, Trojanowski JQ, Smith AB 3rd, Lee VM. 2009. Inhibition of tau fibrillization by oleocanthal via reaction with the amino groups of tau. J Neurochem. 110(4):1339-51.

18. Monti MC, Margarucci L, Riccio R, Casapullo A. 2012. Modulation of tau protein fibrillization by oleocanthal. J Nat Prod. 75(9):1584-8.

19. Wischik CM, Staff RT, Wischik DJ, Bentham P, Murray AD, Storey JM, Kook KA, Harrington CR. 2015. Tau aggregation inhibitor therapy: an exploratory phase 2 study in mild or moderate Alzheimer's disease. J Alzheimers Dis. 44(2):705-20.

20. Gauthier S, Feldman HH, Schneider LS, Wilcock GK, Frisoni GB, Hardlund JH, Moebius HJ, Bentham P, Kook KA, Wischik DJ, Schelter BO, Davis CS, Staff RT, Bracoud L, Shamsi K, Storey JM, Harrington CR, Wischik CM. 2016. Efficacy and safety of tau-aggregation inhibitor therapy in patients with mild or moderate Alzheimer's disease: a randomised, controlled, double-blind, parallel-arm, phase 3 trial. Lancet. 388(10062):2873-2884.

21. Franz F Hefti. 2008. Requirements for a lead compound to become a clinical candidate. BMC Neurosci. 9(Suppl 3): S7.

22. JP Hughes, S Rees, SB Kalindjian, and KL Philpott. 2011. Principles of early drug discovery. Br J Pharmacol. 162(6): 1239–1249.

23. Keseru GM, Makara GM. 2006. Hit discovery and hit-to-lead approaches. Drug Discov Today. 11(15-16):741-8.

24. Khatoon S, Grundke-Iqbal I, Iqbal K. 1994. Levels of normal and abnormally phosphorylated tau in different cellular and regional compartments of Alzheimer disease and control brains. FEBS Lett. 351(1):80-4.

25. Zhang JH, Chung TD, Oldenburg KR. 1999. A Simple Statistical Parameter for Use in Evaluation and Validation of High Throughput Screening Assays. J Biomol Screen. 4(2):67-73.

26. Powell DJ, Hertzberg RP, Macarrón R. 2016. Design and Implementation of High-Throughput Screening Assays. Methods Mol Biol. 1439:1-32.

27. Nakamura N, Ohyagi Y, Imamura T, Yanagihara YT, Iinuma KM, Soejima N, Murai H, Yamasaki R, Kira JI. 2017. Apomorphine Therapy for Neuronal Insulin Resistance in a Mouse Model of Alzheimer's Disease. J Alzheimers Dis. 58(4):1151-1161. doi: 10.3233/JAD-160344.

28. Yaffe K, Krueger K, Cummings SR, Blackwell T, Henderson VW, Sarkar S, Ensrud K, Grady D. 2005. Effect of raloxifene on prevention of dementia and cognitive impairment in older women: the Multiple Outcomes of Raloxifene Evaluation (MORE) randomized trial. Am J Psychiatry. 162(4):683-90.

29. Zhong G, Wang Y, Zhang Y, Zhao Y. 2015. Association between Benzodiazepine Use and Dementia: A Meta-Analysis. PLoS One. 10(5):e0127836.

30. Billioti de Gage S, Moride Y, Ducruet T, Kurth T, Verdoux H, Tournier M, Pariente A, Bégaud B. 2014. Benzodiazepine use and risk of Alzheimer's disease: case-control study. BMJ. 349:g5205.

31. Hu CD, Chinenov Y, Kerppola TK. 2002. Visualization of interactions among bZIP and Rel family proteins in living cells using bimolecular fluorescence complementation.

Mol Cell. 9(4):789-98.

32. Ohashi K, Mizuno K. 2014. A novel pair of split venus fragments to detect protein-protein interactions by in vitro and in vivo bimolecular fluorescence complementation assays. Methods Mol Biol. 1174:247-62.

33. Stibe CM, Lees AJ, Kempster PA, Stern GM. 1988. Subcutaneous apomorphine in parkinsonian on-off oscillations. Lancet. 1(8582):403-6.

34. A J Lees . 1989. The on-off phenomenon. J Neurol Neurosurg Psychiatry. 52(Suppl): 29–37.

35. van Laar T, Jansen EN, Essink AW, Neef C, Oosterloo S, Roos RA. 1993. A double-blind study of the efficacy of apomorphine and its assessment in 'off'-periods in Parkinson's disease. Clin Neurol Neurosurg. 95(3):231-5.

36. Stacy M, Silver D. 2008. Apomorphine for the acute treatment of "off" episodes in Parkinson's disease. Parkinsonism Relat Disord. 14(2):85-92.

37. Neef C, van Laar T. 1999. Pharmacokinetic-pharmacodynamic relationships of apomorphine in patients with Parkinson's disease. Clin Pharmacokinet. 37(3):257-71.

38. Lashuel HA, Hartley DM, Balakhaneh D, Aggarwal A, Teichberg S, Callaway DJ. 2002. New class of inhibitors of amyloid-beta fibril formation. Implications for the mechanism of pathogenesis in Alzheimer's disease. J Biol Chem. 277(45):42881-90.

39. Himeno E, Ohyagi Y, Ma L, Nakamura N, Miyoshi K, Sakae N, Motomura K, Soejima N, Yamasaki R, Hashimoto T, Tabira T, LaFerla FM, Kira J. 2011. Apomorphine treatment in Alzheimer mice promoting amyloid-β degradation. Ann Neurol. 69(2):248-56.

40. Nickelsen T, Lufkin EG, Riggs BL, Cox DA, Crook TH. 1999. Raloxifene hydrochloride, a selective estrogen receptor modulator: safety assessment of effects on cognitive function and mood in postmenopausal women. Psychoneuroendocrinology. 24(1):115-28.

41. Li R, Cui J, Shen Y. 2014. Brain sex matters: estrogen in cognition and Alzheimer's disease. Mol Cell Endocrinol. 389(1-2):13-21.

42. Pike CJ. 2017. Sex and the development of Alzheimer's disease. J Neurosci Res. 95(1-2):671-680.

43. Merlo S, Spampinato SF, Sortino MA. 2017. Estrogen and Alzheimer's disease: Still an attractive topic despite disappointment from early clinical results. Eur J Pharmacol. 817:51-58.

44. Hojo Y, Murakami G, Mukai H, Higo S, Hatanaka Y, Ogiue-Ikeda M, Ishii H, Kimoto T, Kawato S. 2008. Estrogen synthesis in the brain--role in synaptic plasticity and memory. Mol Cell Endocrinol. 290(1-2):31-43.

45. Sohrabji F. 2007. Guarding the blood-brain barrier: a role for estrogen in the etiology of neurodegenerative disease. Gene Expr. 13(6):311-9.

46. Engler-Chiurazzi EB, Brown CM, Povroznik JM, Simpkins JW. 2017. Estrogens as neuroprotectants: Estrogenic actions in the context of cognitive aging and brain injury. Prog Neurobiol. 157:188-211.

47. Duarte AC, Hrynchak MV, Gonçalves I, Quintela T, Santos CR. 2016. Sex Hormone Decline and Amyloid β Synthesis, Transport and Clearance in the Brain. J Neuroendocrinol. 28(11).

48. Liu XA, Zhu LQ, Zhang Q, Shi HR, Wang SH, Wang Q, Wang JZ. 2008. Estradiol attenuates tau hyperphosphorylation induced by upregulation of protein kinase-A. Neurochem Res33(9):1811-20.

49. Shi HR, Zhu LQ, Wang SH, Liu XA, Tian Q, Zhang Q, Wang Q, Wang JZ. 2008. 17beta-estradiol attenuates glycogen synthase kinase-3beta activation and tau hyperphosphorylation in Akt-independent manner. J Neural Transm (Vienna). 115(6):879-88.

50. Zhang Z, Simpkins JW. 2010. Okadaic acid induces tau phosphorylation in SH-SY5Y cells in an estrogen-preventable manner. Brain Res. 1345:176-81.

51. Henderson VW, Ala T, Sainani KL, Bernstein AL, Stephenson BS, Rosen AC, Farlow MR. 2015. Raloxifene for women with Alzheimer disease: A randomized controlled pilot trial. Neurology. 85(22):1937-44.

52. Strickler R, Stovall DW, Merritt D, Shen W, Wong M, Silfen SL. 2000. Raloxifene and estrogen effects on quality of life in healthy postmenopausal women: a placebo-controlled randomized trial. Obstet Gynecol. 96(3):359-65.

53. Shao H, Breitner JC, Whitmer RA, Wang J, Hayden K, Wengreen H, Corcoran C, Tschanz J, Norton M, Munger R, Welsh-Bohmer K, Zandi PP; Cache County Investigators. 2012. Hormone therapy and Alzheimer disease dementia: new findings from the Cache County Study. Neurology. 79(18):1846-52.

54. O'Boyle CP, Kelly J, O'Brien ET, O'Malley K. 1981. Once daily slow-release hydralazine in hypertension. Ir Med J. 74(4):115-6.

55. Shionoiri H, Naruse M, Minamisawa K, Ueda S, Himeno H, Hiroto S, Takasaki I. 1997. Fosinopril. Clinical pharmacokinetics and clinical potential. Clin Pharmacokinet. 32(6):460-80.

56. Davis R, Coukell A, McTavish D. 1997. Fosinopril. A review of its pharmacology and clinical efficacy in the management of heart failure. Drugs. 54(1):103-16.

57. Elliott WJ, Ram CV. 2011. Calcium channel blockers. J Clin Hypertens (Greenwich). 13(9):687-9.

58. Caballero-Gonzalez FJ. 2015. Calcium channel blockers in the management of hypertension in the elderly. Cardiovasc Hematol Agents Med Chem. 12(3):160-5.

59. Iadecola C, Yaffe K, Biller J, Bratzke LC, Faraci FM, Gorelick PB, Gulati M, Kamel H, Knopman DS, Launer LJ, Saczynski JS, Seshadri S, Zeki Al Hazzouri A; American Heart Association Council on Hypertension; Council on Clinical Cardiology; Council on Cardiovascular Disease in the Young; Council on Cardiovascular and Stroke Nursing; Council on Quality of Care and Outcomes Research; and Stroke Council. 2016. Impact of Hypertension on Cognitive Function: A Scientific Statement From the American Heart Association. Hypertension. 68(6):e67-e94.

60. Marfany A, Sierra C, Camafort M, Doménech M, Coca A. 2018. High blood pressure, Alzheimer disease and antihypertensive treatment. Panminerva Med. 60(1):8-16.

61. Miners JS, Ashby E, Van Helmond Z, Chalmers KA, Palmer LE, Love S, Kehoe PG. 2008. Angiotensin-converting enzyme (ACE) levels and activity in Alzheimer's disease, and relationship of perivascular ACE-1 to cerebral amyloid angiopathy. Neuropathol Appl Neurobiol. 34(2):181-93.

62. Poon IO. 2008. Effects of antihypertensive drug treatment on the risk of dementia and cognitive impairment. Pharmacotherapy. 28(3):366-75.

63. Gao Y, O'Caoimh R, Healy L, Kerins DM, Eustace J, Guyatt G, Sammon D, Molloy DW. 2013. Effects of centrally acting ACE inhibitors on the rate of cognitive decline in dementia. BMJ Open. 3(7). pii: e002881.

64. Nagai Y, Yoshida K, Narumi S, Tanayama S, Nagaoka A. 1989. Brain distribution of idebenone and its effect on local cerebral glucose utilization in rats. Arch Gerontol Geriatr. 8(3):257-72.

65. Semsei I, Nagy K, Zs -Nagy I. 1990. In vitro studies on the OH* and O2(-*) free radical scavenger properties of idebenone in chemical systems. Arch Gerontol Geriatr. 11(3):187-97.

66. Jaber S, Polster BM. 2015. Idebenone and neuroprotection: antioxidant, pro-oxidant, or electron carrier? J Bioenerg Biomembr. 47(1-2):111-8.

67. Kutz K, Drewe J, Vankan P. 2009. Pharmacokinetic properties and metabolism of idebenone. J Neurol. 256 Suppl 1:31-5.

68. Thal LJ, Grundman M, Berg J, Ernstrom K, Margolin R, Pfeiffer E, Weiner MF, Zamrini E, Thomas RG. 2003. Idebenone treatment fails to slow cognitive decline in Alzheimer's disease. Neurology. 61(11):1498-502.

69. Weyer G, Babej-Dölle RM, Hadler D, Hofmann S, Herrmann WM. 1997. A controlled study of 2 doses of idebenone in the treatment of Alzheimer's disease. Neuropsychobiology. 36(2):73-82.

70. Gutzmann H, Hadler D. 1998. Sustained efficacy and safety of idebenone in the treatment of Alzheimer's disease: update on a 2-year double-blind multicentre study. J Neural Transm Suppl. 54:301-10.

71. Sui D, Xu X, Ye X, Liu M, Mianecki M, Rattanasinchai C, Buehl C, Deng X, Kuo MH. 2015. Protein interaction module-assisted function X (PIMAX) approach to producing challenging proteins including hyperphosphorylated tau and active CDK5/p25 kinase complex. Mol Cell Proteomics. 14(1):251-62.

72. Mukhopadhyay P, Rajesh M, Yoshihiro K, Haskó G, Pacher P. 2007. Simple quantitative detection of mitochondrial superoxide production in live cells. Biochem Biophys Res Commun. 358(1):203-8.

73. Köpke E, Tung YC, Shaikh S, Alonso AC, Iqbal K, Grundke-Iqbal I. 1993. Microtubule-associated protein tau. Abnormal phosphorylation of a non-paired helical filament pool in Alzheimer disease. J Biol Chem. 268(32):24374-84.

74. Biancalana M, Koide S. 2010. Molecular mechanism of Thioflavin-T binding to amyloid fibrils. Biochim Biophys Acta. 1804(7):1405-12.

75. Gachet MS, Schubert A, Calarco S, Boccard J, Gertsch J. 2017. Targeted metabolomics shows plasticity in the evolution of signaling lipids and uncovers old and new endocannabinoids in the plant kingdom. Sci Rep. 7:41177.

76. Soeda Y, Yoshikawa M, Almeida OF, Sumioka A, Maeda S, Osada H, Kondoh Y, Saito A, Miyasaka T, Kimura T, Suzuki M, Koyama H, Yoshiike Y, Sugimoto H, Ihara Y, Takashima A. 2015. Toxic tau oligomer formation blocked by capping of cysteine residues with 1,2-dihydroxybenzene groups. Nat Commun. 6:10216.

CHAPTER IV

SELECTIVE BENZODIAZEPINES ARE RISK FACTORS OF ALZHEIMER'S DISEASE

ABSTRACT

Alzheimer's disease (AD) is an irreversible neurodegenerative disease that has no cure or prevention to date. One defining feature of AD is neurofibrillary tangles (NFTs) composed of fibrils of hyperphosphorylated tau (p-tau). I have developed a p-tau-based aggregation assay for high-throughput screen of AD durg candidates. P-tau aggregation inhibitors (PTAIs) are potential AD therapeutics, while compounds that enhance p-tau aggregation (PTAE) and cytotoxicity are likely risk factors. Epidemiological studies have linked several common drugs to increased AD risks. Selective benzodiazepines were found in this study enhancing p-tau aggregation and cytotoxicity, lending molecular support to the epidemiological association of long-term use of benzodiazepines and increased risks of dementia. These results lay the foundation for the development of a p-tau aggregation kit, which is a joint effort between our laboratory and the Cayman Chemical company.

INTRODUCTION

Alzheimer's disease (AD) is the most common type of dementia that causes problems of memory, reasoning, and behaviors [1], and is the sixth-leading cause of death in the United States [2, 3]. There is no cure or prevention method. The defining biomarkers of AD are the progressive accumulation of amyloid beta (Aβ) plaques outside neurons and the neurofibrillary tangles (NFTs) consisting of hyperphosphorylated tau (p-tau) protein inside neurons [4, 5]. The lack of correlation between cognitive impairment and Aβ plaque development, as well as a string of failed drug trials cast significant doubt on a direct role of Aβ in AD pathogenesis. Instead, the causative role of oligomeric, hyperphosphorylated tau is gaining wider acceptance [7 – 10].

The microtubule (MT)-binding tau protein is encoded by a single MAPT gene. Alternative splicing generates six tau isoforms that bear 0, 1, or 2 N domains (0 – 2N) and 3 or 4 MT binding repeats (3R and 4R) [3, 6]. The pathological contribution of the N domains is not apparent, whereas the ratio of 3R:4R may differ in different tauopathies. While the 3R isoforms are as abundant as the 4R counterparts in AD, 3R isoforms increases in the brainstem of advanced AD patients [32]. The 3R isoforms are the primary NFT constituent in Pick's disease [33], manifesting its pathogenic potential. In contrast, progressive supranuclear palsy is a 4R tauopathy [6]. Biochemically, how 3R affects 4R to form fibrils is a subject of debate [34, 35]. Arachidonic acid induces 3R and 4R to form fibrils of distinct morphology [29]. Whether hyperphosphorylation causes 3R and 4R isoforms to behave differently is unknow.

While the direct cause for AD remains enigmatic, epidemiological studies suggested potential AD risk factors among certain pharmaceutical compounds. For example, chronic exposure to benzodiazepines [11, 12], anticholinergic drugs [15], antiepileptic drugs [14], or conventional synthetic disease-modifying antirheumatic drugs [13] were found to be linked to increased chance of dementia. From previous Chapters that demonstrate the use of p-tau aggregation inhibition as the first criterion to identify potential AD therapeutics, I hypothesize that the same assay can be used to test for AD risk factors via the identification of chemical compounds displaying significant p-tau aggregation enhancer (PTAE) activity. If true, this hypothesis also indicates that a kit featuring the aggregation of p-tau is likely to help researchers identify AD therapeutics and risk factors among their "favorite" compounds. This Chapter describes my work on the development of a p-tau aggregation kit, using benzodiazepines as the model for PTAE identification.

Benzodiazepines (BZDs) are widely prescribed to treat a variety of neurological conditions, such as anxiety, depression, epilepsy, and others [36]. BZDs constitute a large family of CNS drugs with a wide spectrum of half-lives and metabolites [17]. Epidemiological studies reported increased risks of AD from long-term use of certain BZDs [11, 12]. In the Billioti de Gage *et al* findings, the accumulated use of long-acting BZDS for 180 days or more in five years is linked to 84% increase of AD [12]. Shorter exposure, or the use of low bioavailability BZDs showed significantly lower risks. The core chemical structure of BZD is the fusion of a benzene ring and a diazepine ring, while substituents at positions N-1, C-3 and C-7 influence their pharmacokinetics profiles, including rapidity of absorption, lipophilicity and elimination half-time, the time

needed to reduce the plasma concentration of a drug to half (Fig 4.3A) [17, 18]. BZDs easily cross the blood-brain-barrier and are distributed in the central nervous system due to their high lipophilicity and plasma protein binding ability [20, 21]. The cumulative nature of BZD use and AD risks prompted that hypothesis that BZDs promote AD development by acting as a p-tau aggregation enhancer that potentiates cytotoxic p-tau aggregation. Evidence presented in this Chapter is consistent with this hypothesis.

MATERIALS AND METHODS

Materials. Prednicarbate, diazepam, flurazepam, temazepam, prazepam, nitrazepam, nimetazepam, nordiazepam and oxazepam were from Cayman Chemical (Ann Arbor, MI). Devazepide was purchased from Santa Cruz Biotechnology (Dallas, Texas). Fluorescein diacetate, propidium iodide, clofazimine, hexachlorophene, hydralazine hydrochloride, thioflavin S and Amicon Centrifugal Filter Unit were purchased from Sigma Aldrich (St. Louis, MO). Gibco Dulbecco's Modified Eagle Medium (DMEM), HyClone^{TM} Fetal Bovine Serum, Optical Adhesive Film and fluorescein isothiocyanate (FITC)-conjugated Annexin V were purchased from Thermo Fisher Scientific (Waltham, MA). Small volume, black, flat-bottom, 384-well plate was purchased from Griner Bio-One (Monroe, NC). All other chemicals for common buffers and solutions were from Sigma Aldrich (St. Louis, MO).

Recombinant Protein Expression and Purification. The plasmids and primers used in this work are listed in Tables 4.1 and 4.2. Tau 0N3R, 1N3R or 2N4R was inserted in the pMK1013 or pMK1013-GSK 3β plasmid by ligation independent cloning (LIC) via the LIC sequence including Not I restriction site at N-terminal of Jun. The tau isoform was amplified using ZAC tau S and ZAC tau AS oligos.

Table 4.1 Plasmid constructs used in this study

Plasmid	Main features	Source or reference
pMK1013	His6-Fos-thrombin + Jun-TEV	31
pMK1013-tau 0N3R	His6-Fos-thrombin + Jun-TEV-tau 0N3R	This study
pMK1013-tau 1N3R	His6-Fos-thrombin + Jun-TEV-tau 1N3R	This study
pMK1013-tau 1N4R	His6-Fos-thrombin + Jun-TEV-tau 1N4R	31
pMK1013-tau 2N4R	His6-Fos-thrombin + Jun-TEV-tau 2N4R	This study
pMK1013-GSK-3β	His6-Fos-thrombin-GSK-3β + Jun-TEV	This study
pMK1013-GSK-3β -tau 0N3R	His6-Fos-thrombin-GSK-3β + Jun-TEV-tau 0N3R	This study
pMK1013-GSK-3β -tau 1N3R	His6-Fos-thrombin-GSK-3β + Jun-TEV-tau 1N3R	This study
pMK1013-GSK-3β -tau 1N4R	His6-Fos-thrombin-GSK-3β + Jun-TEV-tau 1N4R	31
pMK1013-GSK-3β -tau 2N4R	His6-Fos-thrombin-GSK-3β + Jun-TEV-tau 2N4R	This study

Table 4.2 Oligos used in this study

Oligo	Sequence
ZAC TAU S	CCAGAGCGGCCTGCTGAGCCCCGCCAG
ZAC TAU AS	AAAGAGCGGCCTTCACAAACCCTGCTTG

Recombinant Protein Expression and Purification. P-tau and tau isoforms 0N3R, 1N3R, 2N4R were purified using the same protocol as 1N4R. The detailed protocol is described in Chapter II.

Mapping p-tau phosphorylation sites by LC-MS/MS. The Mass Spectrometry assay was done by Cayman Chemical (Ann Arbor, MI). The detailed protocol is described in Chapter II.

Thioflavin S Aggregation assay. Before aggregation assays, proteins were removed from the freezer and thawed on ice. Tau or p-tau was diluted to 6 µM tau in aggregation buffer including 20 mM Tris (pH 7.4), 1 mM DTT and 20 µM thioflavin S (ThS). Typically, the assays were assembled in a 384-well low-volume plate. The plate was covered by an Optical Adhesive Film to minimize evaporation during the assay. The plate was set at 37°C briefly before placing to a BioTek Synergy Neo Plate reader. ThS fluorescence was measured every 10 min (excitation 440 nm; emission 490 nm) for 16 hrs and collected using Gen5 software bundled with the BioTek plate reader.

Cytotoxicity of p-tau. Cell viability assays were conducted in 96-well plates. 2,000 HEK 293T cells in 100 µL media (DMEM, 10% FBS, pen/strep) were seeded to a well and cultured for 40 – 48 hours at 37°C, 5% CO_2. The confluency of cells may affect their sensitivity to p-tau. Values of LD_{50} can therefore only be compared among experiments done at the same time. For PTAEs, 10x concentration of p-tau and the test compounds

were assembled for pre-aggregation (without ThS) for 48 hours before adding 10 µl to 100 µl of cells in 96-well plates. 24 hours after the addition of protein/compound, cells were trypsinized and transferred to microcentrifuge tubes, and pelleted at 1,000 x g for 5 min at room temperature. Cell pellets were resuspended in phosphate-buffered saline (PBS, 137 mM NaCl, 2.7 mM KCl, 10 mM Na_2HPO_4, 1.8 mM KH_2PO_4) and incubated with 5 µg/ml fluorescein diacetate (FDA) for 5 min at room temperature. 5 µg/ml propidium iodide (PI) was then added to the mixture. Cells stained by FDA or PI were examined using an Olympus BX51 Fluorescence Microscope. Cells from randomly chosen fields were counted for FDA or PI stainability. At least fifty cells from multiple fields were counted for each treatment well. Viability was calculated using the equation:

Relative viability = FDA stained cells / (FDA stained cells + PI stained cells).

RESULTS

Production of four hyperphosphorylated tau (p-tau) and unphosphorylated tau isoforms by PIMAX system

One of my long-term research goals is to develop a kit featuring p-tau aggregation for interested scientists to test the p-tau aggregation modulation (enhancement and inhibition) by any chemicals. This kit may impact significantly the development of AD therapeutics and risk factor identification. As stated earlier, certain tauopathies are manifested by neurofibrillary tangles of predominantly 3R or 4R isoforms. An ideal kit should include different isoforms of tau. Indeed, the recombinant 3R and 4R tau without any post-translational modification have been shown to exhibit different characters in aggregation and fibril morphology [29]. However, how 3R and 4R tau behaves after they assume the disease-relevant hyperphosphorylation remains unknown. The first step of developing a p-tau aggregation kit was to prepare 4 different tau isoforms: 0N3R, 1N3R, 1N4R and 2N4R by the PIMAX system as the representatives. The four isoforms expressed with or without the GSK-3β kinase exhibited expected differential mobilities on SDS-PAGE gel (Fig 4.1A). Mass spectrometry analysis (Table 4.3) show comparable phosphorylation patterns among these four isoforms. Totally 41 phosphorylated sites were detected in the four isoforms, of which 19 were found in all four isoforms (“4-hitters”, green), 8 were positive in 3 isoforms (“3-hitters”, light green), 7 in 2 isoforms (“2-hitters”, light orange), and another 7 were found only in 1 isoform (“1-hitters”, light blue). Fig 4.1B shows the distribution of the 4-hitters relative to the functional domains of tau, as well as three additional 3-hitters (Ser46, Ser286, Ser305) that were present in all isoforms bearing the corresponding

exons subjected to alternative splicing. Eleven of these 22 sites are phospho-markers for NFT staging (bold and underlines) [10, 11], suggesting disease relevance. It is interesting to note that there was, in general, a very high degree of overlap among these four p-tau isoforms, which indicates that the substrate specificity of GSK-3β is not significantly affected by the 3 alternative spliced exons.

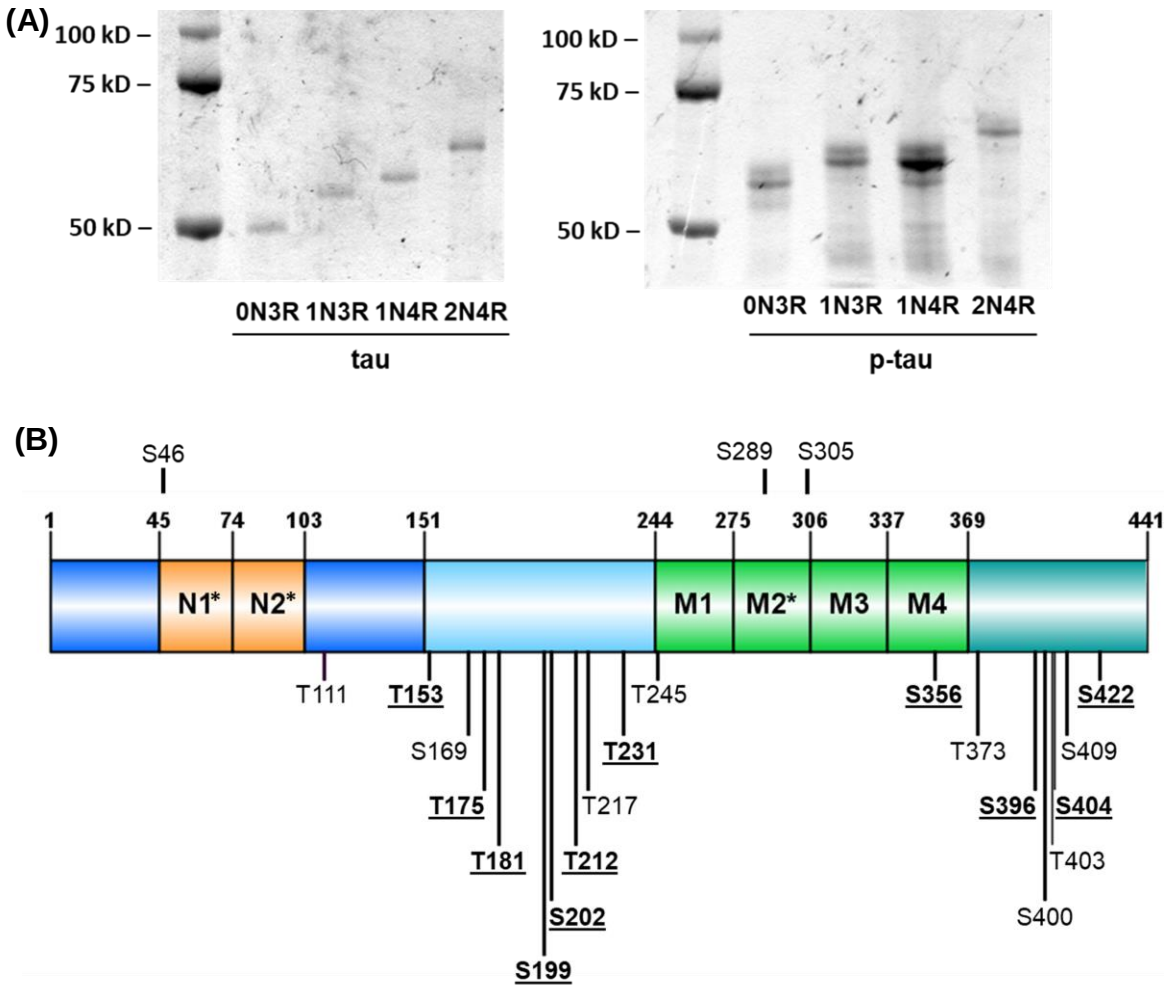

Figure 4.1 Production of hyperphosphorylated tau (p-tau) isoforms via PIMAX and phosphorylation mapping. (A) Purified tau, p-tau (phosphorylated by GSK-3β) 0N3R, 1N3R, 1N4R and 2N4R were resolved by an 8% SDS-PAGE gel. (B) Distribution of phosphorylation sites found in all four tau isoforms under the current study. Only those that were present in all four isoforms are shown. The three sites that are in the exons for alternative splicing are above the domain map. They were found to be phosphorylated in isoforms that contained the corresponding domains. AD staging epitopes are in bold and underlined; *: domains subjected to alternative splicing.

Table 4.3 Summary of p-tau phosphorylation site mapping in four isoforms by mass spectrometry

The first column shows all serine, threonine, and tyrosine residues of the longest tau isoform, 2N4R. Residues found to be phosphorylated are shaded according to the number of repetitions among the four isoforms. Forward slash symbol means the site doesn't exist in the isoform due to the lacking of corresponding N-terminal insertion or repeat domain.

Ser/Thr/Tyr	2N4R	1N4R	1N3R	0N3R	Ser/Thr/Tyr	2N4R	1N4R	1N3R	0N3R
T17					S210				
Y18					T212	+	+	+	+
Y29					S214				
T30					T217	+	+	+	+
T39					T220		+	+	+
S46	+	+	+	/	T231	+	+	+	+
T50		+	+	/	S235		+	+	+
T52	+			/	S237				
S56				/	S238				
S61				/	S241				
T63				/	T245	+	+	+	+
S64				/	S258				
S68				/	S262				
T69			+	/	T263				
T71					S285			/	/
T76					S289	+	+	/	/
T95		/	/	/	S292		+	/	/
T101					S305	+	+	/	/
T102					S316			+	+
T111	+	+	+	+	T319				
S113					S320	+	+		+
T123					S324		+		+
S129					S341				
S131					S352	+			+
T135					S356	+	+	+	+
S137					S361				+
T149		+	+	+	T373	+	+	+	+
T153	+	+	+	+	T377				
S162					T386				
S169	+	+	+	+	Y394		+	+	
T175	+	+	+	+	S396	+	+	+	+
T181	+	+	+	+	S400	+	+	+	+

Table 4.3 (cont'd)

S184					T403	+	+	+	+
S185					S404	+	+	+	+
S191	+		+	+	S409	+	+	+	+
S195				+	S412		+		
Y197					S413				
S198			+		T414				
S199	+	+	+	+	S416	+	+		+
S202	+	+	+	+	S422	+	+	+	+
T205	+		+	+	T427				
S208					S433				
					S435				
					Peptide coverage	100%	98%	100%	98%

Hyperphosphorylated tau isoforms exhibit similar aggregation kinetics

Hyperphosphorylation causes tau to exhibit molecular characters critical to the disease (see Chapter II). One such character is inducer-free aggregation. Intriguingly, it has been reported that tau 3R isoforms do not form fibrils as effectively as their 4R counterparts [29]. This prior work was done with unmodified tau that lacks altogether the disease-related feature of hyperphosphorylation. To see how my p-tau isoforms behave in the prototypical aggregation assays, a quantitative comparison of the aggregation kinetics of p-tau 0N3R, 1N3R, 1N4R and 2N4R isoforms was conducted. A 6 μM, a concentration close to the estimated abundance of oligomeric hyperphosphorylated tau in the AD brain [22], both aggregation kinetics and net changes of ThS fluorescence (indicator of fibril formation) over the course of 16 hours showed hyperphosphorylation-driven aggregation of all four tau isoforms (Fig 4.2B). Each of these four proteins showed fast increase of ThS signal in the first two hours, whereas the non-phosphorylated counterparts remained unchanged throughout the entire course of assay. While the initial (T_0) ThS signal and the net increase (Δ) values appeared to be different, such deviations are common in ThS-based aggregation assays of p-tau. Batch-to-batch variations and sometimes even day-to-day variations caused the net values of T_0 and Δ to fluctuate significantly. However, the apparent differentiation between tau and p-tau (that is, the aggregation-promoting power of hyperphosphorylation) has been highly reproducible. Together with the significant overlap in phosphorylation among these four isoforms, it was concluded that there was no obvious difference in the phosphorylation or aggregation kinetics of the four p-tau

species. As the 1N4R p-tau has been studied in great details in Chapters II and III, all the studies hereafter also used the 1N4R isoform as the representative.

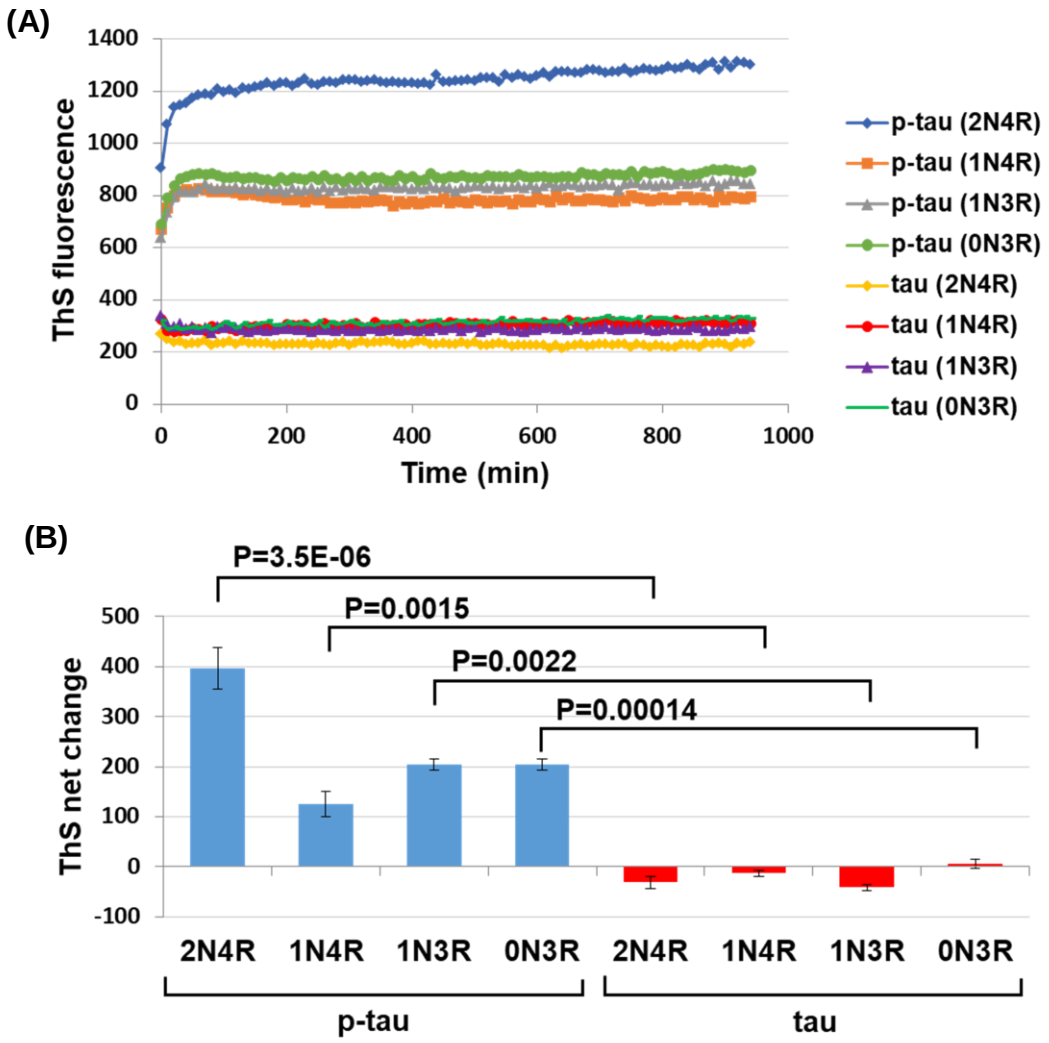

Figure 4.2 Comparison of four p-tau and tau isoforms aggregation. (A) Aggregation of p-tau or tau 0N3R, 1N3R, 1N4R or 2N4R was quantified by real-time thioflavin S (ThS) fluorescence kinetics or (B) by net changes of ThS signal after 16 hours of reaction. Error bars are standard deviation; n = 3. P values were obtained from two-tailed Student's t tests.

Selective prescription benzodiazepines enhance p-tau aggregation and cytotoxicity

The model in Fig 3.2 depicts the potential impact of chemicals that possess a significant modulating power on p-tau aggregation. Two brain permeant PTAIs were discovered in my pilot screen. While two PTAEs (i.e., prednicarbate and carmofur, Fig 3.4D) were identified as well, neither was likely to impose significant relevance to AD due to the treatment duration or application method (see Page 108 for discussion). Instead, I decided to take a targeted approach by examining whether a potential AD risk factor exhibited PTAE activity. To this end, I focused on benzodiazepines (BZDs) [11, 12]. Several prescription BZDs (Fig 4.3B) were acquired from a commercial supplier and tested in the p-tau aggregation and cytotoxicity assay. The PTAE activity of BZDs was tested by adding 6.25 – 150 μM of BZD to our standard 1N4R p-tau aggregation reactions. The ThS net changes are shown in Fig 4.3C. Diazepam (#1), temazepam (#2), flurazepam (#3), prazepam (#4) and devazepide (#5) enhanced p-tau aggregation, similar to the prednicarbate positive control, whereas nordiazepam (#6), oxazepam (#7), nitrazepam (#8) and nimetazepam (#9) had no apparent effect on p-tau aggregation (Fig 4.3C).

(A)

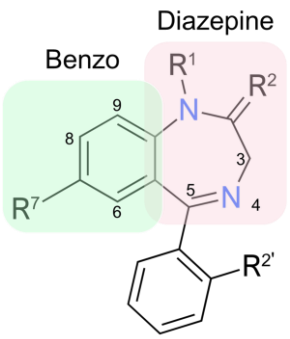
Benzo
Diazepine
R1
R2
R7
R2'
N
9
8
3
5
6
4

(B)

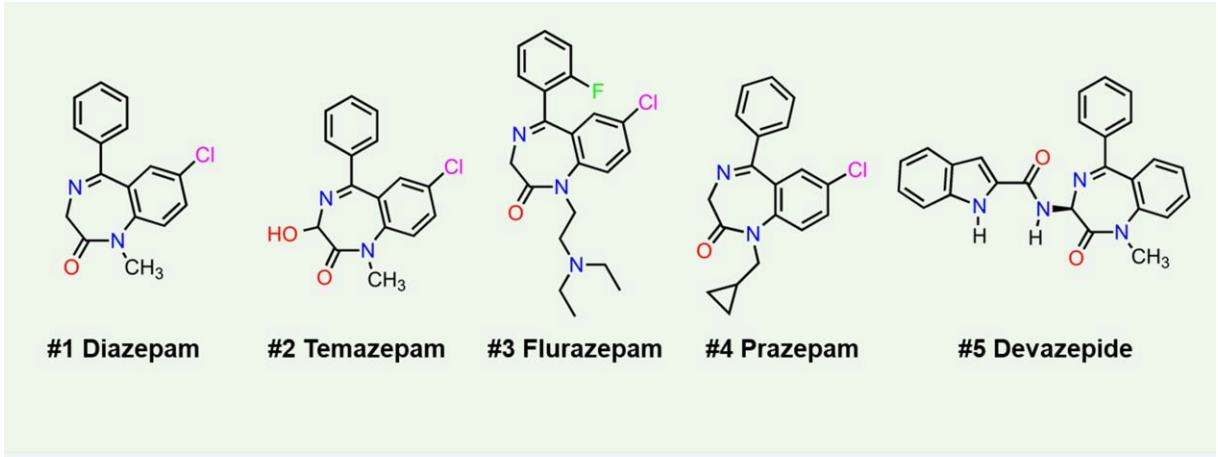
#1 Diazepam
#2 Temazepam
#3 Flurazepam
#4 Prazepam
#5 Devazepide

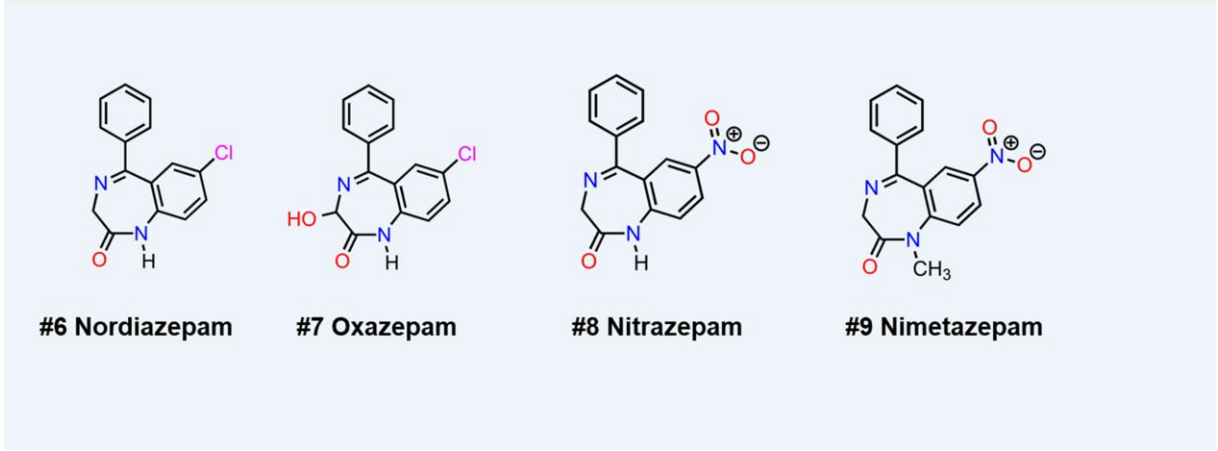
#6 Nordiazepam
#7 Oxazepam
#8 Nitrazepam
#9 Nimetazepam

Figure 4.3 (cont'd)

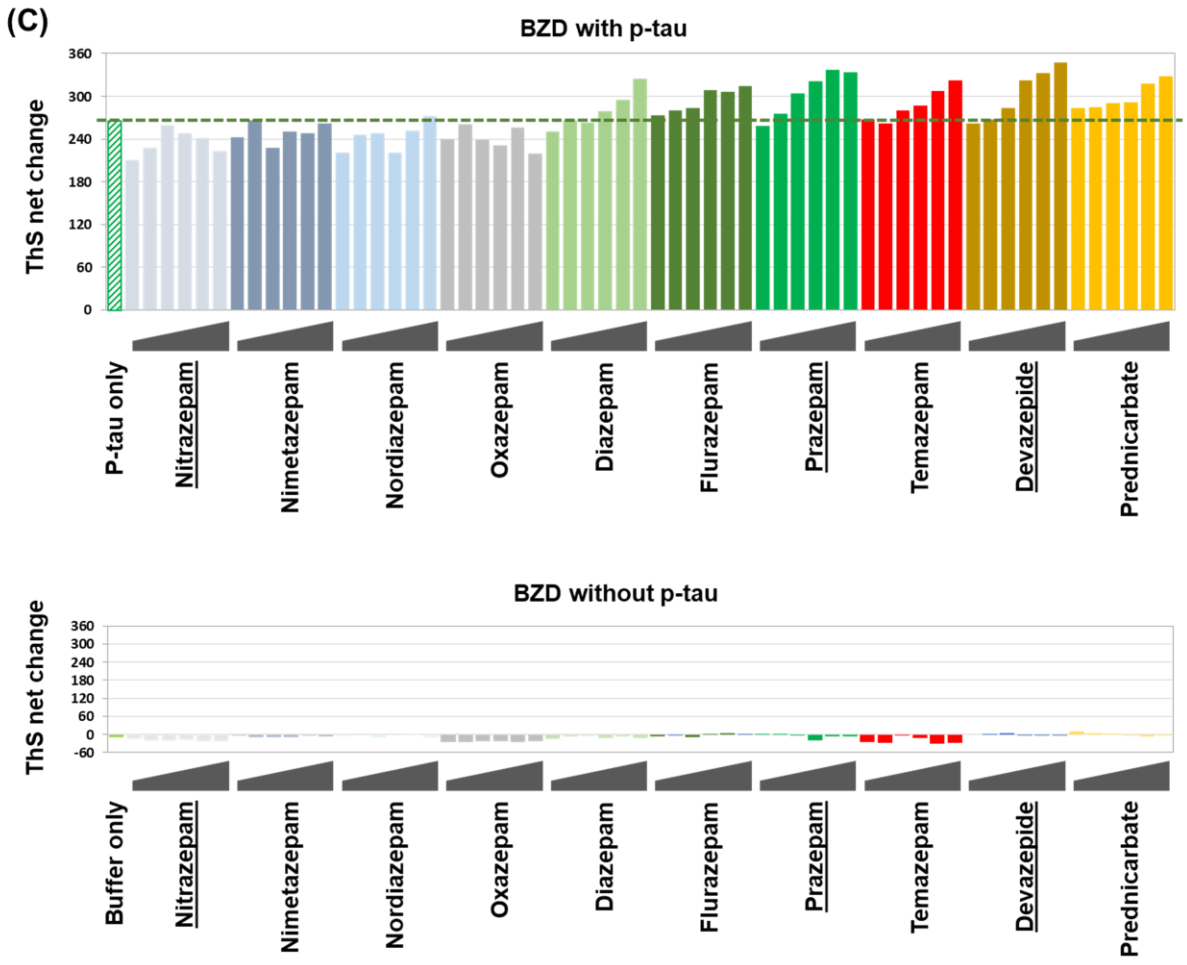

Figure 4.3 Selective prescription benzodiazepines are p-tau aggregation enhancers (PTAEs). (A) Basic structure of benzodiazepine. (B) Structures of candidate benzodiazepiness. (C) Net changes of ThS fluorescence from the aggregation for p-tau under the influence of 6.25 – 150 μM of benzodiazepines or prednicarbate (up) or compound alone (bottom). The three drugs to be tested further in cytotoxicity assays are underlined.

To test whether the PTAE activity corresponded to exacerbated p-tau cytotoxicity, HEK 293T cells were treated with p-tau after pre-incubation with different concentrations of the three representative BZDs: nitrazepam (#8, a non-PTAE), prazepam (#4, a PTAE), or devazepide (#5, a PTAE). The HEK 293T cells were more sensitive to p-tau in the presence of either prazepam or devazepide, but not nitrazepam (Fig 4.4A). The LD_{50} of 48-hr pre-incubated p-tau (concentration of p-tau causing 50% cell death) was found to be around 0.5 μM for HEK 293T. Co-incubation with increasing amounts of prazepam or devazepide caused the LD_{50} values of p-tau to decrease steadily, suggesting strengthening of cytotoxicity by either PTAE. Devazepide in multiple dose-response tests consistently showed the strongest effects on both p-tau aggregation and cell-killing (data not shown). Without p-tau, HEK 293T cells maintained full viability in the presence of the highest dose of the three BZDs tested here (Fig 4.4B), confirming the enhancement of p-tau cytotoxicity. To further substantiate the p-tau aggregation-dependent cell killing enhancement by devazepide, I performed p-tau aggregation assays (no ThS) in the presence of devazepide for 0, 24, 48, or 72 hours. The p-tau/devazepide mix was then added to HEK 293T cells for viability assessment. Fig 4.4C again shows p-tau pre-aggregation duration-dependent increase of cell death. Intriguingly, the 72-hr pre-aggregation was not more toxic than the 48-hr sample, reminiscent of Fig 2.3 A (Chapter II) in which p-tau lost progressively its cell killing power if the pre-aggregation extended for more than 48 hours.

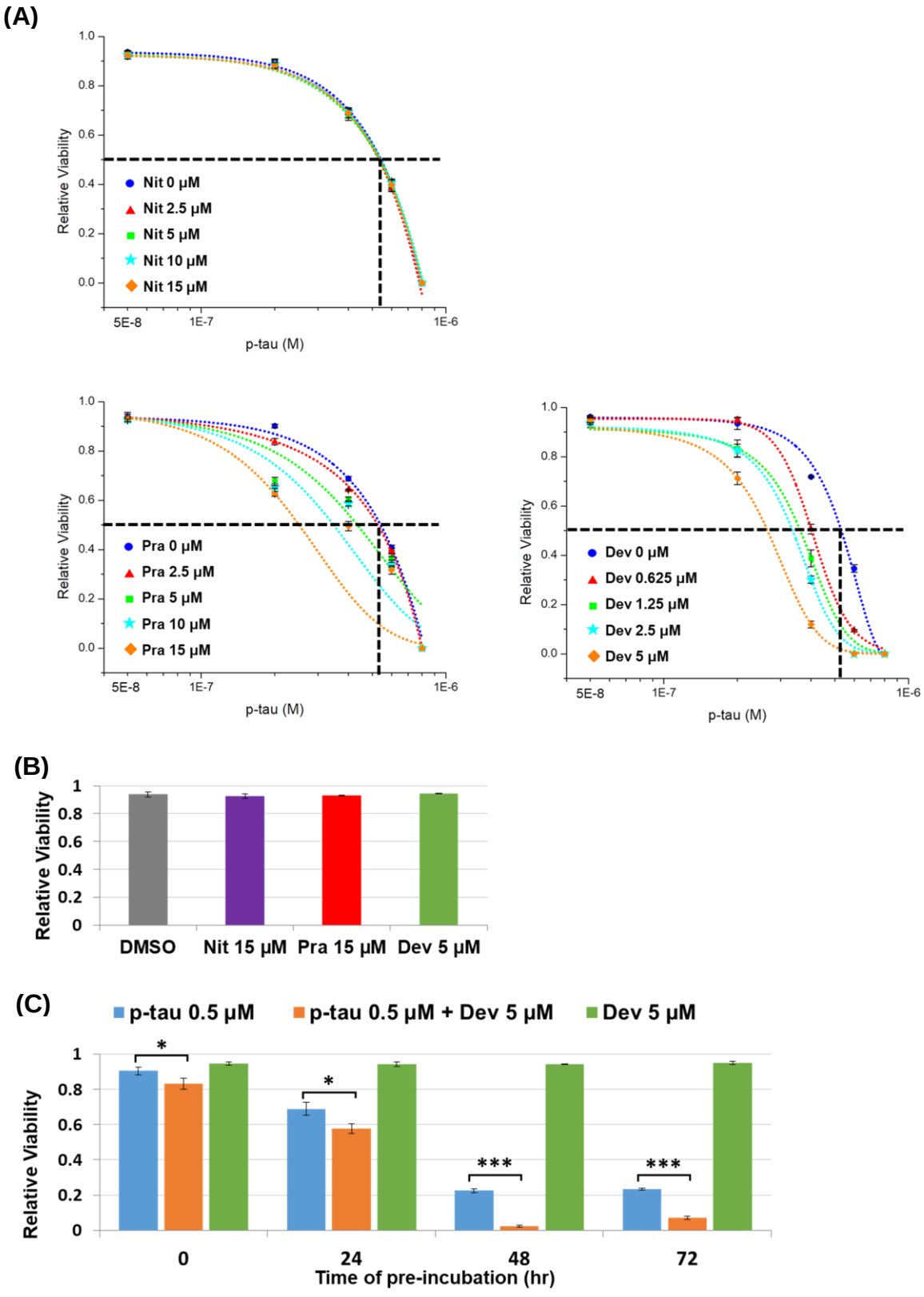

Figure 4.4 Selective prescription benzodiazepines potentiate p-tau cytotoxicity.

Figure 4.4 (cont'd)

(A) PTAE activity correlates with p-tau cytotoxicity changes. HEK 293T cells were treated with 0 – 0.6 μM of p-tau in conjunction with varying doses of nitrazepam, prazepam or devazepide. Devazepide consistently showed stronger exacerbation on p-tau cytotoxicity, hence lower concentrations were used here. The black dotted lines indicate 50% viability. (B) Nitrazepam, prazepam, and devazepide do not affect the viability of HEK 293T cells. (C) 0 – 48 hr pre-incubation promotes devazepide's effect on p-tau cytotoxicity. Error bars are standard deviation; n = 3. P values were obtained from two-tailed Student's t tests; *: P≤0.05, **: P≤0.01, ***: P≤0.001.

DISCUSSION

This Chapter summarizes the results of the characterization of four different p-tau isoforms and, using the 1N4R p-tau as the representative, the correlation between the PTAE activity and exacerbated p-tau cytotoxicity. These results confirmed the hypothesis that the p-tau aggregation assay may be an effective, primary assay for the identification of potential AD therapeutics and risk factors. Our lab is now collaborating with the Cayman Chemical Company (Ann Arbor, MI) to develop a p-tau aggregation kit for interested researchers. The test of whether a prescription drug behaves as a PTAE provides a way to evaluate the drug's safety profile. To differentiate the compound's influence on distinct p-tau isoforms, 0N3R, 1N3R, 1N4R and 2N4R p-tau were generated. The mapping of phosphorylation sites in these four p-tau isoforms are highly overlapped, indicating that the substrate specificity of GSK-3β is not significantly affected by the 3 alternatively spliced exons. Even though there are papers showing 4R isoforms fibrillized more efficiently than 3R isoforms in the presence of an inducer [29, 30], the results of my aggregation assays showed that the four p-tau isoforms behaved similarly in the aggregation kinetics, indicating the diversity between the unmodified tau and p-tau. The 1N4R p-tau has been successfully used for selecting two p-tau aggregation inhibitors, R-(–)-apomorphine and raloxifene, which also attenuated p-tau cytotoxicity. Therefore, the 1N4R p-tau isoform was selected to further examine the potential PTAEs.

It is noteworthy that the four p-tau isoforms exhibited very similar aggregation kinetics (Fig 4.2). Unlike the unmodified tau that the Kanaan group [29] showed had very inefficient, arachidonic acid-induced fibrillization among the 3R isoforms, my data

suggested that hyperphosphorylation was a potent fibrillogenic trigger for both 3R and 4R species. This finding is critical as the 3R isoforms are the predominant species in Pick's disease [33]. The lack of fibrillogenesis of unmodified 3R tau in vitro argues strongly for the pathogenic potential of hyperphosphorylation, and validates the systems described herein.

Long-term usage of BZDs has been reported to be associated with increased risks of dementia [11, 12]. Benzodiazepines (BZDs) are the most commonly used medications for treating anxiety, insomnia, and many neurological conditions [17]. Prescription BZDs function through their enhancement on the effect of the neurotransmitter gamma-aminobutyric acid (GABA) at the $GABA_A$ receptor [23]. In addition, BZDs also bind Translocator protein (TSPO), an important marker for neuroinflammation [24] on the outer mitochondrial membrane [25]. 30.6 million adults, which accounts for 12.6% of the total population in the United States, have reported the usage of BZDs in 2015-2016 [26, 27]. This prescription is most frequent in adults age 50-64 [26], coinciding with the upward trend of AD prevalence. Based on their elimination half-time, BZDs are classified into three categories: short acting (1-12 hrs), intermediate-acting (12 – 40 hrs) and long-acting (40 – 250 hrs) [17]. The time to clear a BZD from the body is about 5 elimination half-times, and can be prolonged in the elderly due to reduced liver activity [28]. Diazepam (#1), prazepam (#4) , flurazepam (#3), and temazepam (#5) have a half-life of 100 hr, 29 – 224 hr, 2.3 hr, and 2 hr. One implication from this work is that by choosing a non-PTAE, or one that has short bioavailability, the risks for AD may be under control.

The structures of BZDs tested in this work also provide interesting clue for future structure-activity relationship (SAR) studies (Fig 4.3A). Diazepam (#1) and temazepam (#2) are N-1-methyl-substituted BZDs, while their N-demethylation products, nordiazepam (#6) and oxazepam (#7) lack the p-tau aggregation and cytotoxicity enhancement activities. Similarly, flurazepam (#3) and prazepam (#4) are modified at N-1 by 2-(diethylamino)ethyl and cyclopropylmethyl respectively. Together with the minimal difference between the diazepam/nordiazepam, and the temazepam/oxazepam pairs, it seems very possible that an alkyl substitution at the N-1 position plays a critical role in defining a damning PTAE BZD. Devazepide (#5) has an N-1-methyl and a unique C-3-indole-2-carboxamide substitution, and was the strongest PTAE in both aggregation and in cell killing assays. Modifications at the C-3 position therefore may further fortify PTAE activity and cytotoxicity. Lastly, the two 7-nitro-benzodiazepines, nitrazepam (#8) and nimetazepam (#9), show no influence on p-tau fibrilization, in spite of the N-1-methyl group in nimetazepam. It is therefore possible that a free C-7 position (or bearing a small atom such as chloride) is necessary for a BZD to exert the PTAE activity.

REFERENCES

REFERENCES

1. Bancher C, Brunner C, Lassmann H, Budka H, Jellinger K, Wiche G, Seitelberger F, Grundke-Iqbal I, Iqbal K, Wisniewski HM. 1989. Accumulation of abnormally phosphorylated tau precedes the formation of neurofibrillary tangles in Alzheimer's disease. Brain Res. 477(1-2):90-9.

2. Arendt T, Stieler JT, Holzer M. 2016. Tau and tauopathies. Brain Res Bull. 126(Pt 3):238-292.

3. Buée L, Bussière T, Buée-Scherrer V, Delacourte A, Hof PR. 2000. Tau protein isoforms, phosphorylation and role in neurodegenerative disorders. Brain Res Brain Res Rev. 33(1):95-130.

4. Neve RL, Harris P, Kosik KS, Kurnit DM, Donlon TA. 1986. Identification of cDNA clones for the human microtubule-associated protein tau and chromosomal localization of the genes for tau and microtubule-associated protein 2. Brain Res. 387(3):271-80.

5. Goedert M, Spillantini MG, Cairns NJ, Crowther RA. 1992. Tau proteins of Alzheimer paired helical filaments: abnormal phosphorylation of all six brain isoforms. Neuron. 8(1):159-68.

6. Flament S, Delacourte A, Verny M, Hauw JJ, Javoy-Agid F. 1991. Abnormal Tau proteins in progressive supranuclear palsy. Similarities and differences with the neurofibrillary degeneration of the Alzheimer type. Acta Neuropathol. 81(6):591-6.

7. Flach K, Hilbrich I, Schiffmann A, Gärtner U, Krüger M, Leonhardt M, Waschipky H, Wick L, Arendt T, Holzer M. 2012. Tau oligomers impair artificial membrane integrity and cellular viability. J Biol Chem. 287(52):43223-33.

8. Berger Z, Roder H, Hanna A, Carlson A, Rangachari V, Yue M, Wszolek Z, Ashe K, Knight J, Dickson D, Andorfer C, Rosenberry TL, Lewis J, Hutton M, Janus C. 2007. Accumulation of pathological tau species and memory loss in a conditional model of tauopathy. J Neurosci. 27(14):3650-62.

9. Wu JW, Hussaini SA, Bastille IM, Rodriguez GA, Mrejeru A, Rilett K, Sanders DW, Cook C, Fu H, Boonen RA, Herman M, Nahmani E, Emrani S, Figueroa YH, Diamond MI, Clelland CL, Wray S, Duff KE. 2016. Neuronal activity enhances tau propagation and tau pathology in vivo. Nat Neurosci. 19(8):1085-92.

10. Frost B, Jacks RL, Diamond MI. 2009. Propagation of tau misfolding from the outside to the inside of a cell. J Biol Chem. 284(19):12845-52.

11. Zhong G, Wang Y, Zhang Y, Zhao Y. 2015. Association between Benzodiazepine Use and Dementia: A Meta-Analysis. PLoS One. 10(5):e0127836.

12. Billioti de Gage S, Moride Y, Ducruet T, Kurth T, Verdoux H, Tournier M, Pariente A, Bégaud B. 2014. Benzodiazepine use and risk of Alzheimer's disease: case-control study. BMJ. 349:g5205.

13. Chou MH, Wang JY, Lin CL, Chung WS. 2017. DMARD use is associated with a higher risk of dementia in patients with rheumatoid arthritis: A propensity score-matched case-control study. Toxicol Appl Pharmacol. 334:217-222.

14. Taipale H, Gomm W, Broich K, Maier W, Tolppanen AM, Tanskanen A, Tiihonen J, Hartikainen S, Haenisch B. 2018. Use of Antiepileptic Drugs and Dementia Risk-an Analysis of Finnish Health Register and German Health Insurance Data. J Am Geriatr Soc. 66(6):1123-1129.

15. Gray SL, Anderson ML, Dublin S, Hanlon JT, Hubbard R, Walker R, Yu O, Crane PK, Larson EB. 2015. Cumulative use of strong anticholinergics and incident dementia: a prospective cohort study. JAMA Intern Med. 175(3):401-7.

16. Richardson K, Fox C, Maidment I, Steel N, Loke YK, Arthur A, Myint PK, Grossi CM, Mattishent K, Bennett K, Campbell NL, Boustani M, Robinson L, Brayne C, Matthews FE, Savva GM. 2018. Anticholinergic drugs and risk of dementia: case-control study. BMJ. 361:k1315.

17. Wick JY. 2013. The history of benzodiazepines. Consult Pharm. 28(9):538-48.

18. Gerecke M. 1983. Chemical structure and properties of midazolam compared with other benzodiazepines. Br J Clin Pharmacol. 16 Suppl 1:11S-16S.

19. Jones DR, Hall SD, Jackson EK, Branch RA, Wilkinson GR. 1988. Brain uptake of benzodiazepines: effects of lipophilicity and plasma protein binding. J Pharmacol Exp Ther. 245(3):816-22.

20. Arendt RM, Greenblatt DJ, Liebisch DC, Luu MD, Paul SM. 1987. Determinants of benzodiazepine brain uptake: lipophilicity versus binding affinity. Psychopharmacology (Berl). 93(1):72-6.

21. Mukhopadhyay P, Rajesh M, Yoshihiro K, Haskó G, Pacher P. 2007. Simple quantitative detection of mitochondrial superoxide production in live cells. Biochem Biophys Res Commun. 358(1):203-8.

22. Khatoon S, Grundke-Iqbal I, Iqbal K. 1994. Levels of normal and abnormally phosphorylated tau in different cellular and regional compartments of Alzheimer disease and control brains. FEBS Lett. 351(1):80-4.

23. Lydiard RB. 2003. The role of GABA in anxiety disorders. J Clin Psychiatry. 64 Suppl 3:21-7.

24. Scarf AM, Kassiou M. 2011. The translocator protein. J Nucl Med. 52(5):677-80.

25. Papadopoulos V, Lecanu L, Brown RC, Han Z, Yao ZX. 2006. Peripheral-type benzodiazepine receptor in neurosteroid biosynthesis, neuropathology and neurological disorders. Neuroscience. 138(3):749–56.

26. Maust DT, Lin LA, Blow FC. 2019. Benzodiazepine Use and Misuse Among Adults in the United States. Send to Psychiatr Serv. 70(2):97-106. Epub 2018 Dec 17.

27. Blanco C, Han B, Jones CM, Johnson K, Compton WM. 2018. Prevalence and Correlates of Benzodiazepine Use, Misuse, and Use Disorders Among Adults in the United States. Send to J Clin Psychiatry. 79(6). pii: 18m12174.

28. Griffin CE 3rd, Kaye AM, Bueno FR, Kaye AD. 2013. Benzodiazepine pharmacology and central nervous system-mediated effects. Ochsner J. 13(2):214-23.

29. Cox K, Combs B, Abdelmesih B, Morfini G, Brady ST, Kanaan NM. 2016. Analysis of isoform-specific tau aggregates suggests a common toxic mechanism involving similar pathological conformations and axonal transport inhibition. Neurobiol Aging. 47:113-126.

30. Zhong Q, Congdon EE, Nagaraja HN, Kuret J. 2012. Tau isoform composition influences rate and extent of filament formation. J Biol Chem. 287(24):20711-9.

31. Sui D, Xu X, Ye X, Liu M, Mianecki M, Rattanasinchai C, Buehl C, Deng X, Kuo MH. 2015. Protein interaction module-assisted function X (PIMAX) approach to producing challenging proteins including hyperphosphorylated tau and active CDK5/p25 kinase complex. Mol Cell Proteomics. 14(1):251-62.

32. Uematsu M, Nakamura A, Ebashi M, Hirokawa K, Takahashi R, Uchihara T. 2018. Brainstem tau pathology in Alzheimer's disease is characterized by increase of three repeat tau and independent of amyloid β. Acta Neuropathol Commun. 6(1):1.

33. Qian W, Liu F. 2014. Regulation of alternative splicing of tau exon 10. Neurosci Bull. 30(2):367-77.

34. Siddiqua A, Margittai M. 2010. Three- and four-repeat Tau coassemble into heterogeneous filaments: an implication for Alzheimer disease. J Biol Chem. 285(48):37920-6.

35. Adams SJ, DeTure MA, McBride M, Dickson DW, Petrucelli L. 2010. Three repeat isoforms of tau inhibit assembly of four repeat tau filaments. PLoS One. 5(5):e10810.

36. O'brien CP. 2005. Benzodiazepine use, abuse, and dependence. J Clin Psychiatry. 66 Suppl 2:28-33.

APPENDICES

APPENDIX A

Reduction of EC_{50} for R-(–)-apomorphine on p-tau cytotoxicity by mixing with curcuminoid

The EC_{50} (the concentration of the compound that gives half-maximal inhibition effect) of R-(–)-apomorphine on 0.8-μM p-tau's cytotoxicity for SH-SY5Y cells is around 3 μM (Fig 3.6C). To reduce the amount of R-(–)-apomorphine required for cell protection, I have tried mixing R-(–)-apomorphine with other compounds and subjected the combination to p-tau treated cells. One that gives positive result is the mixture of R-(–)-apomorphine and 1 μM of one kind curcuminoid (#21), 1,7-Bis(2-hydroxy-5-methoxyphenyl)-1,6-heptadiene-3,5-dione (Fig 5.1A). This curcuminoid is a gift from Dr. Rita P.-Y. Chen [1]. Curcumin is the active ingredient in turmeric, a spice that is commonly used in Asian food. Curcumin is an amyloid beta (Aβ) aggregation inhibitor [2], reduces Aβ level and benefits memory ability in AD transgenic mouse models [3, 4]. In addition, recent publications support that curcumin also works as tau aggregation inhibitor in vitro [5] and reduces tau hyperphosphorylation level in a mouse model [6]. Curcuminoid are derivatives of curcumin with high solubility [1], which may contribute to better efficacy in AD therapeutics development. To examine whether curcuminoid#21 itself exhibits p-tau aggregation inhibitor (PTAI) activity, 12.5 – 50 μM of the compound or DMSO as control was added into the thioflavin S aggregation assay for 6-μM p-tau. The result of ThS net change indicates that the curcuminoid #21 prevents p-tau aggregation in a dose-dependent manner (Fig 5.1B). The curcuminoid #21 also presents protection against p-tau cytotoxicity (Fig 5.1C). 8 μM of this compound can increase SH-SY5Y cell viability to 40% after 0.8-μM p-tau treatment. After mixing this

curcuminoid#21 with R-(–)-apomorphine, the viability curve under 0.8-μM p-tau shows a left shift (blue curve shifts to red curve in Fig 5.1 D). This indicates adding curcuminoid#21 reduces cell death in the presence of R-(–)-apomorphine, even though the compound itself shows no protection at 1 μM. More experiments are needed to test the active curcuminoid species and the active concentration range. This work suggests that the dosage of R-(–)-apomorphine or other compound for AD treatment may be reduced by taking food that contains certain curcuminoids.

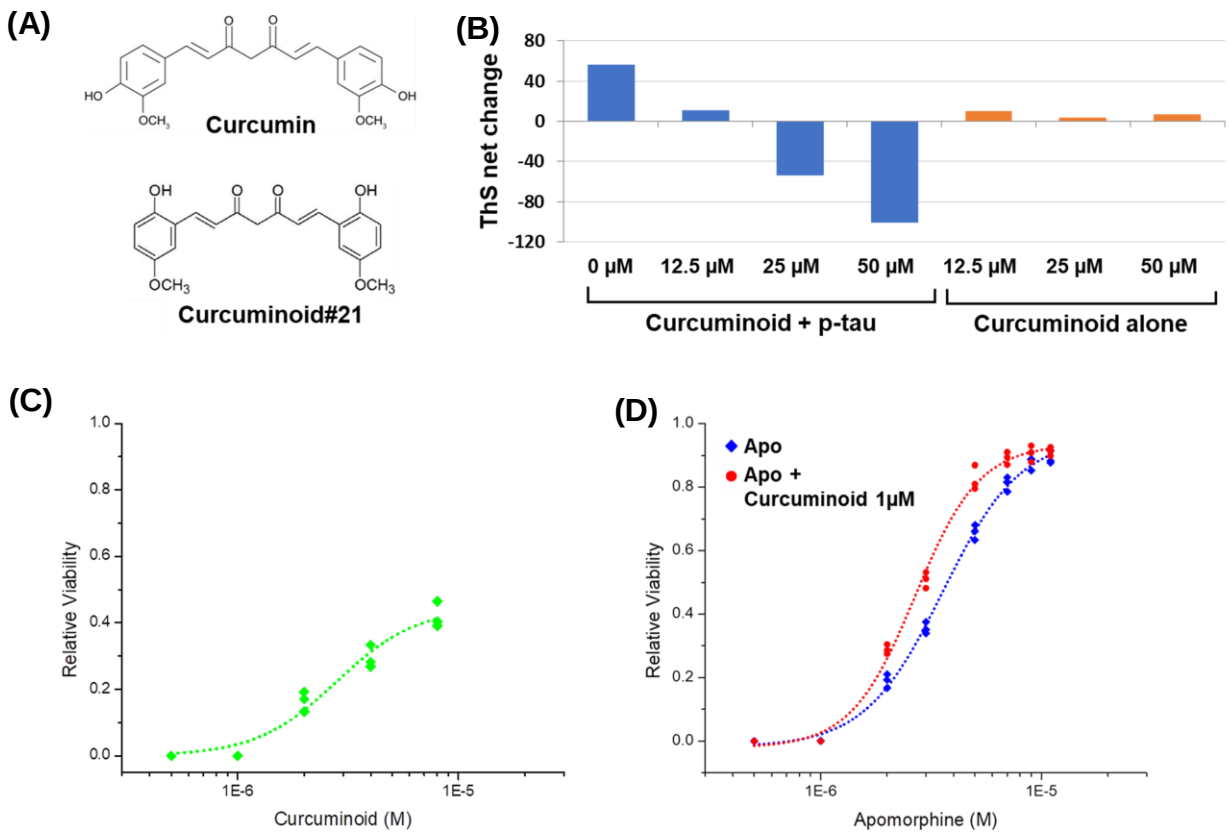

Figure 5.1 Mixture of R-(–)-apomorphine and curcuminoid reduces the EC50 of R-(–)-apomorphine. (A) Structure of Curcumin and Curcuminoid #21. (B) Curcuminoid #21 is a PTAI. 12.5, 25, 50 μM curcuminoid #21 or DMSO was added into the aggregation of 6-μM p-tau. The ThS net change shows a dose-dependent reduction. (C) Viability curve of SH-SY5Y cells treated by 0.8 μM p-tau in the presence of 0 – 10 μM Curcuminoid #21. (D) Viability curve of SH-SY5Y cells treated by 0.8-μM p-tau in the presence of 0 – 17 μM R-(–)-apomorphine or the mixture of R-(–)-apomorphine and 1 μM Curcuminoid #21.

APPENDIX B

Bimolecular fluorescence complementation orthogonal testing

METHODS

Plasmids and Recombinant Genes. The plasmids and primers used in this work are listed in Tables 5.1 and 5.2. Venus (1-210) or Venus (211-238) was inserted at the N-terminal or C-terminal of the 1N4R tau in the pMK1013-GSK-3β-tau plasmid by ligation independent cloning (LIC). A LIC sequence including Not I restriction site was inserted at N-terminal of the 1N4R tau in the pMK1013-GSK 3β-tau plasmid by QuikChange mutagenesis using oligos oXD266 and oXD267, or inserted at C-terminal of the 1N4R tau in the pMK1013-GSK 3β-tau plasmid using oligos oXD268 and oXD269. The Venus(1-210) amplified using oXD270 and oXD271, or Venus(1-210) amplified using oXD272 and oXD273 was inserted to the N-terminal of the 1N4R tau by LIC. The Venus(1-210) containing a stop codon amplified using oXD270 and oXD274, or Venus(1-210) containing a stop codon amplified using oXD272 and oXD275 was inserted to the C-terminal of the 1N4R tau by LIC.

Table 5.1 Plasmid constructs used in this study

Plasmid	Main features	Source or reference
pMK1013-GSK-3β-tau	His6-Fos-thrombin-GSK-3β + Jun-TEV-tau	7
pXD37	pUC57-VENUS, E. coli codon opt	This study
pNK05	His6-Fos-thrombin-GSK-3β + Jun-Vneus(1-210)-TEV-tau	This study
pNK06	His6-Fos-thrombin-GSK-3β + Jun-Vneus(211-238)-TEV-tau	This study
pNK07	His6-Fos-thrombin-GSK-3β + Jun-TEV-tau-Vneus(1-210)	This study
pNK08	His6-Fos-thrombin-GSK-3β + Jun-TEV-tau-Vneus(211-238)	This study

Table 5.2 Oligos used in this study

Oligo	Sequence
oXD266	CAG GGT TCT AGT CCA GAG CGG CCG CTG TTT ATT GCT GAG CCC CGC CAG GAG TTC
oXD267	GAA CTC CTG GCG GGG CTC AGC AAT AAA CAG CGG CCG CTC TGG ACT AGA ACC CTG
oXD268	TCC CTG GCC AAG CAG GGT TTG AGT CCA GAG CGG CCG CTG TTT A TC GAG TCT GGT AAA GAA
oXD269	TTC TTT ACC AGA CTC GA T AAA CAG CGG CCG CTC TGG ACT CAA ACC CTG CTT GGC CAG GGA
oXD270	CCAGAGCGGCCTGTGAGCAAAGGCGAGGAAC
oXD271	AAACAGCGGCCTGTCTTTGCTCAGCTTGCTC
oXD272	CCAGAGCGGCCTCCGAACGAGAAGCGTGAT
oXD273	AAACAGCGGCCTTTTGTACAGCTCGTCCATACC
oXD274	AAACAGCGGCCTTCAGTCTTTGCTCAGCTTGCTC
oXD275	AAACAGCGGCCTTCATTTGTACAGCTCGTCCATACC

Recombinant Protein Expression and Purification. P-tau-VN and VC-p-tau were expressed using the same protocol as PIMAX p-tau (Chapte II) but were present in the inclusion bodies. For purification, the inclusion bodies were collected and rinsed using 20 ml Buffer A. The sample was centrifuged again at 10,000 x g for 5 min at 4°C, and the supernatant was removed. The pellets were resuspended using 20 ml 8 M Urea, 10 mM DTT in Buffer A and rocked for 1hr at 4°C. The mixture was then centrifuged at 10,000 x g for 10 min at 4°C, the supernatant was transferred to a 14 kD cutoff dialysis tube and dialyzed against 500 ml of 6 M, 4 M, 2 M, 1 M, 0.5 M and 0 M Urea in Buffer A sequentially. Each dialysis lasted for 4 hours at 4°C. The final solution containing refolded protein was transferred to a new tube. 0.5 mM DTT and 1 mM EDTA were supplied. The sample was then purified by TEV protease digestion and gel filtration chromatography using the same protocol as p-tau.

Aggregation assay. Before aggregation assays, proteins were removed from the freezer and thawed on ice. P-tau-VN and VC-p-tau was diluted to 3 μM in aggregation buffer containing 20 mM Tris (pH 7.4), 1 mM DTT, 20 μM thioflavin S (ThS), and a compound of interest as the aggregation modulator. Typically, the assays were assembled in a 384-well low-volume plate. The plate was covered by an Optical Adhesive Film to minimize evaporation during the assay. The plate was set at room temperature briefly before placing to a BioTek Synergy Neo Plate reader. Fluorescence was measured every 10 min (excitation 440 nm, emission 490 nm for ThS signal and excitation 505 nm, emission 545 nm for Venus signal) for 16 hrs and collected using Gen5 software bundled with the BioTek plate reader.

RESULTS

In addition to cytotoxicity, I developed another dye-free, Bimolecular fluorescence complementation (BiFC) [8, 9] orthogonal testing to study how a compound may affect p-tau aggregation. P-tau is fused to complementary fragments (VN and VC) of a GFP derivative fluorescent reporter protein called Venus. The fusion proteins do not fluoresce when expressed separately. When p-tau interacts with each other during aggregation, the two complementary fragments are brought together, permitting the reconstruction of a fluorescent Venus (Fig 5.2A). 6.25 - 150 µM R-(–)-apomorphine or DMSO as control was added into the aggregation assay of the mixture of 3-µM p-tau-VN and 3-µM VC-p-tau. R-(–)-apomorphine presents a dose-dependent inhibition and a consistent biphasic pattern on both ThS and Venus signal (Fig 5.2B, C). In the case of raloxifene, the compound at high concentrations (75 and 150 µM) shows prevention on the reconstitution of Venus till 16 hrs after the onset of aggregation (Figure 5.2D). The different behaviors of R-(–)-apomorphine and raloxifene in the BiFC assay indicate the two compounds inhibit p-tau aggregation via distinct mechanisms.

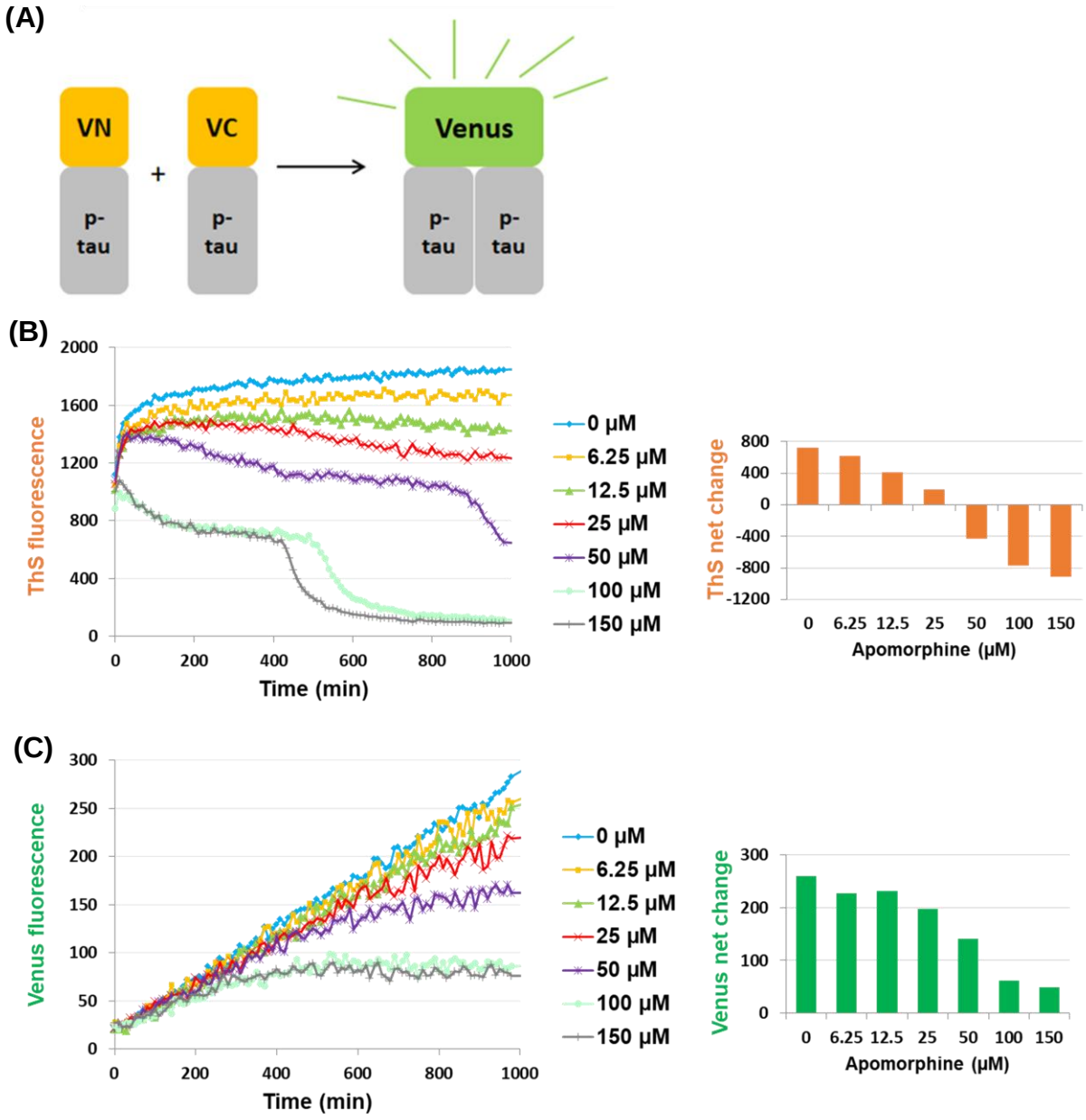
(A)
VN
VC
Venus
p-tau
p-tau
p-tau
p-tau
(B)
ThS fluorescence
Time (min)
0 µM
6.25 µM
12.5 µM
25 µM
50 µM
100 µM
150 µM
ThS net change
Apomorphine (µM)
(C)
Venus fluorescence
Time (min)
Venus net change
Apomorphine (µM)

Figure 5.2 (cont'd)

(D)

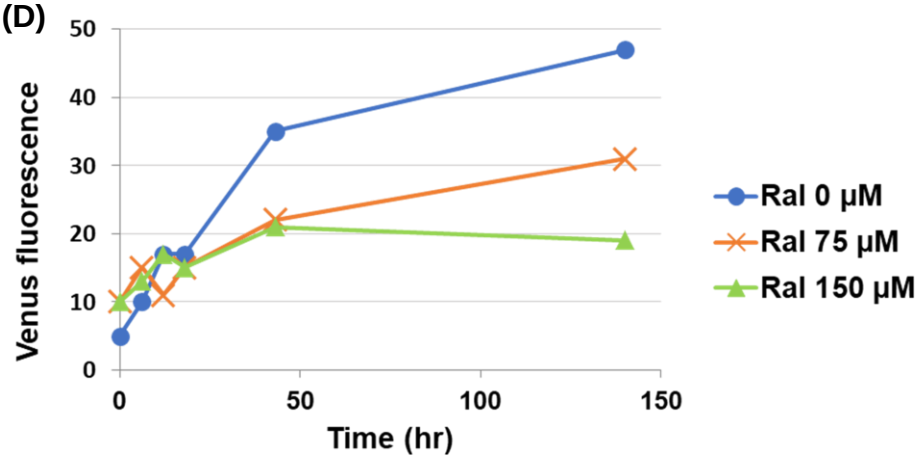

Figure 5.2 R-(–)-apomorphine and raloxifene inhibit p-tau aggregation in BIFC orthogonal assay. (A) Schematic mechanism for Bimolecular Fluorescence Complementation (BiFC) system. VN and VC are the N' (residues 1 - 210) and C' (residues 210 – 238) portions of Venus. (B) ThS and (C) Venus fluorescence changes of 3-µM p-tau-VN and 3-µM VC-p-tau aggregation under the influence of 6.25 – 150 µM R-(–)-apomorphine or DMSO as control. (D) Venus fluorescence changes of 3-µM p-tau-VN and 3-µM VC-p-tau aggregation under the influence of 75 or 150 µM of raloxifene or DMSO as control.

REFERENCES

REFERENCES

1. Chen PT, Chen ZT, Hou WC, Yu LC, Chen RP. 2016. Polyhydroxycurcuminoids but not curcumin upregulate neprilysin and can be applied to the prevention of Alzheimer's disease. Sci Rep. 6:29760.

2. Ono K, Hasegawa K, Naiki H, Yamada M. 2004. Curcumin has potent anti-amyloidogenic effects for Alzheimer's beta-amyloid fibrils in vitro. J Neurosci Res. 75(6):742-50.

3. Lim GP, Chu T, Yang F, Beech W, Frautschy SA, Cole GM. 2001. The curry spice curcumin reduces oxidative damage and amyloid pathology in an Alzheimer transgenic mouse. J Neurosci. 21(21):8370-7.

4. Wang P, Su C, Li R, Wang H, Ren Y, Sun H, Yang J, Sun J, Shi J, Tian J, Jiang S. 2014. Mechanisms and effects of curcumin on spatial learning and memory improvement in APPswe/PS1dE9 mice. J Neurosci Res. 92(2):218-31.

5. Rane JS, Bhaumik P, Panda D. 2017. Curcumin Inhibits Tau Aggregation and Disintegrates Preformed Tau Filaments in vitro. J Alzheimers Dis. 60(3):999-1014.

6. Sun J, Zhang X, Wang C, Teng Z, Li Y. 2017. Curcumin Decreases Hyperphosphorylation of Tau by Down-Regulating Caveolin-1/GSK-3β in N2a/APP695swe Cells and APP/PS1 Double Transgenic Alzheimer's Disease Mice. Am J Chin Med. 45(8):1667-1682.

7. Sui D, Xu X, Ye X, Liu M, Mianecki M, Rattanasinchai C, Buehl C, Deng X, Kuo MH. 2015. Protein interaction module-assisted function X (PIMAX) approach to producing challenging proteins including hyperphosphorylated tau and active CDK5/p25 kinase complex. Mol Cell Proteomics. 14(1):251-62.

8. Hu CD, Chinenov Y, Kerppola TK. 2002. Visualization of interactions among bZIP and Rel family proteins in living cells using bimolecular fluorescence complementation. Mol Cell. 9(4):789-98.

9. Ohashi K, Mizuno K. 2014. A novel pair of split venus fragments to detect protein-protein interactions by in vitro and in vivo bimolecular fluorescence complementation assays. Methods Mol Biol. 1174:247-62.